Universität Rostock

Mathematisch-Naturwissenschaftliche Fakultät
Institute: Leibniz-Institut für Atmosphärenphysik

Effects of sudden stratospheric warmings in the ionosphere/thermosphere system

---

A cumulative dissertation
to obtain the academic degree of Doctor of Science
from the Faculty of Mathematics and Natural Sciences
at the University of Rostock

by

Larisa P. Goncharenko

Reviewers:

Prof. Dr. Jorge L. Chau, Leibniz Institute of Atmospheric Physics
Prof. Dr. Claudia Stolle, Leibniz Institute of Atmospheric Physics
Prof. Christoph Jacobi, Leipzig Institute for Meteorology

Date of submission: 12.02.2024
Date of defense: 07.06.2024

https://doi.org/10.18453/rosdok_id00005218

Abstract

Since the late 2000's, rapid progress has been achieved in understanding of mechanisms coupling the upper atmosphere (thermosphere and ionosphere) with lower atmospheric layers (tropo-, strato-, and mesosphere). Atmospheric coupling studies have particularly benefited from investigations of sudden stratospheric warming (SSW) events, which involve global meteorological disturbances. As the state of the middle atmosphere rapidly changes during SSWs, it disrupts typical propagation paths of atmospheric waves that connect the lower and the upper atmosphere. The modified wave spectrum drives substantial variability in the thermosphere and ionosphere. Still, many key aspects of SSW impacts on the ionosphere and thermosphere are not known. This thesis addresses important open questions about the long-distance influence of SSWs, first from the polar stratosphere to the low-latitude ionosphere, and then inter-hemispheric, e.g., from the polar stratosphere to the middle and high latitudes of the opposite hemisphere.

The strongest Southern Hemisphere SSW in the last 40 years occurred in September 2019. It is examined whether Antarctic SSWs drive low-latitude ionospheric perturbations similarly to how Arctic SSWs do. As a result, quasi-periodic oscillations in TEC with strong 12-hrs, 5-6 days and 2-3 days periodicities are revealed. The anomalies can exceed a factor of 2 of the ionospheric background, comparable to the strongest anomalies associated with Arctic SSWs. In addition, a remarkable longitudinal dependence of the ionospheric disturbances could be related to a modulation of the non-migrating diurnal tide.

To explore the latitudinal extent of the ionospheric and thermospheric anomalies during this remarkable Antarctic SSW event, the inter-hemispheric impacts of Antarctic stratospheric disturbances on the mid-latitude upper atmosphere in the Northern Hemisphere were studied. Persistent (at least 30 days) and strong (up to 80-100%) positive anomalies in the total electron content and increases in the thermospheric O/N_2 ratio were found in the western region of North America, but the anomalies were different over the European sector.

The concept of inter-hemispheric coupling has been extended by providing evidence, for the first time, that large disturbances observed in the Arctic winter polar stratosphere during an SSW event cause large disturbances in both the mesosphere and ionosphere over Antarctica. There, ionospheric anomalies can reach $\sim$100% of the background level and are observed for multiple days. Several possible mechanisms are discussed that contribute to the formation of upper atmospheric anomalies in the Southern Hemisphere.

This thesis quantifies the effects of SSW events in the thermosphere and ionosphere and extends our understanding of physical mechanisms by which the lower atmosphere couples to the upper atmosphere on global scales.

Zusammenfassung

Seit den späten 2000er Jahren wurden erhebliche Fortschritte im Verständnis der Kopplungsmechanismen zwischen der oberen Atmosphäre (Thermo- und Ionosphäre) und den darunterliegenden Atmosphärenschichten (Tropo-, Strato- und Mesosphäre) erzielt. Diese Studien profitierten insbesondere von Untersuchungen zu Zeiten plötzlicher Stratosphärenerwärmung (kurz: SSW – Sudden Stratospheric Warming), welche mit globalen meteorologischen Veränderungen einhergehen. Da sich der dynamische Zustand der mittleren Atmosphäre während SSWs wesentlich ändert, werden typische Ausbreitungswege atmosphärischer Wellen, die maßgeblich zur Kopplung der unteren und der oberen Atmosphäre beitragen, unterbrochen. Das veränderte Wellenspektrum führt zu erheblichen Veränderungen in der Thermosphäre und Ionosphäre. Noch immer sind viele Schlüsselaspekte der Auswirkungen von SSWs auf die Ionosphäre und Thermosphäre nicht bekannt. Diese Arbeit befasst sich mit wichtigen offenen Fragen zur Fernwirkung von SSWs, zum einen von der polaren Stratosphäre auf die Ionosphäre in niedrigen Breiten, und zum anderen interhemisphärisch, z. B. von der polaren Stratosphäre auf die mittleren und hohen Breiten der jeweils anderen Hemisphäre.

Das stärkste SSW-Ereignis der Südhemisphäre in den letzten 40 Jahren trat im September 2019 auf. In dieser Arbeit wird untersucht, ob antarktische SSWs ähnlich wie arktische SSWs Störungen der Ionosphäre in niedrigen Breitengraden verursachen. Als Ergebnis werden quasi-periodische Schwankungen im Elektronengehalt der Ionosphäre (kurz: TEC – Total Electron Content) mit signifikanten 12-Stunden-, 5-6-Tage- und 2-3-Tage-Periodizitäten festgestellt. Die Anomalien können bis zu über einen Faktor 2 des ionosphärischen Hintergrunds erreichen, und ist somit vergleichbar mit den stärksten Anomalien, die mit arktischen SSWs verbunden sind. Es wird weiterhin vorgeschlagen, dass eine ebenso beobachtete Längsabhängigkeit der ionosphärischen Störungen mit einer Modulation der nicht-wandernden täglichen Gezeiten zusammenhängt.

Um die Ausbreitung in latitudinaler Richtung der ionosphärischen und thermosphärischen Anomalien während dieses bemerkenswerten antarktischen SSW-Ereignisses in 2017 zu erforschen, wurden die interhemisphärischen Auswirkungen des SSWs auf die obere Atmosphäre der mittleren Breiten der Nordhemisphäre untersucht. Anhaltende (mindestens 30 Tage) und starke (bis zu 80-100%) positive Anomalien des TECs und Erhöhungen des thermosphärischen O/N2-Verhältnisses wurden in der westlichen Region Nordamerikas festgestellt, jedoch unterscheiden sie sich von den Anomalien, wie sie über dem europäischen Sektor beobachtet wurden.

Das Konzept der interhemisphärischen Kopplung wurde erweitert, indem zum ersten Mal nachgewiesen wurde, dass große Störungen, die während eines SSW-Ereignisses

in der polaren Stratosphäre des arktischen Winters beobachtet wurden, große Störungen sowohl in der Mesosphäre als auch in der Ionosphäre über der Antarktis verursachen. Dort können ionosphärische Anomalien 100% des Hintergrundniveaus erreichen und über mehrere Tage andauern. Hier wurden mehrere mögliche Mechanismen erörtert, die zur Entstehung von Anomalien in der oberen Atmosphäre auf der Südhalbkugel beitragen.

Diese Arbeit quantifiziert die Auswirkungen von SSW-Ereignissen in der Thermosphäre und Ionosphäre und erweitert unser Wissen über physikalische Mechanismen, durch die die untere Atmosphäre auf globaler Ebene in die obere Atmosphäre einkoppelt.

Acknowledgements

First and foremost, I would like to thank my advisors, Prof. Dr. Jorge L. Chau and Prof. Dr. Claudia Stolle for their support and the opportunity to do my PhD thesis at the Institute of Atmospheric Physics. Dr. Jorge L. Chau has been an outstanding and most generous collaborator since early research on this topic started in 2008, and I am truly grateful for many years of inspiration, discussions, and contagious enthusiasm.

My sincere thanks go to program managers at the National Science Foundation of USA, National Aeronautics and Space Administration of USA, and the USA Office of Naval Research who provided sustained support of my research activities through several projects.

My colleagues and friends at MIT Haystack Observatory have always being a source of support and strength. I am especially grateful to Dr. Philip J. Erickson, Dr. Anthea J. Coster, and Dr. Shunrong Zhang for making Haystack Observatory an outstanding place for science and for 20+ years of continuous collaborations and friendship that shaped me as a scientist. I also would like to express my gratitude to now retired Dr. John Foster, who was instrumental to my early years as a researcher at the Haystack Observatory, and Dr. Joseph Salah, who was the most supportive mentor during my post-doc years at Haystack.

Cherished colleagues outside of Haystack Observatory have contributed immensely to my research activity and made my life so much richer. Dr. V. Lynn Harvey, Dr. Huixin Liu, Dr. Katelynn Greer, Dr. Nick Pedatella - many thanks for years and years of inspiring discussions and collaborations!

My husband Steven and children Denys, Anna, and Katherine were always the source of quiet support and strength, and I am thankful for their understanding and for believing in me.

Finally, I'd like to thank my father who taught me the most important lessons in life. His words "there is no such way in that there is no way out" stayed with me through my life and inspired me to never give up and to look for solutions even in the most challenging situations.

Contents

List of Figures

List of Abbreviations

AIM	**A**eronomy of **I**ce in the **M**esosphere
CIPS	**C**loud **I**maging and **P**article **S**ize
COSMIC	**C**onstellation **O**bserving **S**ystem for **M**eteorology, **I**onosphere, and **C**limate
DE3	**D**iurnal **E**astward Propagating Tide with Wavenumber **3**
DW1	**D**iurnal **W**estward Propagating Tide with Wavenumber **1**
EIA	**E**quatorial **I**onization **A**nomaly
ENSO	**E**l **N**iño–**S**outhern **O**scillation
EUV	**E**xtreme **U**ltra-**V**iolet
GIRO	**G**lobal **I**onospheric **R**adio **O**bservatory
GLONASS	**GLO**balnaya **NA**vigatsionnaya **S**putnikovaya **S**istema (in Russian)
GNSS	**G**lobal **N**avigation **S**atellite **S**ystem
GUVI	**G**lobal **U**ltra**v**iolet **I**mager
GW	**G**ravity **W**ave
IHC	**I**nter**h**emispheric **C**oupling
M2	**M**oon (Lunar) Semidiurnal Migrating Tide
MERRA	The **M**odern-**E**ra **R**etrospective analysis for **R**esearch and **A**pplications
MJO	**M**adden-**J**ulian **O**scillation
MLS	**M**icrowave **L**imb **S**ounder
MLT	**M**esosphere and **L**ower **T**hermosphere
NH	**N**orthern **H**emisphere
PMC	**P**olar **M**esospheric **C**loud
PMSE	**P**olar **M**esospheric **S**ummer **E**cho
PW	**P**lanetary **W**ave
PW1	**P**lanetary **W**ave with wavenumber **1**
PW2	**P**lanetary **W**ave with wavenumber **2**
QBO	**Q**uasi-**B**iennial **O**scillation
QSPW	**Q**uasi-**S**tationary **P**lanetary **W**ave
SD-WACCM	**W**hole **A**tmosphere **C**ommunity **C**limate **M**odel with **S**pecified **D**ynamics
SH	**S**outhern **H**emisphere
SW2	**S**emidiurnal **W**estward Propagating Tide with Wavenumber **2**
SSW	**S**udden **S**tratospheric **W**arming
TEC	**T**otal **E**lectron **C**ontent
TIMED	**T**hermosphere **I**onosphere **M**esosphere **E**nergetics and **D**ynamics
TIME-GCM	**T**hermosphere-**I**onosphere-**M**esosphere **E**lectrodynamics **G**eneral **C**irculation **M**odel
UV	**U**ltra-**V**iolet
UFKW	**U**ltra-**F**ast **K**elvin **W**aves
UT	**U**niversal **T**ime
WMO	**W**orld **M**eteorological **O**rganization

This thesis is dedicated to all Ukrainians
who fight for their right to live the lives they choose,
and to my children Denys, Anna, and Katherine,
my pride and joy,
without whom a thesis on a different topic
could probably be written 20-30 years ago
. . .

Chapter 1

Introduction

Better understanding of near-Earth space environment recently became a more urgent issue due to the explosive growth in the space satellite industry and the growing need for accurate nowcast and forecast capabilities. The near-earth space (upper thermosphere and ionosphere, altitudes between ∼100 km and ∼1000 km above ground) is strongly driven by solar radiation and magnetospheric energy inputs, and traditionally has been studied in the context of their changes. However, research activity over the last 20 years has accumulated convincing evidence that significant portion of variations in the upper atmospheric parameters is related to processes that occur at lower altitudes (0 - ∼100 km), and these variations occur on a large variety of spatial and temporal scales. This chapter first introduces main atmospheric layers (Section 1.1) and different internal waves such as planetary waves, tides and gravity waves that couple different atmospheric layers (Section 1.2). Than it briefly describes current understanding of mechanisms through which different waves can influence upper atmosphere (Section 1.3). Section 1.4.1 introduces a sudden stratospheric warming, a type of large-scale meteorological event that influences propagation of internal waves and thus disrupts nominal pathways that couple atmospheric layers. Such events have profound influences on the surface weather patterns (Section 1.4.2) and have been used by the lower atmospheric research community to spearhead physics-based development of weather forecasts multiple weeks in advance. SSW events also strongly affect upper atmosphere (Section 1.4.3), although our knowledge about these effects is rather limited. Section 1.5 describes objectives of this Thesis, to employ SSW events to improve our understanding of how large-scale changes in the upper atmosphere are linked to the lower atmosphere.

1.1 Atmospheric Layers

Earth's atmosphere is a layer of gases surrounding the planet Earth and is a fundamental component of life as we know it. Nitrogen and oxygen account for 99% of gases. Other planets and moons have very different atmospheres, and some of them do not have atmospheres at all. Since the nature of gases and forces that act on them change with altitude, the Earth's atmosphere is traditionally divided into different regions. The most frequently used system subdivides regions based on the temperature gradient, with regions called "spheres", and the boundaries between them called "pauses". Each "pause" denotes a change in temperature gradient. From the ground and up, the layers are typically denoted as the troposphere, stratosphere, mesosphere, thermosphere, and exosphere, as shown in Figure 1.1. The boundaries between atmospheric layers are not clearly defined, and change depending on many factors including latitude and season.

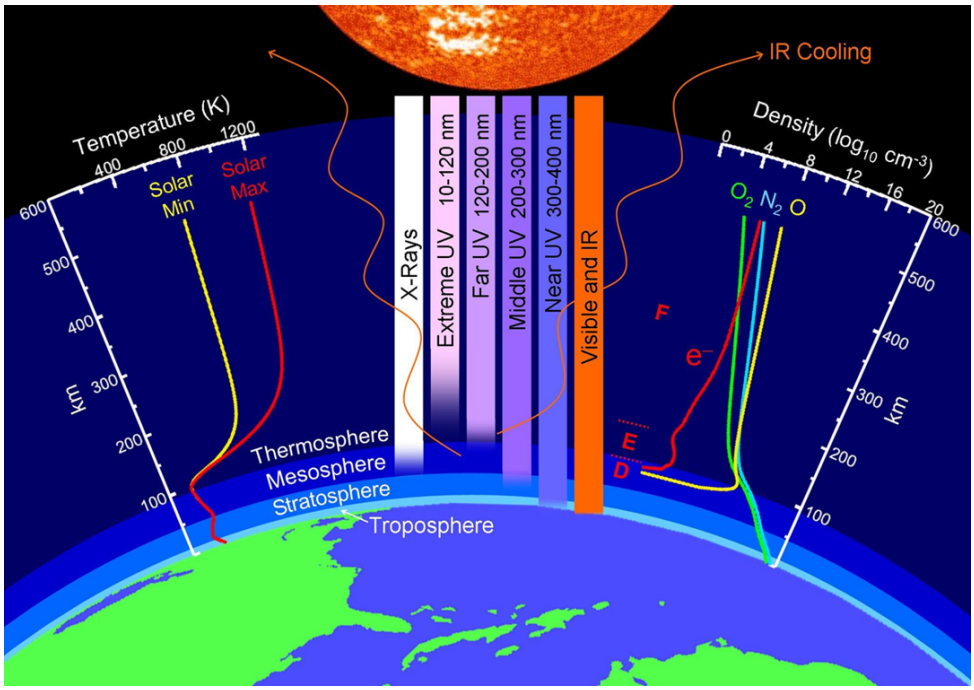

FIGURE 1.1: Regions of the Earth's atmosphere and ionosphere. Image credit: John Emmert, Naval Research Laboratory, USA.

Troposphere. The troposphere marks the region of atmosphere that extends from the Earth's surface to about 10 km. It is characterized by a decrease in temperature with altitude, at the adiabatic lapse rate of ∼7 K per kilometer. The temperature continues to decrease until the tropopause. Almost all weather systems are formed in the troposphere, as it contains the majority of atmospheric water vapor, and most weather events, including rain, snow, thunderstorms, lightning, cyclones and weather fronts, occur within this region. This portion of the atmosphere is the domain of meteorology; it is well studied and understood due to the importance of weather for human society. Currently, tropospheric parameters can be reliably predicted about one week in advance, and predictability decreases after that, although theoretical limits are closer to 3 weeks (Domeisen et al., 2020).

Stratosphere. The stratosphere is located above the troposphere and extends from an altitude of about 10-13 km to its upper boundary of ∼50 km. The stratosphere is crucial to life on Earth, as it contains a thin ozone layer that absorbs the ultraviolet portion of solar radiation which is harmful to human health. Absorption of UV radiation by ozone layer is a primary reason for a positive temperature gradient in the stratosphere, and also a major source of semidiurnal tides (Section 1.2) that play an important role in thermospheric and ionospheric variability (Section 1.3).

Mesosphere. The mesosphere extends from ∼50 km to ∼90km and is characterized by a negative temperature gradient. Radiative cooling and the lack of strong heating mechanisms lead to a sharp temperature decrease in this region, with lowest temperatures at the mesopause dropping to 130 K, making the mesopause the coldest place in the Earth's atmosphere. The mesosphere is a source of a spectacular high-latitude phenomena called polar mesospheric clouds or noctilucent clouds (Lübken et al., 2008). It is also a home for two other prominent and highly dynamic atmospheric phenomena, sprites and elves, that are observed above thunderstorms and are related to electron acceleration physics within lightning regions.

Thermosphere. The thermosphere lies above the mesosphere and is a region where temperature rapidly increases to values well above 1000 K. This temperature increase is caused mainly by the absorption of solar ultraviolet radiation, and variations in the sunlit conditions result in considerable variation in temperature with latitude, local time, season, and the well known 11-year cycle in solar activity. Solar heating causes the atmosphere to expand on the sunlit side of Earth, creating a high-pressure region and setting the characteristics of horizontal pressure gradients and the resulting upper atmosphere wind system. These neutral winds carry energy away from the heat source, and are balanced by upward or downward winds far away from the source, forming together a global circulation pattern. Thermospheric winds are also influenced by other processes, including ion drag, the Coriolis force, the viscous drag force, and momentum advection. Acting together, all these physical pathways make the upper thermosphere a very dynamic and complicated system (Wang et al., 2021). Thermospheric temperatures are also influenced by competing heating and cooling processes, that, in addition to solar extreme ultraviolet (EUV) radiation, include thermal interaction with ionosphere, infrared radiation from minor constituents like CO_2 and NO, and adiabatic heating and cooling due to dynamic variations (Jones Jr et al., 2022). Thermospheric composition, winds, and temperature remain poorly understood in both general and specific characteristics due to the lack of observations, creating what is called a 'thermospheric gap' (Oberheide et al., 2011b).

Exosphere. The exosphere is the uppermost region of the Earth's atmosphere that starts at $\sim$ 500-1000 km, depending on solar radiation, without a clear upper boundary. The composition of the exosphere is dominated by hydrogen, and contains only trace amounts of other gases. As majority of satellites are placed in low Earth orbits, they encounter atmospheric drag from gases in the exosphere that affects satellites' orbits and lifetime. Due to the rapidly increasing number of satellites, accurate knowledge of upper atmosphere density and other parameters recently became an important portion of satellite lifetime planning and collision avoidance.

Ionosphere. The ionosphere is a very different part of the atmosphere. In contrast to other "spheres" that refer to neutral atmospheric layers, the ionosphere is a region of the Earth's atmosphere in which atoms and molecules have become electrically charged. This ionized portion of the upper atmosphere is produced mostly by solar EUV input. Ionosphere has been studied for decades, as ionization of the upper atmosphere is of practical importance due to its influence on propagation of radio waves. In addition, the ionosphere is also known better than the thermosphere because it is easier to observe using radiowave remote sensing techniques. The ionosphere extends from $\sim$60 km up to $\sim$1000 km, and has several distinct layers - D, E, F1 and F2 regions - that are formed by absorption of different portions of solar radiation. On Earth, the ionized portion remains a minor constituent of the atmosphere, and even in the F2-region peak of ionosphere less than 2% of the neutral atmosphere is ionized.

1.2 Wave Coupling in the Atmosphere

The neutral atmosphere is highly dynamic and filled with different waves with a variety of spatial and temporal scales, including planetary waves, tides, and gravity waves. These waves can be observed as perturbations in different atmospheric parameters, including temperature, wind, density, and geopotential height. Horizontal

and vertical propagation of these waves plays an important role in the coupling between different atmospheric layers and in the dynamic and energy balance of the atmosphere, as discussed in Sections 1.3, 1.4, 1.4.2, and 1.4.3.

Planetary waves. Planetary waves (PWs) are large-scale perturbations that extend coherently along longitude, and are responsible for longitudinal variations in atmospheric parameters. These waves can be stationary, meaning that they are fixed in the rotating reference frame and do not propagate along longitude, or travelling, and can have periods from 2 days to several weeks. Quasi-stationary planetary waves with wavenumbers one and two (QSPW1 and QSPW2, also known as PW1 and PW2), which are most relevant to this thesis, dominate spatial and temporal variability in the stratosphere, and have large amplitudes at middle latitudes (50-70°) in winter season (Smith and Perlwitz, 2015). Other important waves that have significant impact on the upper thermosphere and ionosphere are traveling planetary waves with multi-day periods, e.g., 2, 6, 10, 16 days (Q2DW, Q6DW, Q10DW, Q16DW, respectively), and ultra-fast Kelvin waves, UFKW (e.g., Forbes, 2021). Planetary waves in general do not propagate above the lower thermosphere (Pogoreltsev et al., 2007; Forbes et al., 2002), but they can modulate tides or gravity waves that carry planetary wave signatures to higher altitudes.

Tides. Tides are oscillations that are generated by Earth's rotation with respect to the Sun (solar thermal tides) or to the Moon (lunar gravitational tides). Tides have periods that are linked to the fraction of the planet's rotation period; solar tides have periods of 24 hrs (diurnal tide), 12 hrs (semidiurnal tide), 8 hrs (terdiurnal tide), etc., while the M2 lunar tide, vitally important for atmospheric coupling, has a period of 12.421 hrs. Solar tides are excited in the atmosphere by the absorption of different wavelengths of solar radiation by different atmospheric constituents. The diurnal tide is excited in the troposphere by heating of water vapor, while semidiurnal tide is created in the stratosphere by heating of ozone. Tides are also excited *in-situ* in the thermosphere by heating of oxygen and nitrogen (Forbes, 1995), as well as via ion-neutral interactions in the thermosphere-ionosphere (Müller-Wodarg et al., 2001; Jones Jr et al., 2013). Tides are classified into two types: *migrating tides* that propagate westward with the same apparent phase speed as the Sun or Moon, and *non-migrating tides*, that have apparent phase speeds faster or slower than the Sun's motion. Tidal nomenclature uses abbreviations to denote tidal periods (D for diurnal, S for semidiurnal, T for terdiurnal), propagation direction (E for eastward, W for westward, 0 for tides that do not propagate in longitude), and zonal wavenumber, representing the number of maximums and minimums in longitude. The most important tides for atmosphere-ionosphere coupling are DW1 (diurnal westward propagating with wavenumber one) and SW2 (semidiurnal westward propagating with wavenumber two), although other tides like DE3, DW2, SW1, SW3 can significantly contribute to perturbations in the atmospheric parameters (Forbes, 2021).

Gravity waves. Gravity waves (GWs) are small-scale atmospheric oscillations with periods from minutes to several hours. They can be excited when perturbed air parcels are restored to equilibrium by buoyancy and gravity in a stably stratified atmosphere. There are many sources of atmospheric GWs, including winds over mountains (Holton, 1992; Fritts et al., 2016), convective processes (Alexander et al., 1995), imbalances in jet streams and frontal systems (Wu and Zhang, 2004), higher-order wave excitation from wave dissipation (Vadas et al., 2003; Vadas et al., 2018), polar vortex (Yoshiki and Sato, 2000), Joule heating during geomagnetic storms (Hocke, Schlegel, et al., 1996), and episodic events like tsunamis (Garcia et al., 2014)

or volcano eruptions (Wright et al., 2022). Under favorable propagation conditions, GWs can transfer momentum and energy from one atmospheric region to another in both horizontal and vertical directions, so the impact of a specific GW source can be seen at locations far away from their generation.

Nonlinear interactions between planetary waves and tides or between different tides also generate secondary waves (Teitelbaum et al., 1989; Teitelbaum and Vial, 1991). As waves propagate upward, their amplitudes increase due to the exponential decrease in the background neutral density, and reach maximums in the lower thermosphere (90 - 120 km). As the wave sources and the propagation condition (background wind) significantly change in space and time, the resulting waves that enter the upper atmosphere from below display large variability and significantly contribute to overall thermospheric and ionospheric variability.

1.3 Thermospheric and Ionospheric Variability Forced by Lower Atmosphere Waves

Observational and modeling studies in the E and F regions of the ionosphere provide a variety of evidence on the role of multi-scale wave dynamics for understanding thermosphere-ionosphere variations on day-to-day, seasonal, and interannual scales. Statistical studies show that under quiet geomagnetic conditions variability in ionospheric peak electron density N_mF_2 reaches 15-35% of its mean value (Forbes et al., 2000; Rishbeth and Mendillo, 2001), and this variability is attributed to combined influences of different atmospheric waves. In another spectacular example, the low-latitude ionosphere exhibits strong longitudinal variations with four-peak or three-peak structures that are attributed to non-migrating tides DE3 and DE2 (Immel et al., 2006; Hagan et al., 2007; Oberheide et al., 2011a). Pathways that connect lower atmosphere with the upper thermosphere and ionosphere are still not completely understood, although there has been a rapid progress within a last 10-15 years. These transformative developments resulted from the superposition of several factors: growing availability of global observations, development of more capable physics-based models, and very deep and long minimum of solar cycle 23, when the influence of solar and geomagnetic drivers of the upper atmosphere was unusually weak. Numerous mechanisms of coupling between the lower and upper atmosphere are discussed in recent reviews (Liu, 2016; Forbes, 2021).

One of the important mechanisms for ionospheric variability is the E-region dynamo that acts at ∼100-150 km altitude. Tidal winds drive E-region electric currents that generate dynamo electrostatic fields. These fields than map to the F-region and produce plasma drifts in the direction perpendicular to the magnetic field lines. These E×B drifts carry the signatures of the original tidal waves and are very efficient in redistributing ionospheric plasma in the low-latitude ionosphere, leading to the formation of the equatorial ionization anomaly (EIA), known for over a century as a prominent increase of ionization at ±15°–20° magnetic latitude.

Although tidal amplitudes decrease above ∼120-130 km altitude due to tidal dissipation and molecular damping, observations show that tides can nevertheless propagate directly into the upper thermosphere, where they can modulate thermospheric winds, composition and density and strongly affect ionospheric parameters (Forbes et al., 2009; Häusler et al., 2010; Oberheide et al., 2009).

Numerous simulations have demonstrated that dissipation of upward propagating tides can affect the background circulation and vertical transport of atomic oxygen in the lower thermosphere. This manifests in a reduction of thermospheric O/N_2 ratio at low latitudes and, in turn, can contribute to a depletion in ionospheric electron density or total electron content (TEC) (Jones Jr et al., 2014b; Pedatella et al., 2016; Yamazaki and Richmond, 2013). Similarly, a reduction in O/N_2 ratio and electron density is also expected in these situations due to the dissipation of gravity waves (Jones Jr et al., 2020) and planetary waves (Yue and Wang, 2014).

Due to the large change in amplitudes of stratospheric QSPW and background stratospheric winds, sudden stratospheric warming events provide the most striking examples of global perturbations of the ionosphere and thermosphere, and serve as exemplary cases to gain insights into linking of the lower and upper atmosphere through complex interactions among tides, planetary waves, gravity waves, and mean circulation.

1.4 Sudden Stratospheric Warmings and Links to Atmospheric Variability

1.4.1 Sudden Stratospheric Warming: Phenomenology and Definition

The polar winter stratosphere is typically very cold, maintained radiatively in this state by cold polar night conditions, and is characterized by strong eastward winds that form the stratospheric polar vortex. During many winters, the quiet polar vortex becomes disturbed, with stratospheric temperatures rapidly increasing by tens of degrees, and eastward winds decreasing. These events, known as sudden stratospheric warming (SSW), are the most dramatic and dynamic meyeorological phenomenon and a dominant source of variability in the winter stratosphere, particularly in the Northern Hemisphere.

The World Meteorological Organization (WMO) categorizes SSW events into four types: major midwinter, minor, final, and Canadian warmings (Butler et al., 2015). It is now widely accepted to define a SSW to be “major” if, at 10 hectoPascals (hPa) or below, the zonal mean temperature increases poleward from 60° latitude and the circulation at 60° latitude reverses from westerly (eastward) to easterly (westward) winds. “Minor” SSW are defined to occur when the zonal mean temperature increases poleward from 60° latitude but the circulation remains westerly. “Final” warmings are major warmings that occur late enough in the season to mark the transition from winter to summer. Figure 1.2 illustrates a major Arctic sudden warming event in 2018–2019, together with the background climatology and variability of zonal wind, and the average temperature from 65°N to 90°N at 10 hPa. Both lowest and highest temperatures and winds are observed during these winter conditions. The warming (red line) peaks in late December and early January and is followed by another type of anomaly: very low stratospheric temperatures and high eastward winds in February and March, indicating the long-lasting impacts of SSW events.

Different types of SSW events are also classified through their spatial structure, where distinctions are made based on whether there are one (PW-1) or two (PW-2) ridges and troughs around a latitude circle. These two SSW categories are also referred to as “displaced” (also called "vortex-shift") or “split” polar vortex types (Charlton and Polvani, 2007; Matthewman and Esler, 2011; Esler and Matthewman, 2011) in which PW-1 modes dominate “displaced” events and “splits” imply PW-2

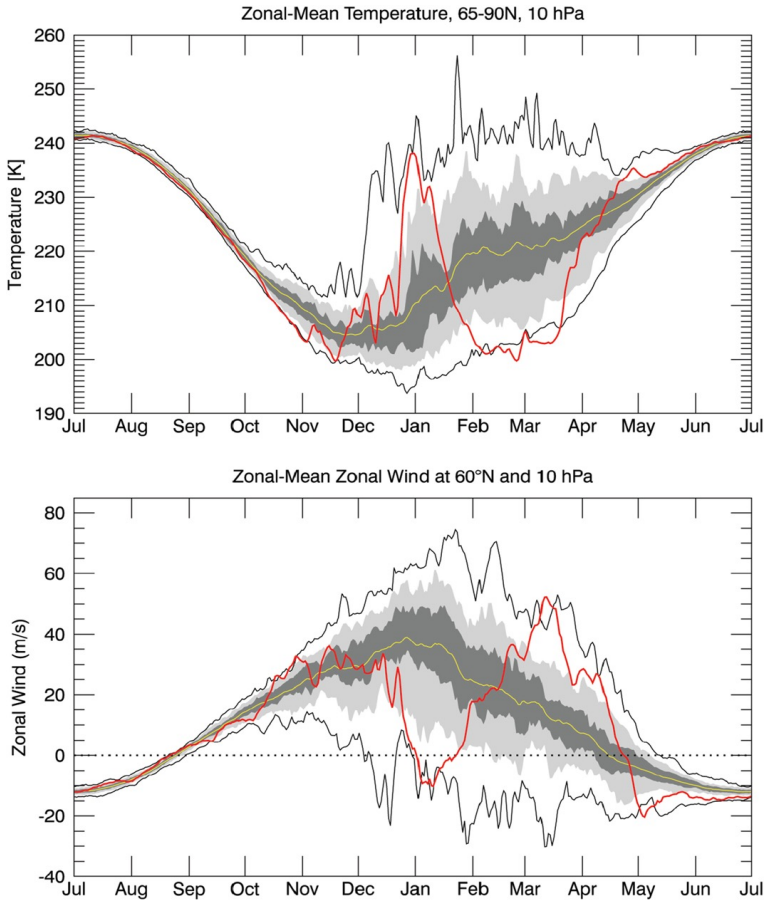

FIGURE 1.2: Zonal-mean temperatures (top) and zonal-mean zonal wind at 60°N (bottom) at 10hPa and 65–90◦N for July 2018 to June 2019 (red lines). An SSW event is seen as the upward spike in temperature and the reduction to less than 0 m/s in zonal wind (easterlies). The yellow lines signify the daily average conditions in the stratosphere for that time of year, while the gray shading shows 30th/70th (dark) and 10th/90th (light) percentiles. Solid black lines show the daily max/min for prior winters 1979–2018. The month ticks indicate the first day of the month. From Baldwin et al. (2021).

signatures. Figure 1.3 shows an example of a typical polar vortex, vortex displacement SSW, and vortex split SSW. Statistical studies show that about a third of observed major SSWs can be classified as split events, with another third as displacement events. For the rest of the events, the polar vortex both displaces and splits within a period of several days (Baldwin et al., 2021).

There is an extensive body of literature on SSW dynamics, ranging from composites (Limpasuvan et al., 2004; Butler et al., 2017) to climatologies (Labitzke et al., 2005; Charlton and Polvani, 2007) and individual case studies. The current knowledge of these events is summarized by Baldwin et al. (2021) and Goncharenko et al. (2021b). The impact of these dramatic changes extends both horizontally into middle and low latitudes and even into the opposite hemisphere and vertically, down into the troposphere and up into the thermosphere and ionosphere, as described in the next sections.

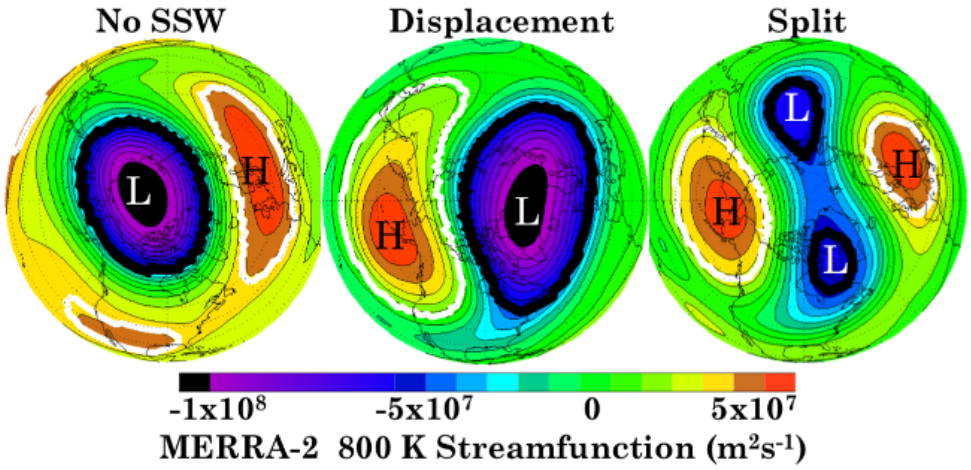

FIGURE 1.3: Arctic vortex (marked with "L" and thick black contours) and stratospheric anticyclones (marked with "H" and white contours) near 30 km on days with (left) no SSW in January 2011, (middle) a vortex shift SSW in January 2008, and (right) a vortex split SSW in January 2009. From Goncharenko et al. (2021b).

1.4.2 Downward Influence of SSW

In the Northern Hemisphere (NH), it is known that stratospheric anomalies can propagate downward into the troposphere on time scales from several days to months (Baldwin and Dunkerton, 2001; Thompson et al., 2002; King et al., 2019). Many studies have linked Arctic SSW with surface weather anomalies, and in particular with extremely low temperatures that last days and weeks (Kidston et al., 2015; Nath et al., 2016; Karpechko et al., 2018; Domeisen et al., 2020). For example, the major SSW event in February 2018 has been linked to persistent cold weather over large parts of Europe in late February and early March after a very warm winter (Karpechko et al., 2018), as well as anomalously wet conditions over southwestern Europe (Ayarzagüena et al., 2018). Additional effects include positive temperature anomalies over Greenland and eastern Canada, and even subtropical Africa and the Middle East (Baldwin et al., 2021). Several mechanisms have been proposed to explain the downward influence of these stratospheric dynamics (Kidston et al., 2015; Tripathi et al., 2015a). However, the exact mechanisms responsible for stratosphere-troposphere connections are not fully known yet, and as a consequence it is still not possible to predict surface weather impact of a specific SSW. These topics are currently a very active and promising research area (Baldwin et al., 2021).

Overall, the morphology of the polar vortex is an important factor that determines the location, strength, and temporal extent of the surface weather response to SSW (Kidston et al., 2015; Domeisen et al., 2020; Lehtonen and Karpechko, 2016). For example, vortex-shift events (related to amplification of PW1 oscillations) influence the occurrence of extreme cold events in East Asia (Lu et al., 2022; Zhong and Wu, 2023). Vortex-split events (related to amplification of PW2 modes) have been associated with extreme cold events over Europe (Seviour et al., 2013; Lü et al., 2020). Regional changes in the perturbed stratospheric vortex can induce zonally asymmetric effects in the troposphere and regionally dependent stratosphere–troposphere coupling (Thompson and Wallace, 2000; Kodera et al., 2016; Domeisen et al., 2020; Hall et al., 2021).

Surface weather anomalies typically develop with a lag of about 3 days after the stratospheric anomalies and can persist for up to 60 days (Domeisen et al., 2020). For longer time scales (longer than 3-4 weeks), surface responses are very similar for vortex-split and vortex-shift SSW events (White et al., 2021). However, closer to the central dates of SSW vortex-split events extend deep into the troposphere faster, within 2-3 days after SSW onset (Kidston et al., 2015), while vortex-shift events are associated with a more gradual downward propagation over ∼10–15 days. In addition to regional and timing differences in the downward influence of SSW events, vortex-split events lead to stronger surface weather responses than vortex-shift events (Lehtonen and Karpechko, 2016).

The impact of stratospheric anomalies on the surface weather is not limited to only SSW events. Another type of stratospheric extreme, a strong and zonally symmetric polar vortex, can lead to extreme Eurasian weather with anomalously high temperatures, as occurred in early 2020 (Rupp et al., 2022). Such stratospheric extremes can develop due to a weak planetary wave activity in the stratosphere associated with a quasi-simultaneous reflection of both PW1 and PW2 modes. Both strong vortex events (Tripathi et al., 2015b) and final warming events (Butler et al., 2019; Hardiman et al., 2011) have been shown to impact surface weather, but their effects are less understood than SSW events.

The impacts of stratospheric anomalies on surface conditions are much less understood for the Southern Hemisphere, as such anomalies are not as frequent as in the Northern Hemisphere. However, they occur episodically in austral spring to early summer (Shiotani and Hirota, 1985; Kuroda and Kodera, 1998). Statistical analysis shows that the warming and weakening of the stratospheric polar vortex increases the chances of hot and dry extremes and associated wildfires over Australia (Lim et al., 2019). The rare Antarctic SSW of September 2019 appeared to be a primary driver of the extreme hot and dry conditions over subtropical eastern Australia that accompanied the severe wildfires in Australia in October-December 2019, below-average rainfall in northeastern Brazil and eastern South Africa, and above-average rainfall in southeastern Brazil, western Patagonia, and southernmost New Zealand (Lim et al., 2020).

As emphasized by Lim et al. (2019), understanding and predicting extreme surface weather conditions - low and high temperatures, low and high rainfall, wildfires and snowstorms - is crucially important for human society because of the risks and impacts on economy and human health, including agriculture, wildfires, utilities, infrastructure, water management, etc. Prolonged temperature or rainfall extremes in a specific area of the world can be felt in a much larger area through its impacts on production and export of agricultural products. The state of the stratospheric polar vortex represents an important source of predictability for surface weather on sub-seasonal and seasonal scales (from two weeks to two months), and significant potential benefit to humanity. Even more broadly, this area of research has enormous potential for large advances within the next decade, as it has several attractive features: already available comprehensive datasets, well-developed models, a large international research workforce, and intrinsic support from governments due to the immediate benefits to society from increased understanding.

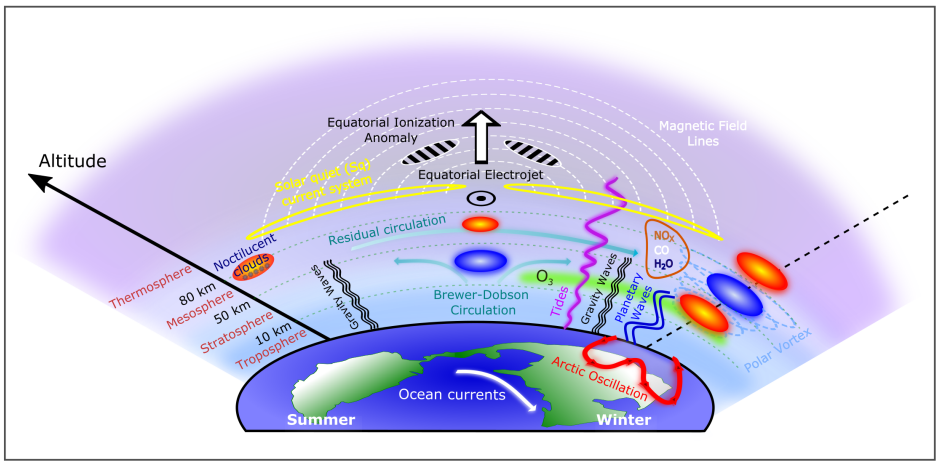

FIGURE 1.4: Schematic of the coupling processes and atmospheric variability that occur during sudden stratospheric warming events. Red and blue circles denote regions of warming and cooling, respectively. From Pedatella et al. (2018).

1.4.3 Upward Influence of SSW

In contrast to a well-developed understanding of SSW impacts on the troposphere and surface weather described in the previous section, community understanding of the influence of such events on upper atmospheric layers is in relatively early stages of development. It is already well recognized that SSW also affect atmospheric layers above the stratosphere. SSW effects in the mesosphere have been known since the 1970s and include high-latitude mesospheric cooling and reversal of mesospheric winds, warming in the tropical mesosphere, and warming in the high-latitude summer (Southern Hemisphere) mesosphere (e.g, Chandran et al., 2014). A review of knowledge on the links between SSW and the ionosphere and thermosphere is provided by Chau et al. (2012), and most recently by Goncharenko et al. (2021b) and Forbes (2021). Figure 1.4 schematically shows several types of upper atmospheric anomalies associated with SSW events. This section will primarily address SSW links with higher atmospheric layers including the lower thermosphere, upper thermosphere, and ionosphere, as physical drivers and responses in these regions are directly related to this thesis work.

Rapid progress in understanding SSW impacts on the thermosphere-ionosphere system began relatively recently, since late 2000's. Initial observations demonstrated lower thermospheric warming and upper thermospheric cooling at middle latitudes (Goncharenko and Zhang, 2008) and strong quasi-semidiurnal anomalies in vertical drifts observed in the low-latitude ionosphere (Chau et al., 2009). Such quasi-semidiurnal anomalies have been observed in various data sets, including tidal winds in the lower thermosphere, electrojet amplitudes, vertical drifts, peak electron density N_mF_2, and TEC. At low latitudes, anomalies in response are bright and can reach as much as 100-150% of the background electron density with persistence for an extended period of time, from several days for short SSW events and up to 30-40 days for prolonged major SSW events (Goncharenko et al., 2013; Goncharenko et al., 2021b; Pedatella et al., 2014).

SSW-related changes in middle atmospheric wind and temperature cause an amplification of several tidal wave modes: the solar semidiurnal migrating tide (SW2), lunar semidiurnal migrating tide (M2) (Jin et al., 2012; Forbes and Zhang, 2012; Pedatella et al., 2014), SW1 tide (Liu et al., 2010; Pedatella et al., 2012), and SW3 tide (Liu et al., 2010). These tidal modes are thought to be the primary mechanism responsible for the quasi-semidiurnal signature in observations. Non-migrating tides SW1 and SW3 are generated through interaction between the strong QSPW and SW2 tide (Forbes, 2021). The increase in tropical ozone during SSW events could also contribute to an enhancement in the SW2 (Goncharenko et al., 2012; Limpasuvan et al., 2016), although it plays a minor role (∼20-30%). Lunar tides in the equatorial electrojet can be amplified during SSW by a factor of 3 (Yamazaki, 2013). On average, SSW leads to a 75% increase in the lunar current system, but to only a 10% increase in the solar current system, and in the absolute sense changes in solar and lunar tidal winds are comparable in magnitude. From a phasing perspective, when SW2 and M2 tides are similar in magnitude, their superposition can be constructive during the first and third quarters of the Moon phase and destructive during the second and forth quarters of the Moon phase, leading to a multi-day modulation of plasma drifts (Yamazaki, 2014; Maute et al., 2016). As SSW also can lead to the amplification in diurnal tides (Sathishkumar and Sridharan, 2013) and terdiurnal tides (Gong and Zhou, 2011; Gong et al., 2016), a rich spectrum of amplified tides results and leads to a highly variable wind system in the lower thermosphere. Amplified E-region winds are the primary reason for the production of enhanced F-region plasma drifts through the E-region dynamo mechanism and, consequently, for a large change in low-latitude ionospheric electron density during SSW (Pedatella et al., 2012; Pedatella et al., 2014).

Direct penetration of amplified tides to the upper thermosphere is an additional mechanism that contributes to observed ionospheric variations, in particular at middle latitudes where the E-region dynamo mechanism is less effective. SSW-modified upper thermospheric winds can move the F-region upward or downward by transporting plasma along magnetic field lines (Pedatella and Maute, 2015). Goncharenko et al. (2018) reported a deep depletion in the nighttime ionosphere reaching a factor of 2-5 relative to non-SSW conditions and attributed it to the SSW modulation of thermospheric wind. Recent simulations and observations confirmed that tidal modification of meridional thermospheric winds during SSW can lead to large decreases in the nighttime electron density in a large range of latitudes (up to 50 degrees in both hemispheres), and such depletions have proved to be a robust feature during SSWs (Jones Jr et al., 2023).

Numerical simulations suggest that SSWs drive other thermospheric disturbances, including thermospheric warming and cooling that depend on local time, latitude, and longitude (Liu et al., 2013; Liu et al., 2014), changes in the meridional circulation (Miyoshi et al., 2015), and changes in the thermospheric composition (Yamazaki and Richmond, 2013; Pedatella et al., 2016) that can impact atomic oxygen and hydrogen density and potentially have implications even at altitudes of several Earth radii above Earth's surface (Jones Jr et al., 2020). Due to the scarcity of thermospheric data many of these predictions have not been tested, although available observations link SSW to a decrease in O/N_2 ratio (Oberheide et al., 2020) and changes in the mean meridional winds (Gasperini et al., 2023), in consistency with simulations.

1.4.4 Summary of SSW Importance

In aggregate, the amplitude and variety of the SSW features discussed above clearly demonstrate the relevance and impact of their dynamic influences on atmospheric variations, and these pathways arguably form a sometimes dominant and always essential driver of whole atmosphere variability. Community understanding of the varieties of SSW mechanisms, and their relative importance over relevant spatial and temporal scales, remain incomplete but ultimately represent a key goal for better quantification of dynamics in the tightly coupled atmosphere-ionosphere system.

1.5 Objectives and Structure of the Thesis

This thesis extends the knowledge of ionospheric and atmospheric variability through SSW-centric observational studies of their drivers and impacts. A study focus on SSW has been a proven strategy to vastly improve our understanding of multiple mechanisms connecting the lower and upper atmosphere. However, the majority of available studies have focused on Arctic SSWs that occur in December - February, and it remains unknown whether Antarctic SSWs can lead to any comparable perturbations in the ionosphere and thermosphere. Studies available to date also suggest that SSW effects are not uniform and are considerably more pronounced in the American longitudinal sector. Given the limitations of single-case studies and the unavoidable differences in methodology employed by different researchers, it is not clear whether such conclusions can be generalized. Longitudinal variations in the ionosphere/thermosphere in response to SSW remain not well documented and not well understood. In addition, available studies focus on ionospheric variability at low latitudes, and perturbations at middle and high latitudes are much less known, despite studies in the available literature that present fascinating examples of SSW-associated perturbations at middle to high latitudes.

This work advances knowledge of SSW pathways and impacts through new studies of SSW dynamics, by first investigating the ionospheric response to a rare Antarctic SSW in September 2019. Chapter 2 provides a summary of observational data and methods that were used to isolate SSW signatures. Chapter 3 summarises investigation of effects of Antarctic SSW at low latitudes. Chapter 4 extends this research to middle latitudes of the Northern Hemisphere. Chapter 5 continues the topic of far-reaching effects of SSW in the opposite hemisphere and discusses responses to Arctic SSW in the mesosphere and ionosphere over Antarctic regions. Finally, conclusions and suggestions for future work are outlined in Chapter 6.

Chapter 2

Data and methods

This section describes major observational techniques and stratospheric, mesospheric, thermospheric and ionospheric datasets used in the studies described in Chapters 3 - 5, as well as methods to identify SSW-associated anomalies in various datasets.

2.1 Total Electron Content from GNSS observations

Total Electron Content (TEC) obtained from the Global Navigation Satellite Systems (GNSS) is one of the most versatile ionospheric datasets used in numerous studies of ionospheric variability. As TEC is highly variable due to changes in solar EUV, season, local time, and other factors, correct attribution of TEC changes to effects of SSW requires careful separation of contributions from different drivers. Although numerous earlier studies successfully used 10-day averaging (or similar approach) to define the background state of the ionosphere (Goncharenko et al., 2010a; Goncharenko et al., 2010b), this approach has limitations and is not always applicable. To improve the description of the background ionospheric state, we utilized additional methods that are described in Sections 2.1.2 and 2.1.3.

2.1.1 TEC database

We use TEC data provided by the Madrigal database and processed by MIT Haystack Observatory as described by Rideout and Coster (2006) and Vierinen et al. (2016). All studies described in the next chapters utilize data product that has 1x1 degree latitude and longitude resolution and 5 minute temporal resolution for locations that are covered by ground-based GNSS receivers, resulting in data gaps over the oceans and areas without GNSS receivers. Figure 2.1 shows example of data coverage for September 15, 2019, during Antarctic SSW. The numbers of GNSS receivers varies with time, increasing from 5360 sites for the January 2013 SSW study (Chapter 5) to 6340 sites for the September 2019 SSW studies (Chapters 3 and 4). MIT Haystack Observatory currently processes data from more than 6000 GNSS receivers. GLONASS data was added to the processing in 2017, resulting in the 30% improvement in the data density. Inspection of the TEC data for the time period between August 1, 2019 and November 1, 2019 shows high data quality, with a median error of a single data point equal to 0.92 TECu (1 TECU = 10^{16} electrons m^{-2}), and 99-th percentile in error equal to 1.36 TECu. The error in TEC data exceeded 3 TECu in 0.01% of original data, and this data was excluded from the subsequent analysis.

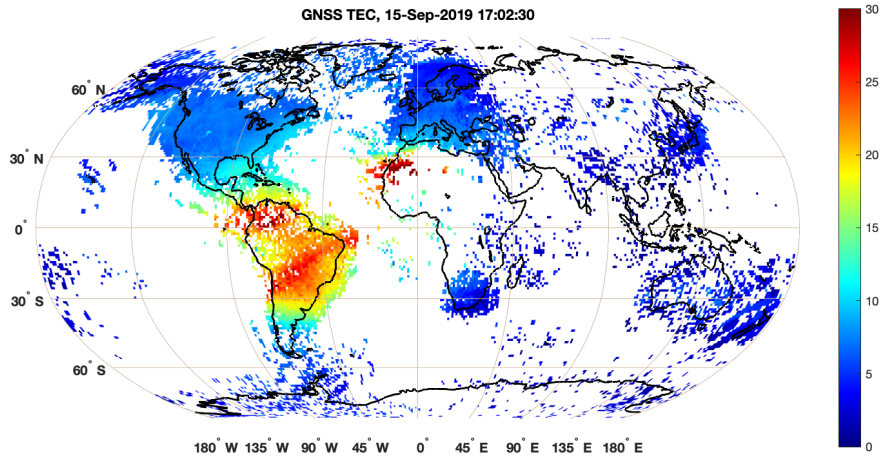

FIGURE 2.1: GNSS TEC data coverage provided by the CEDAR Madrigal database for September 15, 2019.

2.1.2 Background TEC: dynamically quiet state

To accurately isolate effects of SSW, we first characterize the typical 'dynamically quiet' ionospheric state for a given season and solar flux conditions. For the case of September 2019 Antarctic SSW, we calculate median values of TEC and different percentiles for the following conditions: low solar activity (F10.7 daily index is 70 +/- 5 sfu; 81-day average F10.7 index is 70 +/- 5 sfu), low geomagnetic activity (daily Ap index < 15 for the current day and previous 24 hours), average or below average stratospheric planetary wave activity at 10hPa and 60°S, and centered on September 15 with a +/-15-day window. Average level of stratospheric planetary wave activity was calculated from 40+ years of MERRA data. The Madrigal database contains 79 days that satisfy the aforementioned conditions, with data collected in 2008, 2009, and 2018. The TEC observations for the selected 79 days are then binned in 30-min intervals, resulting in several hundred data points per each 1° longitude x 1° latitude bin in areas with good data coverage. Areas with more limited data coverage (like over Africa) have more data from year 2018 in comparison with 2008 and 2009. Median TEC values determined from these bins are then used in this study as a baseline that describes the 'dynamically quiet' ionosphere in each geographic sector with high resolution in latitude and longitude. We have included in the calculation of medians only areas that had more than 50 points in each 1° x 1° x 30-min bin, indicating that medians were calculated based on observations from at least 8-9 different days. As an example, the top two panels of Figure 3.2 show median TEC in the American sector at 17 UT (Fig. 3.2a) and at 21 UT (Fig. 3.2b). In addition, different percentile estimates obtained from these 79 days of data (for example, difference between 10-th and 90-th percentiles or 25-th and 75-th percentiles) enabled quantitative description of typical ionospheric variability during dynamically quiet conditions.

2.1.3 Background TEC: empirical model

To separate effects of meteorological or other types of forcing from known effects of solar, geomagnetic activity, and seasonal change, we have developed an empirical model of TEC in the American sector at 75°W based on 15 years of data (2000 - 2015). The model describes TEC variation as a function of solar flux, season, and

geomagnetic activity through a multiple linear regression fit of the observed TEC to time series of solar flux proxies, seasonal oscillations, geomagnetic activity indices (with multiple delays), and cross-modulation of these terms. Explicitly, the model is formulated as follows:

$$TEC(t, DOY) = TEC_0 + TEC_{sol}(t) + TEC_{seas}(DOY) + TEC_{geo}(t) + TEC_{cr-terms}(t, DOY), \tag{2.1}$$

where

$$TEC_{sol}(t) = b_1 PF_{107}(t) + b_2 PF_{107}^2(t); \tag{2.2}$$

$$TEC_{seas}(DOY) = \sum_{m=1}^{m_{seas}} c_m \sin\left(\frac{2\pi DOY m}{365}\right) + d_m \cos\left(\frac{2\pi DOY m}{365}\right); m = 1, 2 \tag{2.3}$$

$$TEC_{geo}(t) = \sum_{l=0}^{l_{geo}} e_l Ap_3(t-l) + e_{l1} Ap_3^2(t-l_1); l = 0, 3, 6, 9, \, hours; \, l_1 = 0 hours \tag{2.4}$$

$$TEC_{cr-terms}(t, DOY) = f_1 PF_{107}(t) \sin\left(\frac{2\pi DOY}{365}\right) + f_2 PF_{107}(t) \cos\left(\frac{2\pi DOY}{365}\right) \tag{2.5}$$

This formula includes a dependence on a solar flux proxy $PF107 = (F10.7 + F10.7_{81ave})$, where $F10.7$ and $F10.7_{81ave}$ are solar flux for the previous day and 81-day average, respectively, a seasonal variation as a function of day of year (DOY), a dependence on current and previous geomagnetic activity (terms with $Ap3$, where $Ap3$ is a current geomagnetic activity index, $Ap3_{-3}$ is geomagnetic activity during previous 3 hours, etc.). Terms with coefficients f_1 and f_2 represent cross-terms between solar flux and seasonal variations. All coefficients are determined through a multiple linear regression fit to available data. We note that for GNSS TEC data such coefficients are obtained independently for every 1 degree in latitude and for every hour, thus avoiding potential artificial features that can be introduced by fitting with 24hr, 12hr, and 8hr tides. Subtracting the empirical model prediction from the data produces residuals that cannot be directly driven by influences of seasonal change, solar activity, and geomagnetic activity, and contains the potential influence of meteorological origin. Figure 2.2 illustrates the use of the model for a case study of major SSW that occurred in January 2013 and compares expected TEC as provided by the empirical model (top panel) with GNSS TEC observations (middle panel). Data-model differences (bottom panel) are observed in the large range of latitudes and during both daytime and nighttime.

2.2 Peak Electron Density N_mF_2 from Ionosondes

To obtain independent validation of ionospheric anomalies during SSW from different observational technique, we use ionosonde data at several selected locations and the same modeling approach as described for TEC modeling in Section 2.1.3. Ionosonde data is obtained from the GIRO database (Reinisch and Galkin, 2011) or, in case of Vernadsky station, from collaborators. Goncharenko et al. (2018) includes more details on the performance of empirical models and concludes that the local

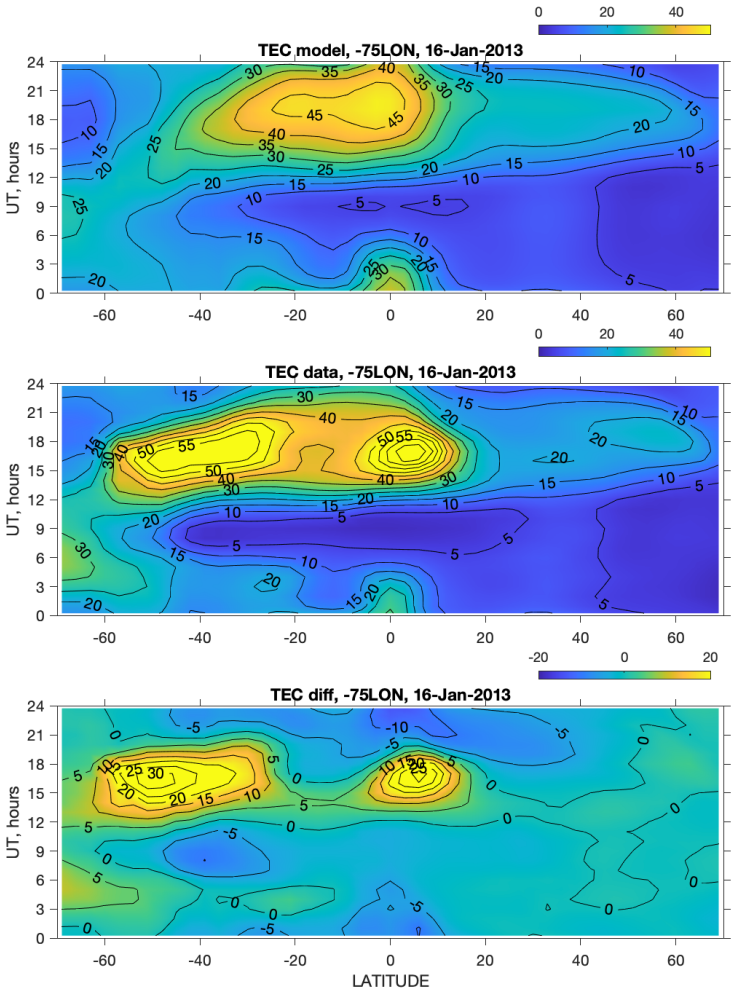

FIGURE 2.2: (top) TEC on January 16, 2013 (during a major SSW) along 75°W longitude as predicted by empirical model; (middle) TEC observations for January 16, 2013; (bottom) data-model difference in TECu. Highly anomalous TEC values are observed from low-latitude Northern Hemisphere to high latitudes of the Southern Hemisphere.

empirical models provide an accurate description of the mean state for various ionospheric features and can serve as the climatological specification of the ionosphere in the American longitudinal sector during the November-March period.

2.3 Thermospheric Composition from TIMED GUVI

We use observations of column O/N_2 ratio ($\sum O/N_2$) by the Global Ultraviolet Imager (GUVI) onboard the Thermosphere, Ionosphere, Mesosphere Energetics, and Dynamics (TIMED) satellite (Strickland et al., 1995; Paxton et al., 2021) to examine whether anomalous O/N_2 variations can be attributed to the SSW of September 2019 (Chapter 4. Background thermospheric O/N_2 is calculated as a median value of all observations collected from 2008-2018, 2020 for low solar flux conditions (F10.7 < 80), low geomagnetic activity (Ap for the current day and previous day < 13), and

centered on September 15 +/- 10 days, in consistency with approach for TEC data described in the Section 2.1.2.

2.4 Stratospheric Winds and Temperature from MERRA-2

The Modern-Era Retrospective analysis for Research and Applications, Version 2 (MERRA-2) temperature and horizontal wind data (Bosilovich, 2015) are used in Chapters 3, 4, and 5 and relevant publications to quantify the background stratospheric and lower mesospheric winds and to demark the stratospheric polar vortex. The stratospheric vortex is identified by employing the method of Harvey et al. (2002). MERRA-2 is provided 4 times daily from the surface to 75 km, at 0.5 degree latitude by 0.625 longitude resolution, and is available 1980 to the present.

2.5 Stratospheric and Mesospheric Temperature from Aura MLS

The Earth Observing System Aura Microwave Limb Sounder (MLS) (Waters et al., 2006) daily global temperature, geopotential height, and derived horizontal wind observations are used in Chapters 3, 4, and 5 to characterize temperature and winds changes from stratosphere up to the lower thermosphere and compute PW amplitudes, phases, and periods up to mesopause altitudes. Data is available for 2004-2023, and covers all longitudes in a near-polar orbit. This data is sufficient for deriving PW attributes (Yamazaki et al., 2020).

2.6 Polar Mesospheric Cloud Frequency from AIM CIPS

Polar mesospheric cloud (PMC) frequencies are derived from measurements made by the Cloud Imaging and Particle Size (CIPS) instrument (McClintock et al., 2009), which is a nadir-viewing panoramic imager that measures scattered radiation at 265 nm. CIPS was launched in 2007 aboard the Aeronomy of Ice in the Mesosphere (AIM) satellite, and was operational until March 2023. CIPS provides high resolution images of PMC albedo near the summer polar mesopause every day over the entire summer polar cap (Lumpe et al., 2013). This work uses the v5.20r05 level 3c data, which has a spatial resolution of 56 km^2. Variations of PMC frequency are used in Goncharenko et al. (2022) and Chapter 5 as additional indicator of Antarctic summer mesopause temperature changes during Arctic SSW.

Chapter 3

Effects of Antarctic SSW in the low-latitude ionosphere

Summary of:

Goncharenko, L. P., Harvey, V. L., Greer, K. R., Zhang, S.-R., Coster, A. J. (2020). Longitudinally dependent low-latitude ionospheric disturbances linked to the Antarctic sudden stratospheric warming of September 2019. Journal of Geophysical Research: Space Physics, 125, e2020JA028199. https://doi.org/10.1029/2020JA028199.

3.1 Introduction

Due to larger planetary waves (PWs) in the Northern Hemisphere (NH) winter as compared to the Southern Hemisphere (SH) winter, Arctic SSWs (e.g., Charlton and Polvani, 2007) are far more common than their Antarctic counterparts (Krüger et al., 2005). An outstanding question is whether Antarctic SSWs can produce similar disturbances in the ionosphere-thermosphere system as Arctic SSWs. As Antarctic SSWs occur much less frequently, only one major SSW was ever recorded, in September 2002, and only several minor SSWs occurred in the satellite era. Ionospheric perturbations during Antarctic SSW of September 2002 included enhanced quasi-two-day oscillations and perturbations consistent with lunar tide (Olson et al., 2013), as well as quasi-10-day oscillations in TEC and location of crests of the Equatorial Ionization Anomaly (EIA) in the Asian sector (Mo and Zhang, 2020). However, both studies noted that enhanced geomagnetic activity during that period complicated the interpretation of the ionospheric observations.

A renewed opportunity to investigate how the ionosphere and thermosphere react to Antarctic SSWs has emerged with the strong minor SSW that occurred over Antarctica in September 2019 (Lim et al., 2020). Yamazaki et al. (2020) examined middle atmospheric observations alongside the ionospheric equatorial electrojet and the topside electron density from the Swarm satellites and reported strong quasi-6-day variations in all parameters during this SSW. Specifically, these variations reached 20-40% for the topside electron density and 5-10% for the topside TEC and were observed simultaneously with 6-day wave activity in the lower thermosphere.

The main objective of this study is to examine ionospheric TEC and attribute anomalies in ionospheric TEC patterns to the Antarctic SSW. This study reports SSW-induced TEC anomalies and their variation as a function of latitude, longitude, and local time, thus presenting different characteristics of ionospheric changes related to the Antarctic SSW of September 2019.

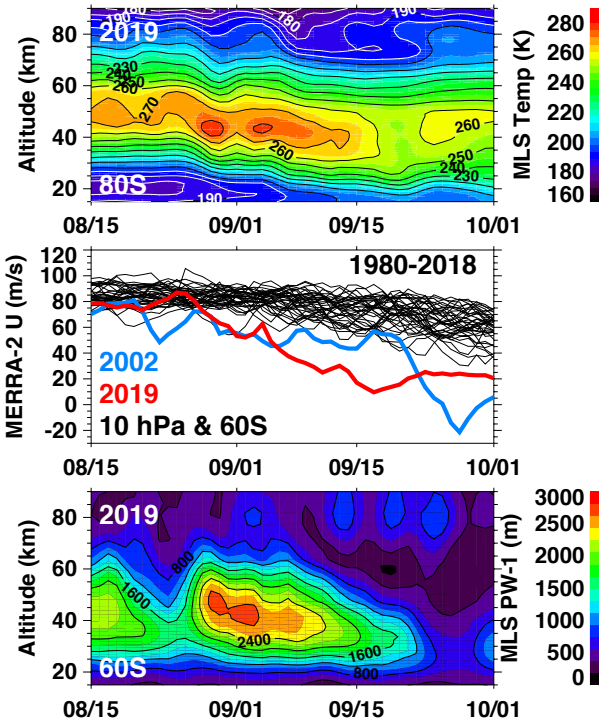

FIGURE 3.1: Time series from 15 August to 1 October 2019 of (top) zonal mean MLS temperatures at 80°S as a function of altitude, (middle) MERRA-2 zonal mean zonal wind at 60°S and 10 hPa for 1980-2018 (black lines) highlighting 2002 (blue) and 2019 (red), and (bottom) MLS planetary wave 1 amplitude at 60°S in 2019.

3.2 Stratospheric and Mesospheric Observations

Figure 3.1 presents an overview of the meteorological conditions in the stratosphere and mesosphere from 15 August to 1 October 2019. The minor SSW is characterized by the descent of the stratopause from 55 km in late August to 40 km in mid-September (top panel). As expected, there is simultaneous cooling in the polar mesosphere. The mesospheric response is most apparent in mid-September, at the same time the zonal winds are weakest (middle panel, red line). The observed vortex weakening in the second week of September is unprecedented in the 40-year data record. During this time the jet encircling the Antarctic vortex is even weaker than during the notorious vortex split year of 2002 (middle panel, blue line). The strong minor SSW and weak polar vortex in the Antarctic in 2019 are driven by large amplitude PWs, as evidenced in the bottom panel of Figure 3.1. Of particular relevance to this work is the PW response in the mesosphere between 70 and 90 km in mid-September. Given the timing of the SSW and mesospheric cooling and the PW activity in the stratosphere and mesosphere, we expect to see largest effects in the thermosphere and ionosphere in mid-September.

3.3 Ionospheric observations

3.3.1 American longitudinal sector

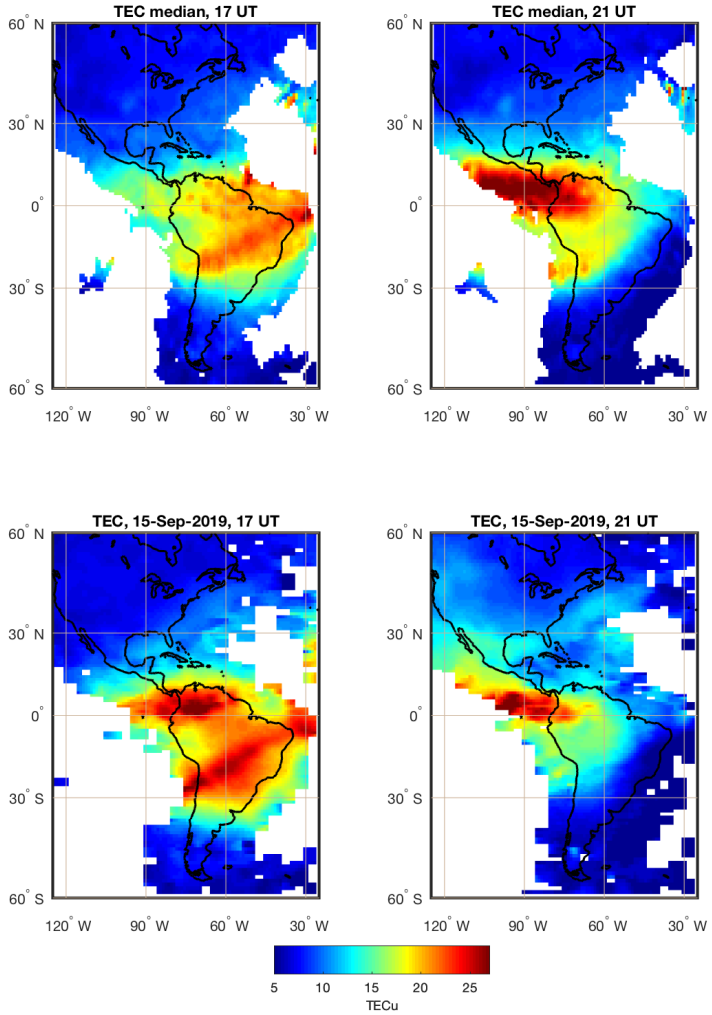

FIGURE 3.2: Maps of TEC over the American sector for low solar, geomagnetic, and stratospheric PW activity levels (top) and for 15 September 2019 (bottom). Left panels show TEC at 17 UT (noon in LT at 75°W), and right panels show TEC at 21 UT (afternoon sector at 75°W). Enhancement of TEC in the noon-time sector on Sep 15, 2019 is followed by a strong depletion several hours later. This behavior is similar to TEC variations observed during Arctic SSW events and is driven by strong enhancements in tidal amplitudes during SSW.

Figure 3.2 compares the median, e.g. 'dynamically quiet state' TEC (as described in Section 2.1.2 in the American sector around noontime (Fig. 3.2a, 17 UT) and afternoon (Fig. 3.2b, 21 UT), with observations during Antarctic SSW on September 15, 2019 during the same time, 17 UT (Fig. 3.2c) and 21 UT (Fig. 3.2d). Large increases in TEC are observed at 17 UT during the SSW, with enhancements in both crests of the EIA, while the opposite behavior is observed several hours later, at 21 UT, with suppression of both crests of EIA. Similar quasi-semidiurnal deviations in TEC in the low-latitude ionosphere in the American sector have been previously reported to occur during Arctic SSW events (Goncharenko et al., 2010a, see their Figure 1). The mechanism driving this quasi-semidiurnal ionospheric variability is amplification of

tidal amplitudes in the lower thermosphere (Liu et al., 2010; Jin et al., 2012; Pedatella et al., 2014). Anomalous tides modulate electric fields through the E-region dynamo process, modify F-region vertical drifts and, subsequently, F-region electron densities. Although the roles of different mechanisms and different tides are a matter of active research (see reviews by Chau et al., 2012 and Goncharenko et al., 2021b), similar quasi-semidiurnal behavior was observed in multiple ionospheric parameters and during multiple Arctic SSW events, both major and minor. We thus conclude that a minor Antarctic SSW of September 2019 causes quasi-semidiurnal perturbations in the low-latitude ionosphere in a manner similar to Arctic SSW events.

3.3.2 Longitudinal dependence of SSW effects

The ionospheric response to the Antarctic SSW is both hemispheric in scale and regional in strength of specific features; in other words, qualitatively similar large-scale low-latitude ionospheric anomalies are observed in different geographic sectors, but the strength of these anomalies is different. Figure 3.3 illustrates this point and presents TEC anomalies observed on 15 September 2019 and calculated as a difference between observations and median values and expressed as percent change from median. Around noontime, positive TEC anomalies are seen over the American, African, and Asian sectors, albeit with varying strengths. In the American sector, the largest anomalies are observed in the areas several degrees poleward of the EIA crests, reaching 40-60% poleward of the northern crest of EIA and 60-80% poleward of the southern crest of EIA. Positive noontime anomalies are larger in the African sector where they reach 100%, while negative anomalies formed within 20^o latitude of the EIA trough. In contrast, in the Asian sector positive TEC anomalies are rather weak and do not exceed 20-30%. To summarize the ionospheric anomalies over the globe, the afternoon and nighttime anomalies are more consistent between different geographic sectors and show predominant suppression of TEC which is stronger in the African and Asian sectors. These negative anomalies could result from a superposition of several mechanisms: a negative phase of a quasi-semidiurnal perturbation, general decrease of a thermospheric O/N_2 ratio related to the dissipation of enhanced tides (Yamazaki and Richmond, 2013; Oberheide et al., 2020), and perturbations in upper thermospheric winds that could contribute to the night-time anomalies (Pedatella and Maute, 2015; Goncharenko et al., 2018).

One of the important distinctive features of this SSW is the fact that ionospheric anomalies are highly dynamic, with their phenomenology strongly varying from one day to another. This contrasts with typical TEC anomalies during Arctic major and minor SSW events where similar quasi-semidiurnal (Goncharenko et al., 2010b; Fagundes et al., 2015) or negative disturbances (Vieira et al., 2017) last for multiple days. A plausible cause for the lack of persistence in quasi-semidiurnal anomalies during September 2019 SSW is the co-occurrence of a very strong quasi 6-day wave.

Figure 3.4 demonstrates another important aspect of ionospheric anomalies observed in September 2019: their phenomenology is different for geographic locations separated by as little as 30 degrees in longitude. It depicts TEC variations in the northern crests of EIA in the African sector at 0^oE and 30^oE (Figures 3.4a and 3.4b) and in the Asian sector at 115^oE and 145^oE. The most dramatic differences between close longitudes are observed in the African sector (Figures 3.4a and 3.4b). The median TEC and quiet dynamic state variability (TEC variation between 10-th and 90-th percentiles) are significantly higher at 0°E than at 30°E. During the Antarctic SSW

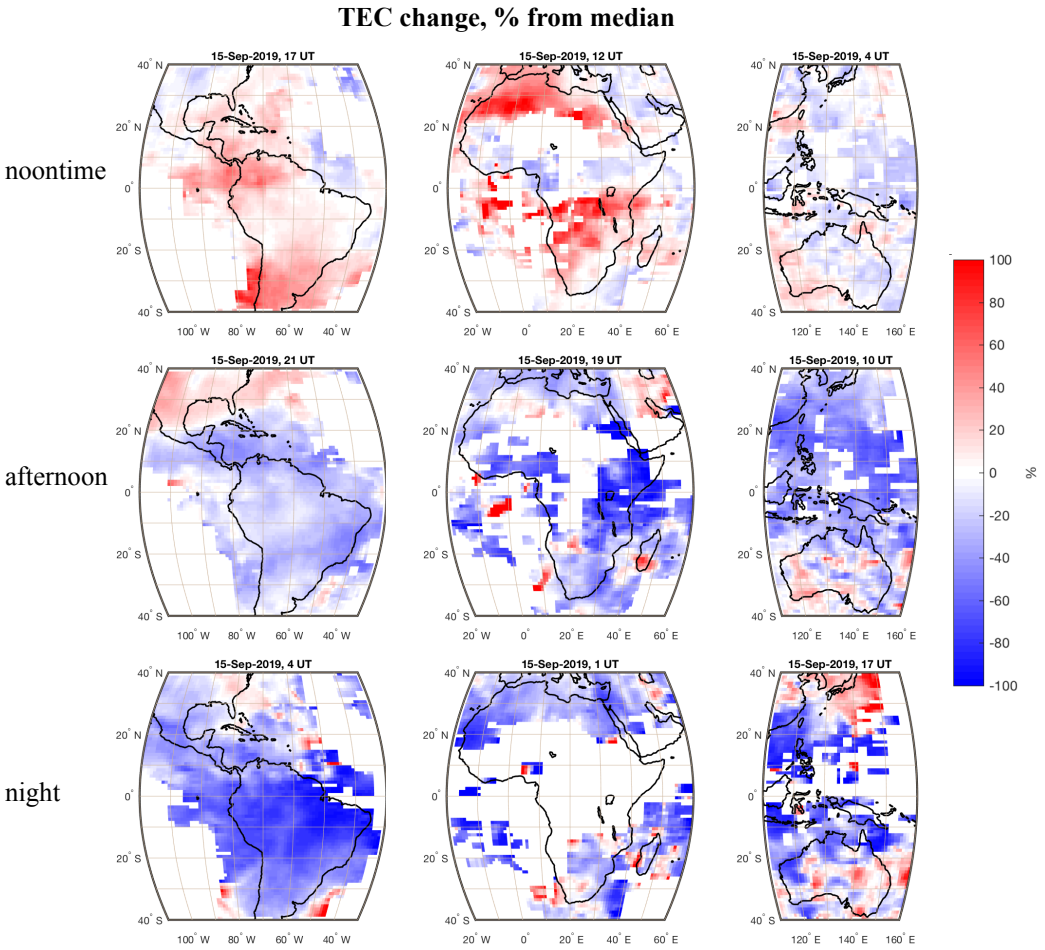

FIGURE 3.3: Change in TEC during Antarctic SSW on September 15, 2019 in different geographic regions and different local time sectors. Change is expressed as percentage from median values. Positive daytime anomalies are strongest in the African sector, but weak in the Asian sector. Negative anomalies in the afternoon and nighttime are more uniform for different geographic regions.

of September 2019, observations reveal increase in TEC above 75-th and 90-th percentiles or suppression below 25-th and 10-th percentiles at both longitudes in the African sector. However, the magnitude of these disturbances is higher at 0°E than at 30°E. Similar longitudinal differences are observed in the Asian sector, as illustrated by Figures 3.4c (115°E) and 3.4d (145°E): longitude with higher median TEC, such as 115°E, has higher quiet dynamic variability and higher disturbances during SSW of September 2019 in comparison with longitude with lower median TEC, such as 145°E. All four locations of EIA crests depicted in figure 3.4 show a mixture of tidal effects and daily mean TEC suppression during SSW, but these effects are stronger at longitudes with higher median TEC.

Longitudinal variations in ionospheric parameters are expected to arise for several different reasons. One set of reasons is related to purely geometric effects arising from the longitudinal differences between the geomagnetic and geographic equator and variations in the magnetic declination as a function of longitude (e.g. England, 2012 and references therein). The longitudinal variation in the difference between the geographic and geomagnetic equator leads to the longitudinal variation in the distance between the region with largest photoionization near the sub-solar point of

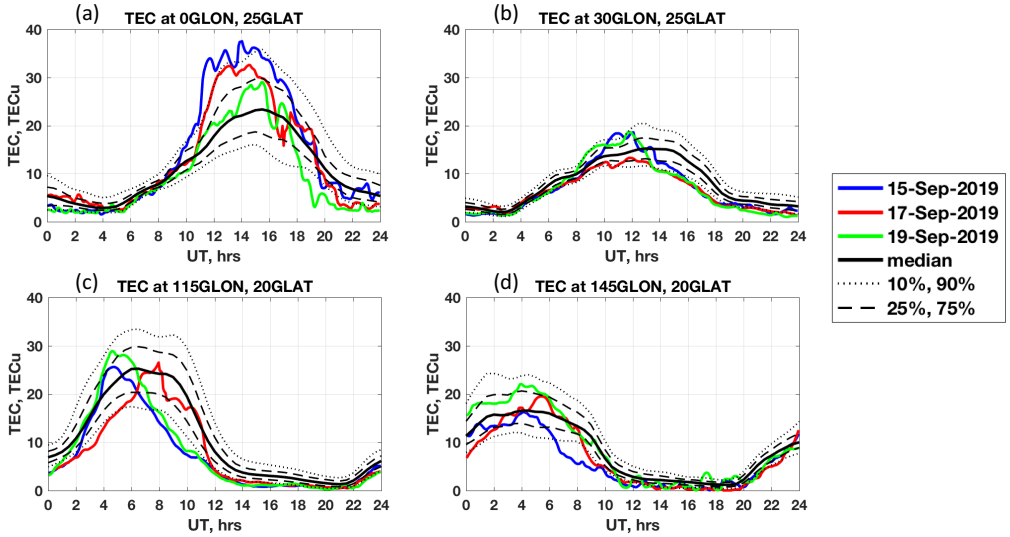

FIGURE 3.4: Variations in TEC during Antarctic SSW in the northern crests of EIA over African sector, panels (a) and (b), and Asian sector, panels (c) and (d).

minimum solar zenith angle and the region of EIA trough as the plasma source of EIA. This reason could contribute to the observed longitudinal differences in TEC in the American sector, but could not be responsible for the observed differences in the African and Asian sectors (Figure 3.4). The longitudinal variation in the magnetic declination changes the angle between the neutral winds and geomagnetic field and, consequently, transport of ionospheric plasma. Effects of varying declination angle for locations separated by 30 degrees in longitude are expected to be strongest in the low-latitude American sector, but weaker in the African and Asian sectors. Thus, geometric effects related to the offset between geographic and geomagnetic equator and declination angle variations could not be a leading cause of the observed longitudinal TEC variations in the African and Asian sectors.

Previous studies concluded that non-migrating tides, in particular non-migrating DE3 (diurnal eastward propagating with zonal wavenumber 3) tide can be a major driver of a 4-peak structure in the longitudinal variation in low-latitude ionospheric electron density (Lin et al., 2007; Kil et al., 2007; Scherliess et al., 2008). Amplitudes of DE3 tide reach their seasonal peaks in September in the lower thermosphere (Akmaev et al., 2008) and throughout the thermosphere (Oberheide et al., 2009). Consequently, the wavenumber-4 signature is expected to be strong in the low-latitude ionosphere in September 2019. Longitudes of higher and lower TEC reported in this study are consistent with longitudinal variations in ionospheric parameters related to DE-3 tide (England et al., 2006; Kil et al., 2008; Scherliess et al., 2008). TEC observations presented in Figure 3.4 strongly suggest that observed longitudinal variations are related to the DE3 tide, and not only for 'dynamically quiet state', but also for the SSW conditions. Moreover, we suggest that Antarctic SSW of September 2019 led to the strong amplification of DE3 tide and, subsequently, to large longitudinal variation in ionospheric perturbations caused by SSW. Previous numerical simulations suggested that modification of semidiurnal non-migrating tides could contribute to ionospheric changes during Arctic SSWs (Pedatella and Forbes, 2010; Fuller-Rowell et al., 2010; McDonald et al., 2015). McDonald et al. (2018) suggested that interference of non-migrating diurnal tides can be a major contributor to TEC enhancements

during Arctic SSW, even without enhanced amplitudes. To the best of our knowledge, our study presents first observational evidence of ionospheric changes that could be related to the amplification of DE3 tide during Antarctic SSW. Additional observational and numerical studies are needed to test our suggestion about SSW modification of DE3 tide.

Our analysis also suggests that large longitudinal variation in ionospheric effects during Antarctic SSW of September 2019 is also manifested in different planetary wave effects. In the American sector at 75°W, a large amplification in the TEC oscillations with a 5-8 day period is observed in the middle of September and coincides with decrease in stratospheric winds during Antarctic SSW. This 5-8 day wave is consistent with amplification in 5-6 day wave reported by Yamazaki et al. (2020). However, TEC observations at 115°E reveal a different behavior: an amplification with 2-3 day periods. Planetary waves are not expected to propagate to ionospheric altitudes directly, but can impact the upper atmosphere indirectly, through modulation of tides extending into upper thermosphere (Oberheide et al., 2009; Liu, 2016), through modulation of equatorial vertical plasma drifts modified by tides propagating to the lower thermosphere (Liu and Richmond, 2013), through changes in thermospheric composition related to tidal dissipation (Yamazaki and Richmond, 2013; Yue and Wang, 2014), or through modulation of gravity waves (Liu, 2016). Our observations of large longitudinal differences in planetary wave oscillations in TEC suggest that longitudes with higher median TEC and higher 'quiet dynamic state' variability are also more influenced by upward propagating stratospheric planetary waves, presumably through modulation of non-migrating tides or gravity waves. This suggestion needs to be further explored in more extended follow-up studies.

3.4 Summary

The rare Antarctic sudden stratospheric warming of September 2019 has provided a unique opportunity to examine whether stratospheric weather over Antarctica can produce ionospheric disturbances. Although the SSW of September 2019 is considered a minor event according to the standard WMO definition, it was associated with several record-breaking changes in the Southern Hemisphere stratosphere. We have examined TEC perturbations in the low-latitude ionosphere and have concluded the following:

1. Comparison of ionospheric TEC in mid-September of 2019 with 'dynamically quiet' mean behavior reveals prominent quasi-semidiurnal variations that are similar to variations associated with Arctic SSW. However, the semidiurnal behavior does not persist for an extended period of time and strongly varies with longitude, indicating that the ionosphere is likely more dynamically disturbed during this Antarctic SSW than during a typical Arctic SSW.

2. We identify both positive and negative ionospheric disturbances that exceed 90-th percentile (or decrease below 10-th percentile) of TEC values for 'dynamically quiet' September equinox and low solar flux conditions. In terms of absolute changes, TEC increased or decreased by up to a factor of 2 and more.

3. The observed TEC disturbances are consistent with several mechanisms previously identified for Arctic SSW events: perturbation of semidiurnal tides, enhanced disturbances with planetary wave periods, in particular the 5-6 day wave and the 2-day wave, and decrease in daily mean TEC that could result

from reduction in thermospheric O/N2 density ratio. The study also suggests new aspects that connect the stratospheric weather to the state of the ionosphere.

4. We demonstrate a strong longitudinal variation in the observed TEC disturbances, when qualitatively different behavior can be observed at locations separated by as little as 30 degrees in longitude.

5. Stronger TEC disturbances are observed at longitudes that correspond to higher electron density in response to variations in non-migrating diurnal eastward propagating (DE3) tide. We suggest that amplification of DE3 tide during SSW plays a major role in the observed ionospheric behavior.

6. Our results indicate that stratospheric weather can strongly influence the state of the ionosphere not only during December-February period (winter in the Northern Hemisphere), but also during September (equinox conditions).

Chapter 4

Effects of Antarctic SSW in the Northern Hemisphere Mid-Latitude Upper Atmosphere

Summary of:

Goncharenko, L. P., Harvey, V. L., Greer, K. R., Zhang, S.-R., Coster, A. J., and Paxton, L. J. (2021). Impact of September 2019 Antarctic Sudden Stratospheric Warming on Mid-Latitude Ionosphere and Thermosphere over North America and Europe. Geophysical Research Letters, 48, e2021GL094517. https://doi.org/10.1029/2021GL094517.

4.1 Introduction

One of the surprising features of ionospheric disturbances during Arctic SSWs is that the largest anomalies are seen not at the high or middle latitudes of the Northern Hemisphere (NH), but instead at low latitudes and middle latitudes of the Southern Hemisphere (SH). Low-latitude variations are better understood; both observational and modeling studies suggest that they are produced mainly through the vertical transport of plasma by enhanced electric field due to amplification of the E-region dynamo mechanism (Fang et al., 2012; Pedatella and Liu, 2013). In contrast, ionospheric variations at the SH middle latitudes have been much less studied and less understood. Limited observational evidence suggests that SSW-induced ionospheric perturbations at SH mid-latitudes can be large, reaching a factor of 2 in TEC (Fagundes et al., 2015) or N_mF2 data (Goncharenko et al., 2018). COSMIC observations during two Arctic SSW events also shows larger ionospheric variations in the SH middle latitudes, and TIME-GCM simulations suggested that the mechanism responsible for these disturbances is a modulation of thermospheric wind by an amplified semidiurnal lunar tide (Pedatella and Maute, 2015), which was particularly strong during these events (Forbes and Zhang, 2012). However, a composite analysis of Whole Atmosphere Community Climate Model with specified dynamics (SD-WACCM) indicated stronger amplification of semidiurnal tides in NH (Limpasuvan et al., 2016). This conclusion implies a stronger ionospheric response to Arctic SSWs in the NH, which contrasts with observational results discussed above.

Extension of SSW-induced ionospheric anomalies across the equator and to the middle latitudes of the opposite hemisphere and the mechanisms responsible for such anomalies are not fully understood. One of the reasons for this is the scarcity of observational data at SH middle latitudes. The record strong Antarctic SSW of September 2019 enables addressing the question of inter-hemispheric coupling during SSWs

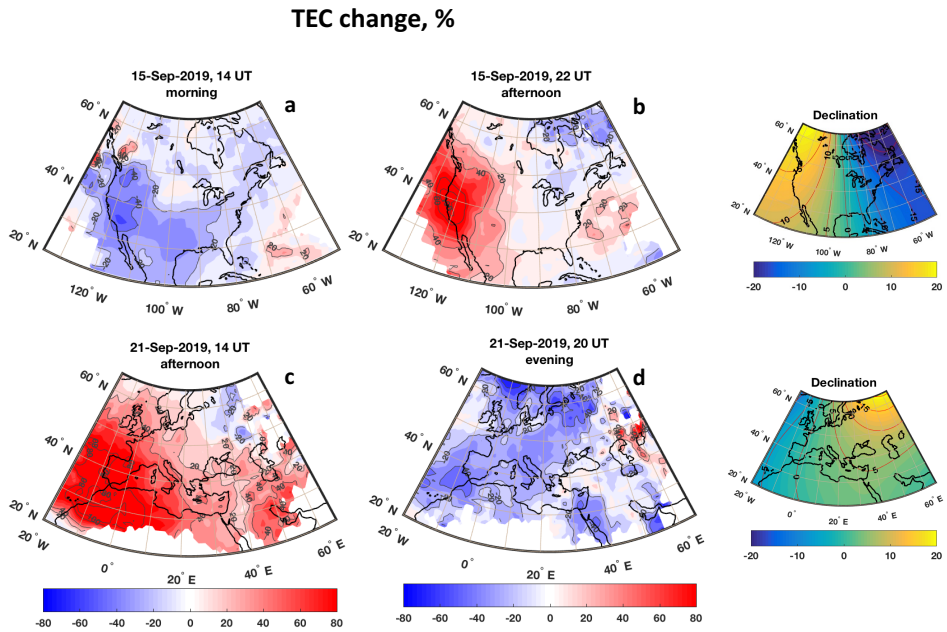

FIGURE 4.1: Ionospheric anomalies observed in September 2019. (a) and (b) Anomalies on September 15, 2019 over North America in the morning (14 UT) and afternoon (22 UT). (c) and (d) Anomalies over North Africa and Europe on September 21, 2019 in afternoon (14 UT) and in the evening (20 UT). Inlets on the right side show the magnetic declination angle over given regions.

with unprecedented detail, as there was an exceptional coverage at NH middle latitudes due to the dense networks of GNSS receivers (Figure 2.1). This study demonstrates that Antarctic SSW produces large anomalies in the middle latitude thermosphere and ionosphere in the NH and suggests mechanisms responsible for these anomalies.

4.2 Ionospheric anomalies

This study focuses on anomalies over North America and Europe, where TEC data quality is highest. To clearly identify effects of the SSW and separate them from ionospheric variations due to changes in solar cycle, season, and geomagnetic activity, we used the 'quiet dynamic state' baseline described in Section 2.1.2.

We hypothesize that the striking regional anomaly over the western U.S. is caused by an abatement or even reversal of the thermospheric zonal wind modified by the SSW, as zonal winds strongly influence ionospheric electron density in areas with larger magnetic declination angles (Zhang et al., 2011; Zhang et al., 2012). Figure 4.1 illustrates the spatial development of ionospheric anomalies at NH middle latitudes. Figures 4.1a and 4.1b show TEC anomalies over North America on September 15, 2019 during morning (14 UT) and afternoon (22 UT) hours, respectively. Anomalies are expressed as a percentage change relative to the quiet time baseline. In the morning sector (Figure 4.1a), the prevailing change is a decrease of TEC by 20-40%, with largest decreases over southern California (110-125°W, 30-50°N). In the afternoon sector (22UT, Figure 4.1b), the most striking feature is an increase up to 80-100% in

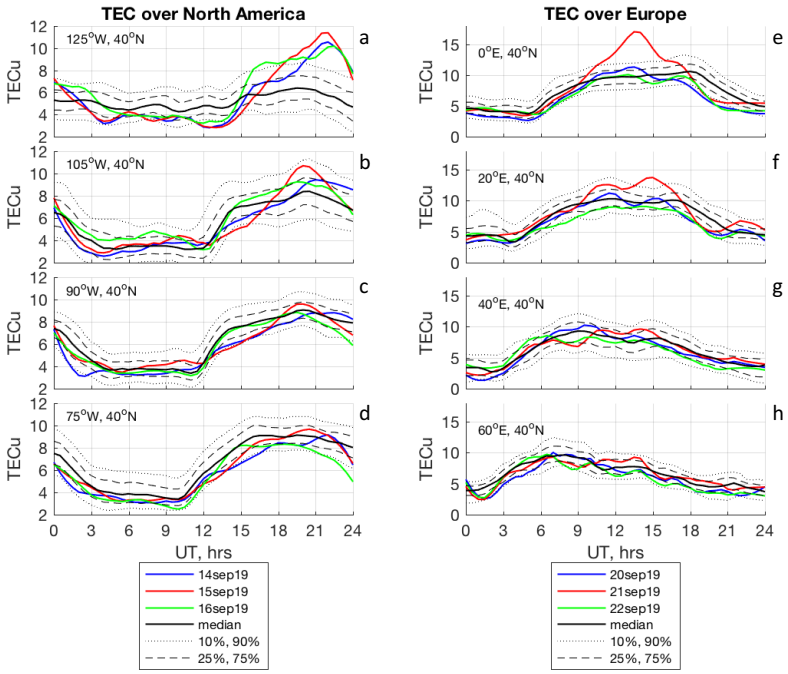

FIGURE 4.2: TEC variations at 40°N at different longitudes in comparison with baseline. Panels (a-d) show variations over North America on September 14-16, 2019. Panels (e-h) show variations over Europe on September 20-22, 2019. Thin dash lines show 25th and 75th percentiles and dotted lines show 10th and 90th percentiles to illustrate the level of typical quiet-time variability.

TEC observed at the same location. This positive daytime anomaly reaches its maximum at 40°N and is separated from low-latitude anomalies seen near the crests of the EIA (see Section 3 and Goncharenko et al., 2020); this indicates that the mechanism responsible for the generation of middle-latitude anomaly is different from the mechanisms driving the low-latitude anomalies. We suggest that the TEC variations observed over the western U.S. where the declination angle exceeds 10° (see inlets on the right side of Figure 4.1) could be generated by an enhanced semidiurnal tide in the zonal wind, with more eastward wind in the morning (providing downward plasma motion and faster recombination) and more westward wind in the afternoon (providing upward plasma motion and slower recombination).

The nature of TEC anomalies over Europe is very different, as illustrated in Figures 4.1c and 4.1d. The largest positive TEC anomalies over Europe are seen on September 15 and September 21, 2019 at 14UT (Figure 4.1c) reaching 100-120% from the baseline at 25-30°N, i.e. near the northern crest of the EIA. The magnetic equator is located at 10°N at these longitudes, and ionospheric disturbances at the EIA crests are likely driven by perturbations in vertical drifts and electric fields through the E-region dynamo. As the SSW of September 2019 is associated with a record strong quasi-6-day wave in the middle atmosphere (Yamazaki et al., 2020; Miyoshi and Yamazaki, 2020; Gu et al., 2021), the timing of the peak TEC anomalies on September 15 and September 21 indicates that they are linked to quasi-6-day oscillations that peak near the crests of EIA. Spectral analysis of TEC (not shown here) confirms the presence of oscillations with periods of 4-8 days in the extended latitudinal span in the European sector.

As geomagnetic activity often increases during equinox (Russell and McPherron, 1973; Lyatsky et al., 2001), our observations of ionospheric anomalies related to this Antarctic SSW illustrate the need to include lower atmospheric forcing in ionosphere and thermosphere studies to avoid incorrect attribution of drivers and mechanisms. The magnitude of the TEC disturbances observed at middle latitudes during this SSW event is comparable to positive and negative effects of geomagnetic storms (Buonsanto, 1999), although geomagnetic activity was quiet.

Another important result of this study is that large ionospheric anomalies are observed only in narrow longitudinal regions. Figure 4.2 compares the baseline (median) with TEC observations during September 14-16, 2019 over North America (left panels, Figures 4.2a-d) and during September 20-22, 2019 over Europe (right panels, Figures 4.2e-h). In the western part of the U.S. (Figure 4.2a) dramatic daytime (18-24 UT) increases in TEC exceed the 90th percentile of typical variability. Over the eastern U.S. (75°W, Figure 4.2d), the dominant signature is TEC suppression which is observed at most times of the day. We note large differences in the baseline TEC behavior (solid black line) between the western U.S. (125°W, Figure 4.2a) and the eastern U.S. (75°W, Figure 4.2d): daytime TEC is much larger over the eastern U.S. than over the western U.S., while nighttime TEC is higher over the western U.S. Such longitudinal differences in the baseline are produced by combined effects of thermospheric zonal winds and magnetic declination (Zhang et al., 2011; Zhang et al., 2012) and are at least partially responsible for the regional nature of the observed TEC anomalies.

The TEC variations over Europe (Figure 4.2e-h) are illustrated for September 20-22, 2019, around the time of the largest disturbances shown in Figure 4.1c. A sharp daytime peak on September 21 to highly anomalous TEC values (30% higher than the 90th percentile) was accompanied by a strong decrease in the afternoon. Similar to observations over North America, significant positive TEC variations are seen only in a narrow longitudinal band; this signature subsides toward the east (at 20°E), and no obvious disturbances are seen at 40°E or 60°E.

4.3 Thermospheric anomalies

Numerous simulations demonstrated that dissipation of upward propagating tides can affect vertical transport of atomic oxygen in the lower thermosphere that results in a reduction of thermospheric O/N_2 ratio and, in turn, can contribute to a depletion in electron density or TEC (Jones Jr et al., 2014b; Jones Jr et al., 2014a; Yamazaki and Richmond, 2013). Similarly, reduction in O/N_2 ratio and electron density is also expected due to the dissipation of gravity waves (Jones Jr et al., 2020) and planetary waves (Yue and Wang, 2014). However, observational evidence to support or challenge these simulations is scarce. We use TIMED/GUVI observations of column O/N_2 ratio (see Section 2.3) to examine whether the SSW of September 2019 leads to any anomalous O/N_2 variations. Figure 4.3 compares background O/N_2 (black) to O/N_2 observations on September 15, 2019 (red) as sampled along different orbits. The main difference between the background and SSW conditions seen at all longitude sectors is a 5-15% depletion in O/N_2 at low latitudes, 20°S to 20°N. This depletion is consistent with a 5-10% O/N_2 decrease in GOLD data during the Arctic SSW in January 2019 (Oberheide et al., 2020) and with numerical simulations cited above. It is likely to be produced by the changes in the residual mean circulation related to the dissipation of SSW-amplified tides and other waves. This decrease in the

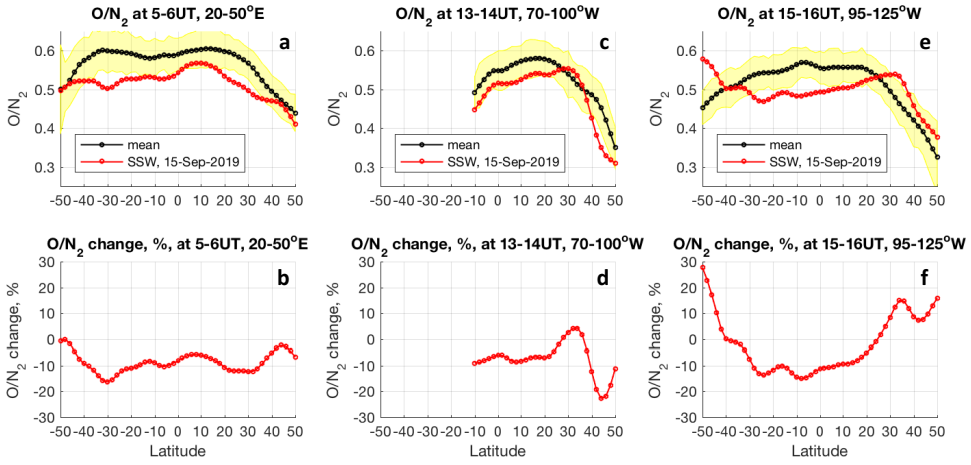

FIGURE 4.3: Evolution of thermospheric O/N_2 at different longitudes. Top panels (a, c, e) compare O/N_2 variations on September 15, 2019 (red) with background O/N_2 behavior (black). Yellow shade indicates 1σ variation. Bottom panels (b, d, f) show change in O/N2 on SSW day in comparison with the background.

low-latitude O/N_2 could contribute to a pronounced depletion of low-latitude TEC (Chapter 3), as changes in O/N_2 are well correlated with changes in TEC. However, at middle latitudes (30-50°S and 30-50°N) the O/N_2 change is more complex and depends on longitude. A decrease in O/N_2 seen at middle latitudes over Europe (Figure 4.3a, b) and the central and eastern U.S. (Figure 4.3c, d) likely contributes to TEC depletions that dominate ionospheric responses at these locations (Figure 4.2d, e, f). However, the O/N_2 anomaly becomes positive at middle latitudes over the western U.S. (Figure 4.3e, f), where an increase in the daytime TEC is observed (Figures 4.1b, 4.2e), and thus can contribute to the formation of positive ionospheric changes over this region.

4.4 Summary

Ionospheric observations in September 2019 provide evidence of large (50-100%) regional anomalies at middle latitudes of the northern hemisphere linked to the Antarctic sudden stratospheric warming. The ionospheric response has a quasi-semidiurnal behavior and is most likely driven by more than one mechanism, including variations in O/N_2 induced by dissipation of waves (tides, gravity waves, planetary waves), variations in plasma drift due to the E-region dynamo, and variations in thermospheric wind. The strongest responses are limited to narrow longitudinal areas with widths of 20-40°, while other longitudes experience similar types of perturbations but with magnitudes within typical day-to-day variability. Positive and negative anomalies over the western U.S. (100-130°W) persist for the entire month of September. Over Europe (20°W to 20°E) the dominating response is long-lasting TEC suppression superimposed on a quasi-6-day variation. Both positive and negative changes are observed in the thermospheric O/N_2 ratio and can contribute to regional increase and suppression of TEC. This study emphasizes the potential role of thermospheric zonal wind and magnetic declination in the formation of regional ionospheric disturbances at middle latitudes, in addition to the role of secondary waves generated through the interaction of quasi-6-day waves and tides.

Chapter 5

Observations of pole-to-pole, stratosphere-to-ionosphere connection

Summary of:

Goncharenko LP, Harvey VL, Randall CE, Coster AJ, Zhang S-R, Zalizovski A, Galkin I and Spraggs M (2022) Observations of Pole-to-Pole, Stratosphere-to-Ionosphere Connection. Front. Astron. Space Sci. 8:768629. doi: 10.3389/fspas.2021.768629

5.1 Introduction

Current knowledge of ionospheric physics is heavily influenced by observational data in the northern hemisphere, while the ionosphere above the sparsely instrumented southern hemisphere remains less understood. This study leverages instrumentation in South America and Antarctica to show that ionospheric variations at summer high latitudes may be attributed to SSW. Observations from independent techniques show a formation of large-scale mesospheric and ionospheric variations in response to the well documented major Arctic SSW of January 2013 (Goncharenko et al., 2013; Jonah et al., 2014; De Wit et al., 2015). These variations are observed not only at low latitudes, but at the middle and polar latitudes of the southern (opposite) hemisphere. The interhemispheric coupling concept (IHC, Becker et al., 2004) is well known in the middle atmosphere research community. It means that dynamic variability in the winter stratosphere is linked to variability of the polar upper mesosphere in the summer hemisphere. Here we demonstrate variability in the summer polar mesosphere and ionosphere over Antarctica induced by Arctic SSW, and extend the concept of interhemispheric coupling to the upper thermosphere and ionosphere.

5.2 Observations of TEC

In the American longitudinal sector evolution of TEC with latitude can be investigated in detail due to the dense network of GNSS receivers. Earlier studies reported that in response to the January 2013 SSW large low-latitude ionospheric disturbances peaked in mid-January (Goncharenko et al., 2013; Jonah et al., 2014). Figure 5.1A illustrates the latitudinal variation in the TEC anomaly at 75°W on January 16, 2013. The TEC anomaly is calculated as a difference between TEC observations and expected TEC behavior, which is provided by the empirical TEC model (see Section

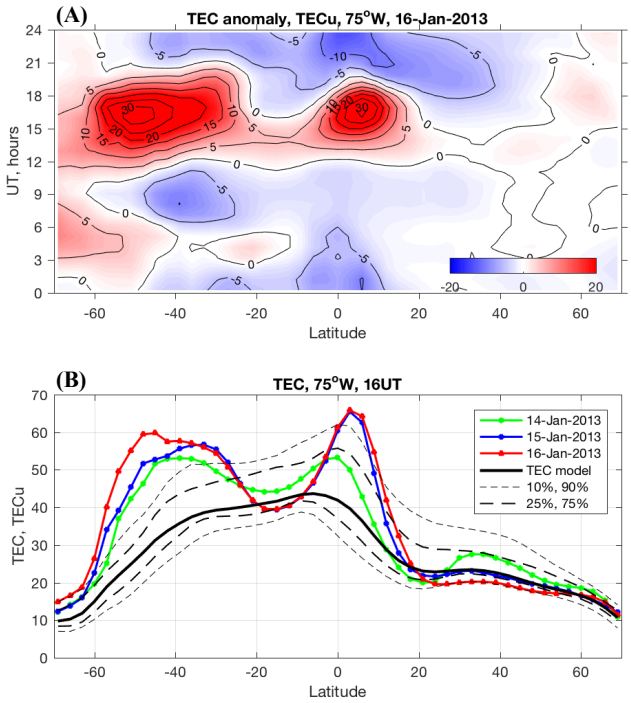

FIGURE 5.1: (A) Anomaly in the total electron content at 75°W on Jan 16, 2013 extends from equatorial to high latitudes of the southern hemisphere. (B) TEC variation with latitude for 75°W and 16 UT (11 AM Local Time). TEC values observed on January 14-16, 2013 (green, blue, red) are compared with TEC values expected for this season and solar activity as predicted by the empirical model (black).

2.1.3). The anomaly in TEC (Figure 5.1A) includes a well-known low-latitude features: large increase in the northern crest of the EIA, (0-15°N) in the morning-noon sector (12-18 UT) and a decrease in the afternoon and evening sectors (21-3 UT) (see reviews by Chau et al., 2012 and Goncharenko et al., 2021b).

Even larger morning-noon TEC anomaly develops in the southern hemisphere, centered at 40-60°S and extended to high latitudes, as seen in the Figure 5.1A. In addition to the morning-noon enhancement, nighttime (3-8 UT) electron density is also enhanced at latitudes higher than 45°S (Figure 5.1A); in particular, the ionospheric Weddell Sea Anomaly, a phenomenon when the nighttime electron density exceeds the daytime electron density (Penndorf, 1965; He et al., 2009), is modified during both nighttime and daytime hours, as seen in Figure 5.1A at 60-70°S. Figure 5.1B shows the latitudinal variation in TEC at 16 UT (11:00 AM local time) for three consecutive geomagnetically quiet days, 14-16 January 2013; similar TEC variations are observed over the 10-day period. Thick dash lines show 25th and 75th percentiles of all available data, thin dash lines show 10th and 90th percentiles. Percentiles were calculated using TEC observations with close solar flux and seasonal conditions. Continuous extension of TEC anomalies up to a factor of 2 from the expected value (and in excess of 75th and even 90th percentile) is observed from 20°S all the way to the high latitudes in the southern hemisphere. These results provide strong evidence that the impact of Arctic SSW is persistent for multiple days, global in scope, and extends across the equator up to high latitudes of the opposite hemisphere.

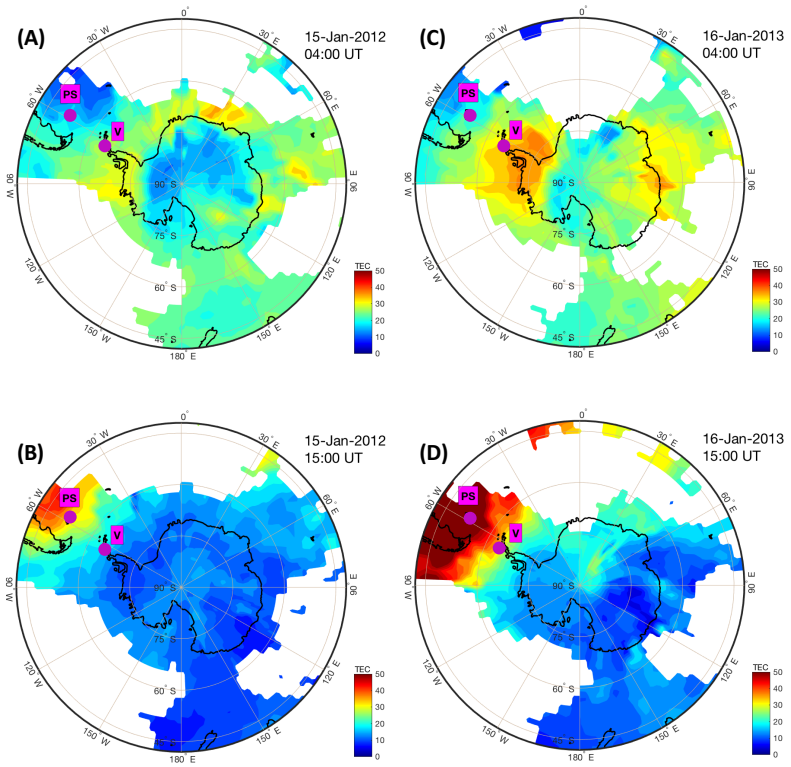

FIGURE 5.2: Southern hemisphere polar maps showing the TEC behavior during undisturbed Arctic conditions in January 2012 (left side, A and B) and during an SSW in January 2013 (right side, C and D). Top panels show snapshots at 4 UT and demonstrate increases in TEC over the entire Antarctic continent, with particularly large enhancement around the Antarctic Peninsula (30-120oW). Bottom panels (snapshot at 15 UT) demonstrate a strong increase in TEC from 60oE to 120oW, with largest increases in the American longitudinal sector. Magenta dots indicate the locations of the Port Stanley and Vernadsky ionosondes stations.

Figure 5.1 extends only to 70ºS, as empirical TEC model did not include higher latitudes due to the data scarcity. Figure 5.2 further illustrates extension of the observed ionospheric anomalies to the high latitudes in the southern hemisphere, up to the South Pole. Polar maps compare TEC distributions on 15 January 2012, an undisturbed Arctic winter day the previous year (panels A and B), to 16 January 2013, a SSW day (panels C and D). The TEC increase on 16 January 2013 (SSW day) at 4 UT is observed over the entire Antarctic continent, as seen in Figure 5.2C. The largest enhancements are over the Antarctic Peninsula and the Weddell Sea in the western hemisphere and near the Antarctic coast and 90ºE. At 15 UT (Figure 5.2D), increases in TEC over the Antarctic Peninsula and the Weddell Sea are clearly an extension of the TEC change that peaked in the middle latitudes of the southern hemisphere, as shown in Figures 5.1A and 5.1B. Ionospheric disturbances similar to those presented in Figures 5.2C and 3D were observed for several days and maximized on January 14-16, 2013, simultaneously with disturbances at lower latitudes seen in Figure 5.1.

5.3 Observations of $NmF2$

Independent confirmation of the impact of an Arctic SSW on the ionosphere over the middle and high latitudes of southern hemisphere is further obtained using

a different observational technique, namely ionosondes. Figure 5.3 shows diurnal variations in the peak electron density N_mF2 at mid- and high-latitude stations: Port Stanley (51.6ºS, 57.9ºW) and Vernadsky (65.1ºS, 64.2ºW), respectively. Typical diurnal variations of N_mF2 (black lines) at these locations are very different. Daytime N_mF2 (at 12-18 UT) over Port Stanley (Figure 5.3A) exceeds nighttime N_mF2 (at 1-6 UT) by 50-60%, as expected in the mid-latitude summer hemisphere, consistent with effects of maximum photo-ionization rates at noon and indicating that solar photo-ionization is the dominant mechanism responsible for N_mF2 behavior. In contrast to middle latitude, at high latitude over the Vernadsky location (Figure 5.3B) nighttime N_mF2 exceeds daytime N_mF2 by a factor of 2, as expected for the area of the Weddell Sea Anomaly. This behavior in typical N_mF2 indicates significant contributions to N_mF2 from ionospheric dynamics, including thermospheric neutral wind and E x B drift (Chen et al., 2011; Richards et al., 2017). During the SSW, similar ionospheric anomalies are observed at both locations: dramatic increases (up to a factor of 2) in N_mF2 during daytime hours (12-18 UT), weaker increases at night (1-6 UT), and a slight decrease in the morning hours (6-9 UT). These anomalies are fully consistent with the GNSS TEC observations shown in Figures 5.1 and 5.2. The similarity of the diurnal behavior in ionospheric anomalies in the geographic mid- and high-latitude southern hemisphere suggest that they could be driven by the same mechanism, despite very different mechanisms being responsible for the typical/climatological ionospheric behavior in these regions.

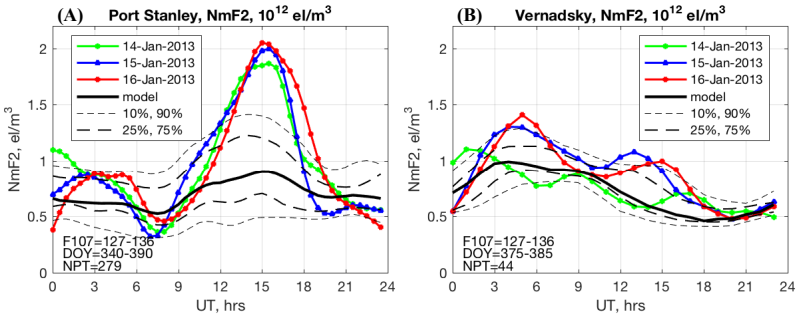

FIGURE 5.3: Variations in the peak electron density N_mF2 as measured by ionosondes at Port Stanley (A) and Vernadsky (B). Highly anomalous increases in N_mF2 are observed at both locations during the SSW, as illustrated with data from January 14-16, 2013.

5.4 Potential mechanisms

Our observations demonstrate that during the 2013 Arctic SSW event, an extended region of atmospheric anomalies formed in the southern hemisphere. This region spans the mesosphere (60–90 km) to the ionosphere (100–1000 km) in the vertical direction, summer mid-latitudes to the South Pole in the horizontal direction, and anomalies persists for days. The formation of such extended anomaly region in the southern hemisphere during the Arctic winter SSW presents a fascinating example of atmospheric coupling that is most likely driven by multiple mechanisms.

We suggest that SSW-associated semidiurnal variations in the upper thermospheric wind system is likely a leading mechanism responsible for large ionospheric disturbances in the high-latitude southern hemisphere during this SSW event, as variations in the meridional wind are an important driver of the Weddell Sea Anomaly

(Jee et al., 2009). At thermospheric altitudes, the wind changes could result from the superposition of migrating semidiurnal solar tides (SW2), non-migrating solar semidiurnal tides (SW1), and semidiurnal lunar tides (M1, M2). Earlier observations and simulations provide evidence of SSW-induced variations in all these tidal components. Superposition of these tidal components (SW2, SW1, M1, M2) of varying amplitudes and phases creates a complicated pattern of anomalies in the thermospheric wind and, consequently, in the ionosphere above Antarctica.

Additional potential mechanism involves changes in thermospheric composition. Miyoshi et al. (2015) found that Arctic winter SSW weakens the summer residual circulation between 80 km and 400 km, including decreased descent in the summer polar lower thermosphere and weakened ascent above 120 km. In general, upwelling decreases the O/N_2 ratio and tends to decrease ionospheric electron density (Rishbeth, 1998). Weaker upwelling in the upper thermosphere at high latitudes of the southern hemisphere predicted by Miyoshi et al. (2015) would result in a higher thermospheric O/N2 ratio and contribute to an overall increase in TEC over Antarctica. Such an increase is seen in Figure 5.1A as a general enhancement in TEC at 60-70ºS, which is observed in addition to the quasi-semidiurnal variation discussed above. The topic of changes in thermospheric composition has not been explored yet with sufficient detail and requires additional observational and modeling effort.

Finally, we cannot rule out the influence on ionospheric electron density that is produced by electric fields.Usually, electric fields are not expected to contribute significantly to variations in electron density at middle and high latitudes, due to the high inclination angle of the Earth's magnetic field lines closer to its poles. However, the inclination angle at high latitudes in the southern hemisphere (58º at Vernadsky) is smaller than in the northern hemisphere (for American longitudes), and an electric field can produce non-negligible electron density variations. Numerical simulations demonstrate significant perturbations in the mid-to-high latitude F-region vertical ion drift due to planetary waves at the model's lower boundary (Liu et al., 2010), so electric fields could be expected to play a certain role in the observed anomalies.

5.5 Summary

This study investigated the behavior of the mesosphere and ionosphere at high latitudes of the southern hemisphere during the Arctic SSW of January 2013. Stratospheric, mesospheric, and ionospheric data reveal anomalous behavior in multiple parameters during a multi-day period in January 2013 – neutral temperature, PMC frequency, TEC, and N_mF2. Persistent mesospheric and ionospheric anomalies that are observed above Antarctica in January 2013 may be related to the SSW in the Arctic stratosphere. These results provide strong observational evidence that SSW events generate truly global disturbances that reach the high latitudes of the opposite hemisphere; thus, this study extends the concept of inter-hemispheric coupling to polar ionosphere. A variety of mechanisms is proposed to interpret the observed atmospheric and ionospheric variations at middle and high latitudes in the southern hemisphere, but their relative importance is not known yet. This paper aims to encourage the scientific community to quantify the contributions of the different mechanisms proposed here, and to suggest or consider other mechanisms responsible for the mesospheric and ionospheric variability seen in the observations.

Chapter 6

Conclusion and Outlook

6.1 Thesis summary

This thesis, with three comprehensive studies at its core, is focused on understanding ionospheric and thermospheric variability linked to sudden stratospheric warmings, which are extreme disturbances in the high-latitude middle atmosphere that occur during the local winter season. The primary dataset to investigate the ionospheric state utilizes extensive, global coverage ionospheric total electron content obtained from GNSS receivers. We also use ionosonde data on peak electron density as a supporting dataset to characterize ionospheric variability, along with thermospheric composition (O/N_2) data to characterize thermospheric changes. In addition, we use a variety of middle atmosphere data gauging atmospheric parameters (winds, temperature, geopotential height, polar mesospheic clouds frequency) to identify the spatio-temporal evolution of disturbances from the stratosphere to the upper mesosphere.

The work described here builds upon 15+ years of previous effort in this research area and investigates several of the unsolved issues identified in a recent review on the topic (Goncharenko et al., 2021b). In particular, the thesis addresses the topics "How does the thermosphere-ionosphere system respond to less frequent SSW events occurring in the Southern Hemisphere?" and "How significant are longitudinal differences in ionospheric disturbances related to SSW, and what mechanisms drive these differences?". Understanding of the answers to these questions provides a new and incisive amount of information on SSW sources, forcing mechanisms, and atmosphere–ionosphere responses.

A very strong Antarctic SSW of September 2019 presented a perfect opportunity to address these topical issues, as that particular SSW occurred during a solar minimum and quiet geomagnetic activity. During this interval, ionospheric effects are easier to isolate, and observational resources from the stratosphere to the ionosphere are much more abundant than during an earlier major Antarctic SSW in 2002, that occurred almost 2 decades earlier with much more sparse coverage from e.g. GNSS derived TEC. In a common theme of these studies, a careful characterization of typical baseline ionosphere behavior is critical to isolating and quantifying SSW-driven anomalies. Accordingly, we developed and tested two methods (Chapter 2) to describe the baseline ionosphere, a 'dynamically quiet state' and local empirical ionospheric models for TEC and N_mF_2. We confirmed in detailed analysis that our results and findings are robust and do not depend on the selected method to describe baseline conditions.

In Goncharenko et al. (2020) (Chapter 3), we analyzed TEC variations during the Antarctic SSW of September 2019 at low latitudes and in different longitudinal sectors (American, African, and Asian), and isolated quasi-semidiurnal ionospheric perturbations that reach a factor of 2 in amplitude compared to the baseline state. The nature and magnitude of quasi-semidiurnal ionospheric perturbations is for the first time seen as very similar to perturbations during a typical Arctic SSW. In addition, analysis shows strong longitudinal differences in the observed perturbations as an important feature, since anomalies are strikingly different at locations separated by only 30 degrees in longitude. Our results thus demonstrate that stratospheric weather is a key driver of variability and can strongly influence the state of the ionosphere not only during December-February period (winter in the Northern Hemisphere), but also during September (equinox conditions).

In Goncharenko et al. (2021a) (Chapter 4), we extended study of the same Antarctic SSW of September 2019 to middle latitudes of the northern hemisphere, with focus on SSW-linked variability over North America and Europe. Quasi-semidiurnal perturbations in TEC that strongly exceed expected quiet-time variability are identified in narrow longitudinal regions on the western coast of US (100-130°W) and over Europe (20°W - 20°E). In addition, we identify both positive and negative disturbances in thermospheric composition that can contribute to the formation of ionospheric perturbations. Ionospheric and thermospheric perturbations are most likely driven by superposition of different mechanisms, including variations in O/N_2 induced by dissipation of waves (tides, gravity waves, planetary waves), variations in plasma drift due to the E-region dynamo mechanism, and variations in thermospheric wind. This study emphasizes in particular the potential significant role of thermospheric zonal wind and magnetic declination in the formation of regional ionospheric disturbances at middle latitudes, in addition to the role of secondary waves generated through the interaction of quasi-6-day waves and tides. The results indicate that these observed features form a complex spatio-temporal response to lower atmosphere forcing that is well beyond conventional, and often simplified, assumptions.

Finally, the Goncharenko et al. (2022) study (Chapter 5) extends the observational evidence of far-reaching impacts of variability in the polar vortex, demonstrating that large disturbances observed in the Arctic winter polar stratosphere (60–90°N) during a sudden stratospheric warming event are communicated across the globe and cause large disturbances in the summertime mesosphere and ionospheric plasma over Antarctica (60–90°S).

6.2 Thesis conclusions

In conclusion, these studies in aggregate highlight that stratospheric polar vortex is a key driver and an important source of predictability of the thermosphere-ionosphere system on a wide range of spatial and temporal scales. Impacts of stratospheric weather, most easily seen during large amplitude SSW–associated forcing, are regularly observed in the upper atmosphere and ionosphere from mid-latitudes in the winter hemisphere, across the equator and to polar regions of the summer hemisphere, and can be expected during both northern hemisphere and southern hemisphere winters. As polar vortex variations have long timescales and can be successfully predicted two weeks in advance (Domeisen et al., 2020), a comprehensive understanding of mechanisms connecting stratosphere, mesosphere, thermosphere

and ionosphere is not only scientifically productive but holds a tantalizing prospect of multi-day predictions of thermospheric and ionospheric parameters.

An additional key conclusion of these studies is that we cannot fundamentally understand the variability and response of the thermosphere and ionosphere without understanding the episodic forcing from below and the extent of the persistent response of the system. In essence, our ability to interpret ionospheric observations is limited by uncertainty about the behavior of underlying thermospheric parameters, in particular the precise details of altitude profiles of winds, composition, and neutral density. For these reasons, continuous, high-quality and high spatial resolution observations of mesospheric, thermospheric and ionospheric parameters must form an essential part of future community observational systems, as they are critical for the robust identification of essential features and understanding physical mechanisms responsible for their formation. Without these additional tools, progress in understanding mechanisms responsible for the observed ionospheric behavior will continue to be hindered by the lack of thermospheric observations with appropriate spatio-temporal resolution.

Ultimately, this work demonstrates that a sustained scientific focus on SSW events and their whole atmosphere response, using multiple tools, can and does form the basis of compelling and information-rich details on complex and fascinating variations in the upper atmospheric system. Efforts in these areas will continue to lead towards a better understanding of Earth atmospheric dynamics and its impacts on radio communication, propagation, and other societal infrastructure.

6.3 Suggestions for future research

Despite significant progress in understanding connections between the lower and upper thermosphere within the last 15+ years, there are a number of questions and topics that remain not answered and that form the basis of future studies. In addition to those questions outlined in Chapters 3, 4 and 5 and in recent reviews by Goncharenko et al. (2021b) and Forbes (2021), below we list several topics that will serve as the core of future studies to further illuminate the variety of mechanisms coupling different atmospheric layers and, hopefully, inspire new generation of scientists:

1. **Studies of polar vortex impacts on ionospheric and thermospheric variability on shorter temporal scales (gravity wave and traveling ionospheric disturbances)**: There is limited observational and modeling work to date that suggests suppression of gravity waves and traveling ionospheric disturbances during SSW and enhancement during strong polar vortex conditions (Becker et al., 2022a; Becker et al., 2022b; Harvey et al., 2023). Following up on these suggestions is essential to forward variability progress.

2. **Studies of SSW impacts on ionosphere on longer temporal scales (planetary wave scales)**: Several available studies have found that planetary waves with different periods (2-day waves, 5-6 day waves, 10-day waves) and zonal wave numbers can be amplified during SSW due to the variations in zonal mean wind. In the ionosphere, modulation on planetary wave time scales can be observed in a limited range of longitudes (Goncharenko et al., 2020). However, underlying reasons for these features are not completely understood. As oscillations on planetary wave time scales represent a large and important portion

of ionospheric variability, further exploration of these links represents a fruitful research direction.

3. **Studies of SSW impacts at middle and high latitudes**: Although increased upper atmospheric and ionospheric variability during SSW at middle and high latitudes was noted over a decade ago and is further explored in this thesis (Goncharenko et al., 2021a; Goncharenko et al., 2022), understanding of these links remains insufficient, as observational evidence is limited, perturbations most likely are driven by a constructive or destructive superposition of several mechanisms, and models have limited success in reproducing essential features of observations. Advancing progress and resolving these limitations is important for a full understanding of the middle (heavily populated) and high latitude ionospheric and upper atmospheric state.

4. **Links between SSW, night-time ionospheric state, and plasma bubbles and scintillations**: Earlier work documented a large-scale depletion during SSW in the nighttime ionosphere and suggested that SSW can affect development of equatorial spread F and plasma irregularities (Goncharenko et al., 2018). More recent whole atmosphere simulations and observations have indeed confirmed that nighttime ionospheric depletions are a robust feature during SSWs, at least in the American longitudinal sector, and that they result from tidal modifications of themospheric meridional wind (Jones Jr et al., 2023). Although several studies have attempted to link SSW to changes in the thermospheric wind system and than to the formation of plasma irregularities and scintillations (De Paula et al., 2015; Patra et al., 2014; Valladares et al., 2022), results are mixed to date. As plasma irregularities, scintillations and plasma bubbles are important space weather phenomena, further research in this area is important for numerous applications including transionospheric communications.

5. **Analysis of other minor Antarctic SSW events**: Beyond the September 2019 event described here, further studies are needed to explore repeatability of ionospheric features and responses at low and middle latitudes during SSW events located in the opposite hemisphere.

6. **Studies of ionospheric/thermospheric variability during strong polar vortex events:** A strong polar vortex event is an anomaly opposite to SSW, when stratospheric eastward winds remain abnormally strong. There have been very few studies of strong polar vortex events in general, and in particular very few studies of their manifestations in the thermosphere and ionosphere. Existing work suggests anomalies may occur opposite to SSW response studied to date, in the form of a suppression of tidal amplitudes (Pedatella and Harvey, 2022; Kumar et al., 2023) and a minor decrease in thermospheric composition. However, experimental observations demonstrate longitudinally dependent anomalies and include strong amplifications in thermospheric composition and ionospheric electron density (Greer et al., 2023). Resolving theory and observations for these conditions is a compelling future direction.

7. **Anomalies following sudden stratospheric warming events:** It is known that many SSW events are followed by long-lasting stratospheric anomalies of an opposite nature. For example, Figure 1.2 illustrates these conditions, as a record low stratospheric temperature in February and March 2019 occurred after a major SSW that peaked in early January 2019. These historically cold stratospheric conditions were also accompanied by strong eastward wind (e.g.

strong polar vortex state) lasting from mid-February to mid-April in a manner expected to affect upward propagation of planetary waves, tides, and gravity waves. However, such anomalies remain unexplored to date. Further study of these anomalies forms a scientifically rich avenue of exploration, and will illustrate the persistence and complexity of these tight atmosphere-ionosphere coupling processes.

8. **Other significant lower atmospheric phenomena (QBO, MJO):** In addition to SSW, a polar phenomenon in the stratosphere, there are several other lower atmospheric phenomena that potentially can influence the upper atmosphere. Some of them, like quasi-biennual oscillation (QBO) and semi-annual oscillation (SAO), occur in the tropical stratosphere. Others, like Madden-Julian Oscillation (MJO) and the El Niño-Southern Oscillation (ENSO), are linked to the ocean-atmosphere interactions. Although effects of such phenomena are very challenging to distinguish in the upper atmosphere, recent progress in data analysis and simulations demonstrated statistically significant response in tidal fields to MJO (Kumari et al., 2020) and ENSO (Liu et al., 2017; Sun et al., 2019). As these patterns regularly occur in the lower atmosphere, further investigations of these links hold a promise of better space weather predictability on sub-seasonal and seasonal scales.

Bibliography

Akmaev, RA, TJ Fuller-Rowell, F Wu, JM Forbes, X Zhang, AF Anghel, MD Iredell, S Moorthi, and H-M Juang (2008). "Tidal variability in the lower thermosphere: Comparison of Whole Atmosphere Model (WAM) simulations with observations from TIMED". In: *Geophysical Research Letters* 35.3.

Alexander, MJ, James R Holton, and Dale R Durran (1995). "The gravity wave response above deep convection in a squall line simulation". In: *Journal of the Atmospheric Sciences* 52.NAS 1.26: 202110.

Ayarzagüena, Blanca, David Barriopedro, JM Garrido-Perez, Marta Abalos, A de la Cámara, Ricardo García-Herrera, N Calvo, and C Ordóñez (2018). "Stratospheric connection to the abrupt end of the 2016/2017 Iberian drought". In: *Geophysical Research Letters* 45.22, pp. 12–639.

Baldwin, Mark P, Blanca Ayarzagüena, Thomas Birner, Neal Butchart, Amy H Butler, Andrew J Charlton-Perez, Daniela IV Domeisen, Chaim I Garfinkel, Hella Garny, Edwin P Gerber, et al. (2021). "Sudden stratospheric warmings". In: *Reviews of Geophysics* 59.1, e2020RG000708.

Baldwin, Mark P and Timothy J Dunkerton (2001). "Stratospheric harbingers of anomalous weather regimes". In: *Science* 294.5542, pp. 581–584.

Becker, E, A Müllemann, F-J Lübken, H Körnich, P Hoffmann, and M Rapp (2004). "High Rossby-wave activity in austral winter 2002: Modulation of the general circulation of the MLT during the MaCWAVE/MIDAS northern summer program". In: *Geophysical Research Letters* 31.24.

Becker, Erich, Larisa Goncharenko, V Lynn Harvey, and Sharon L Vadas (2022a). "Multi-step vertical coupling during the January 2017 sudden stratospheric warming". In: *Journal of Geophysical Research: Space Physics* 127.12, e2022JA030866.

Becker, Erich, Sharon L Vadas, Katrina Bossert, V Lynn Harvey, Christoph Zülicke, and Lars Hoffmann (2022b). "A high-resolution whole-atmosphere model with resolved gravity waves and specified large-scale dynamics in the troposphere and stratosphere". In: *Journal of Geophysical Research: Atmospheres* 127.2, e2021JD035018.

Bosilovich, Michael G (2015). *MERRA-2: Initial evaluation of the climate*. National Aeronautics and Space Administration, Goddard Space Flight Center.

Bossert, Katrina, Larry J Paxton, Tomoko Matsuo, Larisa Goncharenko, Komal Kumari, and Mark Conde (2022). "Large-Scale Traveling Atmospheric and Ionospheric Disturbances Observed in GUVI With Multi-Instrument Validations". In: *Geophysical Research Letters* 49.16, e2022GL099901.

Buonsanto, M Ji (1999). "Ionospheric storms—A review". In: *Space Science Reviews* 88.3-4, pp. 563–601.

Butler, Amy H, Andrew Charlton-Perez, Daniela IV Domeisen, Isla R Simpson, and Jeremiah Sjoberg (2019). "Predictability of Northern Hemisphere final stratospheric warmings and their surface impacts". In: *Geophysical Research Letters* 46.17-18, pp. 10578–10588.

Butler, Amy H, Dian J Seidel, Steven C Hardiman, Neal Butchart, Thomas Birner, and Aaron Match (2015). "Defining sudden stratospheric warmings". In: *Bulletin of the American Meteorological Society* 96.11, pp. 1913–1928.

Butler, Amy H, Jeremiah P Sjoberg, Dian J Seidel, and Karen H Rosenlof (2017). "A sudden stratospheric warming compendium". In: *Earth System Science Data* 9.1, pp. 63–76.

Chandran, A, RL Collins, and VL Harvey (2014). "Stratosphere-mesosphere coupling during stratospheric sudden warming events". In: *Advances in Space Research* 53.9, pp. 1265–1289.

Charlton, Andrew J and Lorenzo M Polvani (2007). "A new look at stratospheric sudden warmings. Part I: Climatology and modeling benchmarks". In: *Journal of climate* 20.3, pp. 449–469.

Chau, JL, BG Fejer, and LP Goncharenko (2009). "Quiet variability of equatorial E× B drifts during a sudden stratospheric warming event". In: *Geophysical Research Letters* 36.5.

Chau, Jorge L, Larisa P Goncharenko, Bela G Fejer, and Han-Li Liu (2012). "Equatorial and low latitude ionospheric effects during sudden stratospheric warming events: Ionospheric effects during SSW events". In: *Space Science Reviews* 168, pp. 385–417.

Chen, CH, JD Huba, A Saito, CH Lin, and JY Liu (2011). "Theoretical study of the ionospheric Weddell Sea Anomaly using SAMI2". In: *Journal of Geophysical Research: Space Physics* 116.A4.

De Paula, ER, OF Jonah, AO Moraes, EA Kherani, BG Fejer, MA Abdu, MTAH Muella, IS Batista, SLG Dutra, and RR Paes (2015). "Low-latitude scintillation weakening during sudden stratospheric warming events". In: *Journal of Geophysical Research: Space Physics* 120.3, pp. 2212–2221.

De Wit, Rosmarie Johanna, RE Hibbins, Patrick Joseph Espy, and Endre Asheim Hennum (2015). "Coupling in the middle atmosphere related to the 2013 major sudden stratospheric warming". In: *Annales geophysicae*. Vol. 33. 3. Copernicus GmbH Göttingen, Germany, pp. 309–319.

Domeisen, Daniela IV, Amy H Butler, Andrew J Charlton-Perez, Blanca Ayarzagüena, Mark P Baldwin, Etienne Dunn-Sigouin, Jason C Furtado, Chaim I Garfinkel, Peter Hitchcock, Alexey Yu Karpechko, et al. (2020). "The role of the stratosphere in subseasonal to seasonal prediction: 2. Predictability arising from stratosphere-troposphere coupling". In: *Journal of Geophysical Research: Atmospheres* 125.2.

England, SL (2012). "A review of the effects of non-migrating atmospheric tides on the Earth's low-latitude ionosphere". In: *Space science reviews* 168, pp. 211–236.

England, SL, S Maus, TJ Immel, and SB Mende (2006). "Longitudinal variation of the E-region electric fields caused by atmospheric tides". In: *Geophysical Research Letters* 33.21.

Esler, JG and N Joss Matthewman (2011). "Stratospheric sudden warmings as self-tuning resonances. Part II: Vortex displacement events". In: *Journal of the atmospheric sciences* 68.11, pp. 2505–2523.

Fagundes, PR, LP Goncharenko, AJ De Abreu, K Venkatesh, M Pezzopane, R De Jesus, M Gende, AJ Coster, and VG Pillat (2015). "Ionospheric response to the 2009 sudden stratospheric warming over the equatorial, low, and middle latitudes in the South American sector". In: *Journal of Geophysical Research: Space Physics* 120.9, pp. 7889–7902.

Fang, Tzu-Wei, Tim Fuller-Rowell, Rashid Akmaev, Fei Wu, Houjun Wang, and David Anderson (2012). "Longitudinal variation of ionospheric vertical drifts during the

2009 sudden stratospheric warming". In: *Journal of Geophysical Research: Space Physics* 117.A3.

Forbes, Jeffrey M (1995). "Tidal and planetary waves". In: *The upper mesosphere and lower thermosphere: A review of experiment and theory* 87, pp. 67–87.

– (2021). "Atmosphere-ionosphere (A-I) coupling by solar and lunar tides". In: *Upper atmosphere dynamics and energetics*, pp. 157–181.

Forbes, Jeffrey M, Sean L Bruinsma, Xiaoli Zhang, and Jens Oberheide (2009). "Surface-exosphere coupling due to thermal tides". In: *Geophysical Research Letters* 36.15.

Forbes, Jeffrey M, Scott E Palo, and Xiaoli Zhang (2000). "Variability of the ionosphere". In: *Journal of Atmospheric and Solar-Terrestrial Physics* 62.8, pp. 685–693.

Forbes, Jeffrey M and Xiaoli Zhang (2012). "Lunar tide amplification during the January 2009 stratosphere warming event: Observations and theory". In: *Journal of Geophysical Research: Space Physics* 117.A12.

Forbes, JM, X Zhang, W Ward, and ER Talaat (2002). "Climatological features of mesosphere and lower thermosphere stationary planetary waves within$\pm$40 latitude". In: *Journal of Geophysical Research: Atmospheres* 107.D17, ACL–1.

Fritts, David C, Ronald B Smith, Michael J Taylor, James D Doyle, Stephen D Eckermann, Andreas Dörnbrack, Markus Rapp, Bifford P Williams, P-Dominique Pautet, Katrina Bossert, et al. (2016). "The Deep Propagating Gravity Wave Experiment (DEEPWAVE): An airborne and ground-based exploration of gravity wave propagation and effects from their sources throughout the lower and middle atmosphere". In: *Bulletin of the American Meteorological Society* 97.3, pp. 425–453.

Fuller-Rowell, Tim, Fei Wu, Rashid Akmaev, Tzu-Wei Fang, and Eduardo Araujo-Pradere (2010). "A whole atmosphere model simulation of the impact of a sudden stratospheric warming on thermosphere dynamics and electrodynamics". In: *Journal of Geophysical Research: Space Physics* 115.A10.

Gan, Q, J Oberheide, L Goncharenko, L Qian, J Yue, W Wang, WE McClintock, and RW Eastes (2023). "GOLD Synoptic Observations of Quasi-6-Day Wave Modulations of Post-Sunset Equatorial Ionization Anomaly During the September 2019 Antarctic Sudden Stratospheric Warming". In: *Geophysical Research Letters* 50.12, e2023GL103386.

Garcia, Raphael F, Eelco Doornbos, Sean Bruinsma, and Hélène Hebert (2014). "Atmospheric gravity waves due to the Tohoku-Oki tsunami observed in the thermosphere by GOCE". In: *Journal of Geophysical Research: Atmospheres* 119.8, pp. 4498–4506.

Gasperini, Federico, McArthur Jones Jr, Brian J Harding, and Thomas J Immel (2023). "Direct observational evidence of altered mesosphere lower thermosphere mean circulation from a major sudden stratospheric warming". In: *Geophysical Research Letters* 50.7, e2022GL102579.

Goncharenko, L, JL Chau, P Condor, A Coster, and L Benkevitch (2013). "Ionospheric effects of sudden stratospheric warming during moderate-to-high solar activity: Case study of January 2013". In: *Geophysical Research Letters* 40.19, pp. 4982–4986.

Goncharenko, Larisa and Shun-Rong Zhang (2008). "Ionospheric signatures of sudden stratospheric warming: Ion temperature at middle latitude". In: *Geophysical Research Letters* 35.21.

Goncharenko, Larisa P, AJ Coster, S-R Zhang, PJ Erickson, L Benkevitch, N Aponte, VL Harvey, BW Reinisch, I Galkin, M Spraggs, et al. (2018). "Deep ionospheric hole created by sudden stratospheric warming in the nighttime ionosphere". In: *Journal of Geophysical Research: Space Physics* 123.9, pp. 7621–7633.

Goncharenko, Larisa P, V Lynn Harvey, Katelynn R Greer, S-R Zhang, and Anthea J Coster (2020). "Longitudinally dependent low-latitude ionospheric disturbances

linked to the Antarctic sudden stratospheric warming of September 2019". In: *Journal of Geophysical Research: Space Physics* 125.8, e2020JA028199.

Goncharenko, Larisa P, V Lynn Harvey, Katelynn R Greer, Shun-Rong Zhang, Anthea J Coster, and Larry J Paxton (2021a). "Impact of September 2019 Antarctic sudden stratospheric warming on mid-latitude ionosphere and thermosphere over North America and Europe". In: *Geophysical Research Letters* 48.15, e2021GL094517.

Goncharenko, Larisa P, V Lynn Harvey, Huixin Liu, and Nicholas M Pedatella (2021b). "Sudden Stratospheric Warming Impacts on the Ionosphere–Thermosphere System: A Review of Recent Progress". In: *Ionosphere dynamics and applications*, pp. 369–400.

Goncharenko, Larisa P, V Lynn Harvey, Cora E Randall, AJ Coster, S-R Zhang, A Zalizovski, I Galkin, and M Spraggs (2022). "Observations of pole-to-pole, stratosphere-to-ionosphere connection". In: *Frontiers in Astronomy and Space Sciences* 8, p. 768629.

Goncharenko, Larisa P, Cole A Tamburri, W Kent Tobiska, Samuel J Schonfeld, Phillip C Chamberlin, Thomas N Woods, Leonid Didkovsky, Anthea J Coster, and Shun-Rong Zhang (2021c). "A new model for ionospheric total electron content: The impact of solar flux proxies and indices". In: *Journal of Geophysical Research: Space Physics* 126.2, e2020JA028466.

Goncharenko, LP, JL Chau, H-L Liu, and AJ Coster (2010a). "Unexpected connections between the stratosphere and ionosphere". In: *Geophysical Research Letters* 37.10.

Goncharenko, LP, AJ Coster, JL Chau, and CE Valladares (2010b). "Impact of sudden stratospheric warmings on equatorial ionization anomaly". In: *Journal of Geophysical Research: Space Physics* 115.A10.

Goncharenko, LP, AJ Coster, R Alan Plumb, and Daniela IV Domeisen (2012). "The potential role of stratospheric ozone in the stratosphere-ionosphere coupling during stratospheric warmings". In: *Geophysical Research Letters* 39.8.

Gong, Yun and Qihou Zhou (2011). "Incoherent scatter radar study of the terdiurnal tide in the E-and F-region heights at Arecibo". In: *Geophysical Research Letters* 38.15.

Gong, Yun, Qihou Zhou, Shaodong Zhang, Nestor Aponte, and Michael Sulzer (2016). "An incoherent scatter radar study of the midnight temperature maximum that occurred at Arecibo during a sudden stratospheric warming event in January 2010". In: *Journal of Geophysical Research: Space Physics* 121.6, pp. 5571–5578.

Greer, Katelynn R, Larisa Goncharenko, V Lynn Harvey, and Nicholas Pedatella (2023). "Polar vortex strength impacts on the longitudinal structure of thermospheric composition and ionospheric electron density". In: *Journal of Geophysical Research: Space Physics* 128.9, e2023JA031797.

Gu, Sheng-Yang, Chen-Ke-Min Teng, Na Li, Mingjiao Jia, Guozhu Li, Haiyong Xie, Zonghua Ding, and Xiankang Dou (2021). "Multivariate analysis on the ionospheric responses to planetary waves during the 2019 Antarctic SSW event". In: *Journal of Geophysical Research: Space Physics* 126.3, e2020JA028588.

Hagan, ME, Astrid Maute, RG Roble, AD Richmond, TJ Immel, and SL England (2007). "Connections between deep tropical clouds and the Earth's ionosphere". In: *Geophysical Research Letters* 34.20.

Hall, Richard J, Daniel M Mitchell, William JM Seviour, and Corwin J Wright (2021). "Tracking the stratosphere-to-surface impact of sudden stratospheric warmings". In: *Journal of Geophysical Research: Atmospheres* 126.3, e2020JD033881.

Hardiman, Steven C, Neal Butchart, Andrew J Charlton-Perez, Tiffany A Shaw, Hideharu Akiyoshi, Andreas Baumgaertner, Slimane Bekki, Peter Braesicke, Martyn

Chipperfield, Martin Dameris, et al. (2011). "Improved predictability of the troposphere using stratospheric final warmings". In: *Journal of Geophysical Research: Atmospheres* 116.D18.

Harvey, V Lynn, R Bradley Pierce, T Duncan Fairlie, and Matthew H Hitchman (2002). "A climatology of stratospheric polar vortices and anticyclones". In: *Journal of Geophysical Research: Atmospheres* 107.D20, ACL–10.

Harvey, V Lynn, Cora E Randall, Scott M Bailey, Erich Becker, Jorge L Chau, Chihoko Y Cullens, Larisa P Goncharenko, Larry L Gordley, Neil P Hindley, Ruth S Lieberman, et al. (2022). "Improving ionospheric predictability requires accurate simulation of the mesospheric polar vortex". In: *Frontiers in astronomy and space sciences* 9, p. 1041426.

Harvey, VL, CE Randall, LP Goncharenko, E Becker, JM Forbes, J Carstens, S Xu, JA France, S-R Zhang, and SM Bailey (2023). "CIPS observations of gravity wave activity at the edge of the polar vortices and coupling to the ionosphere". In: *Journal of Geophysical Research: Atmospheres* 128.12, e2023JD038827.

Häusler, K, Hermann Lühr, ME Hagan, Astrid Maute, and RG Roble (2010). "Comparison of CHAMP and TIME-GCM nonmigrating tidal signals in the thermospheric zonal wind". In: *Journal of Geophysical Research: Atmospheres* 115.D1.

He, Maosheng, Libo Liu, Weixing Wan, Baiqi Ning, Biqiang Zhao, Jin Wen, Xin'an Yue, and Huijun Le (2009). "A study of the Weddell Sea Anomaly observed by FORMOSAT-3/COSMIC". In: *Journal of Geophysical Research: Space Physics* 114.A12.

Hocke, K, K Schlegel, et al. (1996). "A review of atmospheric gravity waves and travelling ionospheric disturbances: 1982–1995". In: *Annales geophysicae*. Vol. 14. 9, p. 917.

Holton, JR (1992). "An introduction to dynamic meteorology". In: *International geophysics series* 48, pp. 1–497.

Immel, TJ, E Sagawa, SL England, SB Henderson, ME Hagan, SB Mende, HU Frey, CM Swenson, and LJ Paxton (2006). "Control of equatorial ionospheric morphology by atmospheric tides". In: *Geophysical Research Letters* 33.15.

Jee, Geonhwa, AG Burns, Y-H Kim, and Wenbin Wang (2009). "Seasonal and solar activity variations of the Weddell Sea Anomaly observed in the TOPEX total electron content measurements". In: *Journal of Geophysical Research: Space Physics* 114.A4.

Jin, H, Y Miyoshi, D Pancheva, P Mukhtarov, H Fujiwara, and H Shinagawa (2012). "Response of migrating tides to the stratospheric sudden warming in 2009 and their effects on the ionosphere studied by a whole atmosphere-ionosphere model GAIA with COSMIC and TIMED/SABER observations". In: *Journal of Geophysical Research: Space Physics* 117.A10.

Jonah, Olusegun Folarin, ER De Paula, Esphan Alam Kherani, Severino Luiz Guimaraes Dutra, and Ricardo da Rosa Paes (2014). "Atmospheric and ionospheric response to sudden stratospheric warming of January 2013". In: *Journal of Geophysical Research: Space Physics* 119.6, pp. 4973–4980.

Jones Jr, M, Jeffrey M Forbes, and Maura E Hagan (2014a). "Tidal-induced net transport effects on the oxygen distribution in the thermosphere". In: *Geophysical Research Letters* 41.14, pp. 5272–5279.

Jones Jr, M, JM Forbes, ME Hagan, and Astrid Maute (2013). "Non-migrating tides in the ionosphere-thermosphere: In situ versus tropospheric sources". In: *Journal of Geophysical Research: Space Physics* 118.5, pp. 2438–2451.

– (2014b). "Impacts of vertically propagating tides on the mean state of the ionosphere-thermosphere system". In: *Journal of Geophysical Research: Space Physics* 119.3, pp. 2197–2213.

Jones Jr, M, LP Goncharenko, SE McDonald, KA Zawdie, J Tate, F Gasperini, NM Pedatella, DP Drob, and JP McCormack (2023). "Understanding Nighttime Ionospheric Depletions Associated With Sudden Stratospheric Warmings in the American Sector". In: *Journal of Geophysical Research: Space Physics* 128.6, e2022JA031236.

Jones Jr, M, DE Siskind, DP Drob, JP McCormack, JT Emmert, MS Dhadly, HE Attard, MG Mlynczak, PG Brown, Gunter Stober, et al. (2020). "Coupling from the middle atmosphere to the exobase: Dynamical disturbance effects on light chemical species". In: *Journal of Geophysical Research: Space Physics* 125.10, e2020JA028331.

Jones Jr, McArthur, John T Emmert, Quan Gan, and Jia Yue (2022). "On the importance of neutral composition and temperature measurements in the 100–200 km altitude region". In: *Frontiers in Astronomy and Space Sciences* 9, p. 1062967.

Karpechko, Alexey Yu, Andrew Charlton-Perez, Magdalena Balmaseda, Nicholas Tyrrell, and Frederic Vitart (2018). "Predicting sudden stratospheric warming 2018 and its climate impacts with a multimodel ensemble". In: *Geophysical Research Letters* 45.24, pp. 13–538.

Kidston, Joseph, Adam A Scaife, Steven C Hardiman, Daniel M Mitchell, Neal Butchart, Mark P Baldwin, and Lesley J Gray (2015). "Stratospheric influence on tropospheric jet streams, storm tracks and surface weather". In: *Nature Geoscience* 8.6, pp. 433–440.

Kil, H, ER Talaat, S-J Oh, LJ Paxton, SL England, and S-Y Su (2008). "Wave structures of the plasma density and vertical E$\times$ B drift in low-latitude F region". In: *Journal of Geophysical Research: Space Physics* 113.A9.

Kil, Hyosub, S-J Oh, MC Kelley, LJ Paxton, SL England, E Talaat, K-W Min, and S-Y Su (2007). "Longitudinal structure of the vertical E$\times$ B drift and ion density seen from ROCSAT-1". In: *Geophysical Research Letters* 34.14.

King, Andrew D, Amy H Butler, Martin Jucker, Nick O Earl, and Irina Rudeva (2019). "Observed relationships between sudden stratospheric warmings and European climate extremes". In: *Journal of Geophysical Research: Atmospheres* 124.24, pp. 13943–13961.

Kodera, Kunihiko, Hitoshi Mukougawa, Pauline Maury, Manabu Ueda, and Chantal Claud (2016). "Absorbing and reflecting sudden stratospheric warming events and their relationship with tropospheric circulation". In: *Journal of Geophysical Research: Atmospheres* 121.1, pp. 80–94.

Krüger, Kirstin, Barbara Naujokat, and Karin Labitzke (2005). "The unusual midwinter warming in the Southern Hemisphere stratosphere 2002: A comparison to Northern Hemisphere phenomena". In: *Journal of the atmospheric sciences* 62.3, pp. 603–613.

Kumar, Sunil, Tarique A Siddiqui, Claudia Stolle, Nicholas M Pedatella, and Duggirala Pallamraju (2023). "Impact of strong and weak stratospheric polar vortices on geomagnetic semidiurnal solar and lunar tides". In: *Earth, Planets and Space* 75.1, p. 52.

Kumari, Komal, Jens Oberheide, and Xian Lu (2020). "The tidal response in the mesosphere/lower thermosphere to the Madden-Julian oscillation observed by SABER". In: *Geophysical Research Letters* 47.16, e2020GL089172.

Kuroda, Yuhji and Kunihiko Kodera (1998). "Interannual variability in the troposphere and stratosphere of the Southern Hemisphere winter". In: *Journal of Geophysical Research: Atmospheres* 103.D12, pp. 13787–13799.

Labitzke, Karin, Barbara Naujokat, and Markus Kunze (2005). "The lower Arctic stratosphere in winter since 1952: an update". In: *Sparc Newsletter* 24, pp. 27–28.

Lehtonen, Ilari and Alexey Yu Karpechko (2016). "Observed and modeled tropospheric cold anomalies associated with sudden stratospheric warmings". In: *Journal of Geophysical Research: Atmospheres* 121.4, pp. 1591–1610.

Lim, Eun-Pa, Harry H Hendon, Ghyslaine Boschat, Debra Hudson, David WJ Thompson, Andrew J Dowdy, and Julie M Arblaster (2019). "Australian hot and dry extremes induced by weakenings of the stratospheric polar vortex". In: *Nature Geoscience* 12.11, pp. 896–901.

Lim, Eun-Pa, Harry H Hendon, Amy H Butler, Rene D Garreaud, Inna Polichtchouk, Theodore G Shepherd, Adam Scaife, Ruth Comer, Lawrence Coy, Paul A Newman, et al. (2020). "The 2019 Antarctic sudden stratospheric warming". In: *SPARC newsletter* 54, pp. 10–13.

Limpasuvan, Varavut, Yvan J Orsolini, Amal Chandran, Rolando R Garcia, and Anne K Smith (2016). "On the composite response of the MLT to major sudden stratospheric warming events with elevated stratopause". In: *Journal of Geophysical Research: Atmospheres* 121.9, pp. 4518–4537.

Limpasuvan, Varavut, David WJ Thompson, and Dennis L Hartmann (2004). "The life cycle of the Northern Hemisphere sudden stratospheric warmings". In: *Journal of climate* 17.13, pp. 2584–2596.

Lin, CH, CC Hsiao, JY Liu, and CH Liu (2007). "Longitudinal structure of the equatorial ionosphere: Time evolution of the four-peaked EIA structure". In: *Journal of Geophysical Research: Space Physics* 112.A12.

Liu, H-L (2016). "Variability and predictability of the space environment as related to lower atmosphere forcing". In: *Space weather* 14.9, pp. 634–658.

Liu, H-L and AD Richmond (2013). "Attribution of ionospheric vertical plasma drift perturbations to large-scale waves and the dependence on solar activity". In: *Journal of Geophysical Research: Space Physics* 118.5, pp. 2452–2465.

Liu, H-L, Wenbin Wang, AD Richmond, and RG Roble (2010). "Ionospheric variability due to planetary waves and tides for solar minimum conditions". In: *Journal of Geophysical Research: Space Physics* 115.A6.

Liu, Huixin, Hidekatsu Jin, Yasunobu Miyoshi, Hitoshi Fujiwara, and Hiroyuki Shinagawa (2013). "Upper atmosphere response to stratosphere sudden warming: Local time and height dependence simulated by GAIA model". In: *Geophysical Research Letters* 40.3, pp. 635–640.

Liu, Huixin, Yasunobu Miyoshi, Saburo Miyahara, Hidekatsu Jin, Hitoshi Fujiwara, and Hiroyuki Shinagawa (2014). "Thermal and dynamical changes of the zonal mean state of the thermosphere during the 2009 SSW: GAIA simulations". In: *Journal of Geophysical Research: Space Physics* 119.8, pp. 6784–6791.

Liu, Huixin, Yang-Yi Sun, Yasunobu Miyoshi, and Hidekatsu Jin (2017). "ENSO effects on MLT diurnal tides: A 21 year reanalysis data-driven GAIA model simulation". In: *Journal of Geophysical Research: Space Physics* 122.5, pp. 5539–5549.

Liu, Jing, Donghe Zhang, Larisa P Goncharenko, Shun-Rong Zhang, Maosheng He, Yongqiang Hao, and Zuo Xiao (2021). "The latitudinal variation and hemispheric asymmetry of the ionospheric lunitidal signatures in the American sector during major Sudden Stratospheric Warming events". In: *Journal of Geophysical Research: Space Physics* 126.5, e2020JA028859.

Lu, Qian, Jian Rao, Chunhua Shi, Dong Guo, Guiqin Fu, Ji Wang, and Zhuoqi Liang (2022). "Possible influence of sudden stratospheric warmings on the atmospheric environment in the Beijing–Tianjin–Hebei region". In: *Atmospheric Chemistry and Physics* 22.19, pp. 13087–13102.

Lü, Zhuozhuo, Fei Li, Yvan J Orsolini, Yongqi Gao, and Shengping He (2020). "Understanding of European cold extremes, sudden stratospheric warming, and Siberian

snow accumulation in the winter of 2017/18". In: *Journal of Climate* 33.2, pp. 527–545.

Lübken, F-J, G Baumgarten, J Fiedler, M Gerding, J Höffner, and U Berger (2008). "Seasonal and latitudinal variation of noctilucent cloud altitudes". In: *Geophysical Research Letters* 35.6.

Lumpe, JD, SM Bailey, JN Carstens, CE Randall, DW Rusch, GE Thomas, K Nielsen, C Jeppesen, WE McClintock, AW Merkel, et al. (2013). "Retrieval of polar mesospheric cloud properties from CIPS: Algorithm description, error analysis and cloud detection sensitivity". In: *Journal of Atmospheric and Solar-Terrestrial Physics* 104, pp. 167–196.

Lyatsky, W, PT Newell, and A Hamza (2001). "Solar illumination as cause of the equinoctial preference for geomagnetic activity". In: *Geophysical Research Letters* 28.12, pp. 2353–2356.

Matthewman, N Joss and JG Esler (2011). "Stratospheric sudden warmings as self-tuning resonances. Part I: Vortex splitting events". In: *Journal of the Atmospheric Sciences* 68.11, pp. 2481–2504.

Maute, A, BG Fejer, JM Forbes, X Zhang, and V Yudin (2016). "Equatorial vertical drift modulation by the lunar and solar semidiurnal tides during the 2013 sudden stratospheric warming". In: *Journal of Geophysical Research: Space Physics* 121.2, pp. 1658–1668.

McClintock, WE, David W Rusch, Gary E Thomas, Aimee W Merkel, Mark R Lankton, Virginia A Drake, Scott M Bailey, and JM Russell III (2009). "The cloud imaging and particle size experiment on the Aeronomy of Ice in the mesosphere mission: Instrument concept, design, calibration, and on-orbit performance". In: *Journal of Atmospheric and Solar-Terrestrial Physics* 71.3-4, pp. 340–355.

McDonald, SE, F Sassi, and AJ Mannucci (2015). "SAMI3/SD-WACCM-X simulations of ionospheric variability during northern winter 2009". In: *Space Weather* 13.9, pp. 568–584.

McDonald, SE, F Sassi, J Tate, J McCormack, DD Kuhl, DP Drob, C Metzler, and AJ Mannucci (2018). "Impact of non-migrating tides on the low latitude ionosphere during a sudden stratospheric warming event in January 2010". In: *Journal of Atmospheric and Solar-Terrestrial Physics* 171, pp. 188–200.

Miyoshi, Yasunobu, Hitoshi Fujiwara, Hidekatsu Jin, and Hiroyuki Shinagawa (2015). "Impacts of sudden stratospheric warming on general circulation of the thermosphere". In: *Journal of Geophysical Research: Space Physics* 120.12, pp. 10–897.

Miyoshi, Yasunobu and Yosuke Yamazaki (2020). "Excitation mechanism of ionospheric 6-day oscillation during the 2019 September sudden stratospheric warming event". In: *Journal of Geophysical Research: Space Physics* 125.9, e2020JA028283.

Mo, Xiaohua and Donghe Zhang (2020). "Quasi-10 d wave modulation of an equatorial ionization anomaly during the Southern Hemisphere stratospheric warming of 2002". In: *Annales Geophysicae*. Vol. 38. 1. Copernicus Publications Göttingen, Germany, pp. 9–16.

Müller-Wodarg, ICF, AD Aylward, and TJ Fuller-Rowell (2001). "Tidal oscillations in the thermosphere: a theoretical investigation of their sources". In: *Journal of Atmospheric and Solar-Terrestrial Physics* 63.9, pp. 899–914.

Nath, Debashis, Wen Chen, Cai Zelin, Alexander Ivanovich Pogoreltsev, and Ke Wei (2016). "Dynamics of 2013 Sudden Stratospheric Warming event and its impact on cold weather over Eurasia: Role of planetary wave reflection". In: *Scientific Reports* 6.1, p. 24174.

Oberheide, J, JM Forbes, K Häusler, Qian Wu, and SL Bruinsma (2009). "Tropospheric tides from 80 to 400 km: Propagation, interannual variability, and solar cycle effects". In: *Journal of Geophysical Research: Atmospheres* 114.D1.

Oberheide, J, JM Forbes, X Zhang, and SL Bruinsma (2011a). "Wave-driven variability in the ionosphere-thermosphere-mesosphere system from TIMED observations: What contributes to the "wave 4"?" In: *Journal of Geophysical Research: Space Physics* 116.A1.

Oberheide, J, JM Forbes, X Zhang, and SLhttps Bruinsma (2011b). "Climatology of upward propagating diurnal and semidiurnal tides in the thermosphere". In: *Journal of Geophysical Research: Space Physics* 116.A11.

Oberheide, J, NM Pedatella, Q Gan, K Kumari, AG Burns, and RW Eastes (2020). "Thermospheric composition O/N response to an altered meridional mean circulation during sudden stratospheric warmings observed by GOLD". In: *Geophysical Research Letters* 47.1, e2019GL086313.

Olson, ME, BG Fejer, Claudia Stolle, Hermann Lühr, and JL Chau (2013). "Equatorial ionospheric electrodynamic perturbations during Southern Hemisphere stratospheric warming events". In: *Journal of Geophysical Research: Space Physics* 118.3, pp. 1190–1195.

Patra, AK, P Pavan Chaitanya, S Sripathi, and S Alex (2014). "Ionospheric variability over Indian low latitude linked with the 2009 sudden stratospheric warming". In: *Journal of Geophysical Research: Space Physics* 119.5, pp. 4044–4061.

Paxton, Larry J, Yongliang Zhang, Hyosub Kil, and Robert K Schaefer (2021). "Exploring the upper atmosphere: Using optical remote sensing". In: *Upper Atmosphere Dynamics and Energetics*, pp. 487–522.

Pedatella, NM, JL Chau, Hauke Schmidt, LP Goncharenko, Claudia Stolle, K Hocke, VL Harvey, Bernd Funke, and TA Siddiqui (2018). "How Sudden stratospheric warmings affect the whole atmosphere". In: *EOS* 99.

Pedatella, NM and JM Forbes (2010). "Evidence for stratosphere sudden warming-ionosphere coupling due to vertically propagating tides". In: *Geophysical Research Letters* 37.11.

Pedatella, NM, T Fuller-Rowell, H Wang, H Jin, Y Miyoshi, H Fujiwara, H Shinagawa, H-L Liu, F Sassi, Hauke Schmidt, et al. (2014). "The neutral dynamics during the 2009 sudden stratosphere warming simulated by different whole atmosphere models". In: *Journal of Geophysical Research: Space Physics* 119.2, pp. 1306–1324.

Pedatella, NM and VL Harvey (2022). "Impact of strong and weak stratospheric polar vortices on the mesosphere and lower thermosphere". In: *Geophysical Research Letters* 49.10, e2022GL098877.

Pedatella, NM and H-L Liu (2013). "The influence of atmospheric tide and planetary wave variability during sudden stratosphere warmings on the low latitude ionosphere". In: *Journal of Geophysical Research: Space Physics* 118.8, pp. 5333–5347.

Pedatella, NM, H-L Liu, AD Richmond, Astrid Maute, and T-W Fang (2012). "Simulations of solar and lunar tidal variability in the mesosphere and lower thermosphere during sudden stratosphere warmings and their influence on the low-latitude ionosphere". In: *Journal of Geophysical Research: Space Physics* 117.A8.

Pedatella, NM and A Maute (2015). "Impact of the semidiurnal lunar tide on the midlatitude thermospheric wind and ionosphere during sudden stratosphere warmings". In: *Journal of Geophysical Research: Space Physics* 120.12, pp. 10–740.

Pedatella, NM, AD Richmond, A Maute, and H-L Liu (2016). "Impact of semidiurnal tidal variability during SSWs on the mean state of the ionosphere and thermosphere". In: *Journal of Geophysical Research: Space Physics* 121.8, pp. 8077–8088.

Penndorf, Rudolf (1965). "The average ionospheric conditions over the Antarctic". In: *Geomagnetism and Aeronomy: studies in the ionosphere, geomagnetism and atmospheric radio noise* 4, pp. 1–45.

Pogoreltsev, AI, AA Vlasov, K Fröhlich, and Ch Jacobi (2007). "Planetary waves in coupling the lower and upper atmosphere". In: *Journal of Atmospheric and Solar-Terrestrial Physics* 69.17-18, pp. 2083–2101.

Reinisch, Bodo W and Ivan A Galkin (2011). "Global ionospheric radio observatory (GIRO)". In: *Earth, planets and space* 63, pp. 377–381.

Richards, PG, RR Meier, Shih-Ping Chen, DP Drob, and P Dandenault (2017). "Investigation of the causes of the longitudinal variation of the electron density in the Weddell Sea Anomaly". In: *Journal of Geophysical Research: Space Physics* 122.6, pp. 6562–6583.

Rideout, William and Anthea Coster (2006). "Automated GPS processing for global total electron content data". In: *GPS solutions* 10, pp. 219–228.

Rishbeth, H (1998). "How the thermospheric circulation affects the ionospheric F2-layer". In: *Journal of Atmospheric and Solar-Terrestrial Physics* 60.14, pp. 1385–1402.

Rishbeth, H and M Mendillo (2001). "Patterns of ionospheric variability". In: *J. Atmos. Sol. Terr. Phys* 63, pp. 1661–1680.

Rupp, Philip, Sheena Loeffel, Hella Garny, Xiaoyang Chen, Joaquim G Pinto, and Thomas Birner (2022). "Potential links between tropospheric and stratospheric circulation extremes during early 2020". In: *Journal of Geophysical Research: Atmospheres* 127.3, e2021JD035667.

Russell, CT and RLhttps McPherron (1973). "Semiannual variation of geomagnetic activity". In: *Journal of geophysical research* 78.1, pp. 92–108.

Sathishkumar, S and S Sridharan (2013). "Lunar and solar tidal variabilities in mesospheric winds and EEJ strength over Tirunelveli (8.7 N, 77.8 E) during the 2009 major stratospheric warming". In: *Journal of Geophysical Research: Space Physics* 118.1, pp. 533–541.

Scherliess, L, DC Thompson, and RW Schunk (2008). "Longitudinal variability of low-latitude total electron content: Tidal influences". In: *Journal of Geophysical Research: Space Physics* 113.A1.

Seviour, William JM, Daniel M Mitchell, and Lesley J Gray (2013). "A practical method to identify displaced and split stratospheric polar vortex events". In: *Geophysical Research Letters* 40.19, pp. 5268–5273.

Shiotani, M and I Hirota (1985). "Planetary wave-mean flow interaction in the stratosphere: A comparison between northern and southern hemispheres". In: *Quarterly Journal of the Royal Meteorological Society* 111.468, pp. 309–334.

Smith, AK and J Perlwitz (2015). "Middle atmosphere: Planetary waves. Encyclopedia of atmospheric sciences". In.

Strickland, DJ, JS Evans, and LJ Paxton (1995). "Satellite remote sensing of thermospheric O/N2 and solar EUV: 1. Theory". In: *Journal of Geophysical Research: Space Physics* 100.A7, pp. 12217–12226.

Sun, Yang-Yi, Huixin Liu, Yasunobu Miyoshi, Loren C Chang, and Libo Liu (2019). "El Niño–Southern Oscillation effect on ionospheric tidal/SPW amplitude in 2007–2015 FORMOSAT-3/COSMIC observations". In: *earth, planets and space* 71.1, pp. 1–9.

Teitelbaum, H, F Vial, AH Manson, R Giraldez, and M Massebeuf (1989). "Nonlinear interaction between the diurnal and semidiurnal tides: terdiurnal and diurnal secondary waves". In: *Journal of Atmospheric and Terrestrial Physics* 51.7-8, pp. 627–634.

Teitelbaum, Hector and François Vial (1991). "On tidal variability induced by nonlinear interaction with planetary waves". In: *Journal of Geophysical Research: Space Physics* 96.A8, pp. 14169–14178.

Thompson, David WJ, Mark P Baldwin, and John M Wallace (2002). "Stratospheric connection to Northern Hemisphere wintertime weather: Implications for prediction". In: *Journal of Climate* 15.12, pp. 1421–1428.

Thompson, David WJ and John M Wallace (2000). "Annular modes in the extratropical circulation. Part I: Month-to-month variability". In: *Journal of climate* 13.5, pp. 1000–1016.

Tripathi, Om P, Mark Baldwin, Andrew Charlton-Perez, Martin Charron, Stephen D Eckermann, Edwin Gerber, R Giles Harrison, David R Jackson, Baek-Min Kim, Yuhji Kuroda, et al. (2015a). "The predictability of the extratropical stratosphere on monthly time-scales and its impact on the skill of tropospheric forecasts". In: *Quarterly Journal of the Royal Meteorological Society* 141.689, pp. 987–1003.

Tripathi, Om P, Andrew Charlton-Perez, Michael Sigmond, and Frederic Vitart (2015b). "Enhanced long-range forecast skill in boreal winter following stratospheric strong vortex conditions". In: *Environmental Research Letters* 10.10, p. 104007.

Vadas, Sharon L, David C Fritts, and M Joan Alexander (2003). "Mechanism for the generation of secondary waves in wave breaking regions". In: *Journal of the Atmospheric Sciences* 60.1, pp. 194–214.

Vadas, Sharon L, Jian Zhao, Xinzhao Chu, and Erich Becker (2018). "The excitation of secondary gravity waves from local body forces: Theory and observation". In: *Journal of Geophysical Research: Atmospheres* 123.17, pp. 9296–9325.

Valladares, Cesar E, Yun-Ju Chen, Marc R Hairston, Jorge L Chau, and Ramani Dhanya (2022). "Observation of scintillation enhancements and large-scale structures within the equatorial ionization anomaly during a Sudden Stratospheric Warming event". In: *Authorea Preprints*.

Vieira, F, PR Fagundes, K Venkatesh, LP Goncharenko, and VG Pillat (2017). "Total electron content disturbances during minor sudden stratospheric warming, over the Brazilian region: A case study during January 2012". In: *Journal of Geophysical Research: Space Physics* 122.2, pp. 2119–2135.

Vierinen, Juha, Anthea J Coster, William C Rideout, Philip J Erickson, and Johannes Norberg (2016). "Statistical framework for estimating GNSS bias". In: *Atmospheric Measurement Techniques* 9.3, pp. 1303–1312.

Wang, Wenbin, Alan G Burns, and Jing Liu (2021). "Upper Thermospheric Winds: Forcing, Variability, and Effects". In: *Upper atmosphere dynamics and energetics*, pp. 41–63.

Waters, Joe W, Lucien Froidevaux, Robert S Harwood, Robert F Jarnot, Herbert M Pickett, William G Read, Peter H Siegel, Richard E Cofield, Mark J Filipiak, Dennis A Flower, et al. (2006). "The earth observing system microwave limb sounder (EOS MLS) on the Aura satellite". In: *IEEE transactions on geoscience and remote sensing* 44.5, pp. 1075–1092.

White, Ian P, Chaim I Garfinkel, Judah Cohen, Martin Jucker, and Jian Rao (2021). "The impact of split and displacement sudden stratospheric warmings on the troposphere". In: *Journal of Geophysical Research: Atmospheres* 126.8, e2020JD033989.

Wright, Corwin J, Neil P Hindley, M Joan Alexander, Mathew Barlow, Lars Hoffmann, Cathryn N Mitchell, Fred Prata, Marie Bouillon, Justin Carstens, Cathy Clerbaux, et al. (2022). "Surface-to-space atmospheric waves from Hunga Tonga–Hunga Ha'apai eruption". In: *Nature* 609.7928, pp. 741–746.

Wu, Dong L and Fuqing Zhang (2004). "A study of mesoscale gravity waves over the North Atlantic with satellite observations and a mesoscale model". In: *Journal of Geophysical Research: Atmospheres* 109.D22.

Yamazaki, Yosuke (2013). "Large lunar tidal effects in the equatorial electrojet during northern winter and its relation to stratospheric sudden warming events". In: *Journal of Geophysical Research: Space Physics* 118.11, pp. 7268–7271.

– (2014). "Solar and lunar ionospheric electrodynamic effects during stratospheric sudden warmings". In: *Journal of Atmospheric and Solar-Terrestrial Physics* 119, pp. 138–146.

Yamazaki, Yosuke, Vivien Matthias, Yasunobu Miyoshi, Claudia Stolle, Tarique Siddiqui, Guram Kervalishvili, J Laštovička, Michal Kozubek, W Ward, David R Themens, et al. (2020). "September 2019 Antarctic sudden stratospheric warming: Quasi-6-day wave burst and ionospheric effects". In: *Geophysical Research Letters* 47.1, e2019GL086577.

Yamazaki, Yosuke and Arthur D Richmond (2013). "A theory of ionospheric response to upward-propagating tides: Electrodynamic effects and tidal mixing effects". In: *Journal of Geophysical Research: Space Physics* 118.9, pp. 5891–5905.

Yoshiki, Motoyoshi and Kaoru Sato (2000). "A statistical study of gravity waves in the polar regions based on operational radiosonde data". In: *Journal of Geophysical Research: Atmospheres* 105.D14, pp. 17995–18011.

Yue, Jia and Wenbin Wang (2014). "Changes of thermospheric composition and ionospheric density caused by quasi 2 day wave dissipation". In: *Journal of Geophysical Research: Space Physics* 119.3, pp. 2069–2078.

Zhang, Shun-Rong, John C Foster, Anthea J Coster, and Philip J Erickson (2011). "East-West Coast differences in total electron content over the continental US". In: *Geophysical Research Letters* 38.19.

Zhang, Shun-Rong, John C Foster, John M Holt, Philip J Erickson, and Anthea J Coster (2012). "Magnetic declination and zonal wind effects on longitudinal differences of ionospheric electron density at midlatitudes". In: *Journal of Geophysical Research: Space Physics* 117.A8.

Zhong, Wogu and Zhiwei Wu (2023). "Interannual Variability of the Wintertime Asian–Bering–North American Teleconnection Linked to Eurasian Snow Cover and Maritime Continent Sea Surface Temperature". In: *Journal of Climate* 36.9, pp. 2815–2831.

Contribution to the Manuscripts

Individual contributions of the PhD candidate to the manuscripts submitted in this cumulative thesis are listed below.

For all three manuscripts, the candidate was responsible for the acquisition of the financial support for the projects leading to these publications, planning, management and coordination of the research activities, and oversight and leadership, including mentorship of students and early career scientists.

In Goncharenko et al. (2020), the candidate was responsible for conceptualization, development of methodology, provision and data curation of GNSS TEC data, formal analysis of GNSS TEC data, and visualization of GNSS TEC data (Figures 2-7). The candidate was also responsible for the organization of discussions with coauthors, preparation and writing of the original draft, as well as preparation of the revised draft and other pre-publication stages.

Similarly, in Goncharenko et al. (2021a), the candidate was leading the conceptualization of research activities, curation and analysis of GNSS TEC data, analysis of anomalies in O/N_2 data, and preparation of Figures 2-4. The candidate was also responsible for investigation and verification of consistency between the 'quiet dynamic state' TEC and available empirical models of TEC. The candidate was in charge of organising discussions with coauthors, preparation of the initial draft of the manuscript, and addressing reviewers' comments.

In Goncharenko et al. (2022), the candidate formulated the concept in collaboration with coauthors, and conducted analysis of ionospheric data, including GNSS TEC and ionosonde N_mF2. The candidate was also responsible for the development of empirical models of TEC and N_mF2, including data curation and development of algorithms and software. The candidate prepared Figures 2-4, wrote initial draft, and coordinated pre-publication activities with all coauthors.

Appendix A

Goncharenko et al., 2020

Goncharenko, L. P., Harvey, V. L., Greer, K. R., Zhang, S.-R., Coster, A. J. (2020). Longitudinally dependent low-latitude ionospheric disturbances linked to the Antarctic sudden stratospheric warming of September 2019. Journal of Geophysical Research: Space Physics, 125, e2020JA028199. https://doi.org/10.1029/2020JA028199

JGR Space Physics

RESEARCH ARTICLE
10.1029/2020JA028199

Longitudinally Dependent Low-Latitude Ionospheric Disturbances Linked to the Antarctic Sudden Stratospheric Warming of September 2019

L. P. Goncharenko[1], V. L. Harvey[2], K. R. Greer[2], S.-R. Zhang[1], and A. J. Coster[1]

[1]Haystack Observatory, Massachusetts Institute of Technology, Westford, MA, USA, [2]Laboratory for Atmospheric and Space Physics, University of Colorado, Boulder, CO, USA

Key Points:
- Minor Antarctic sudden stratospheric warming of September 2019 produces large ionospheric anomalies at low latitudes
- Changes of total electron content exceeding a factor of 2 are observed
- Large longitudinal differences in total electron content response to Antarctic SSW are reported

Correspondence to:
L. P. Goncharenko,
lpg@mit.edu

Citation:
Goncharenko, L. P., Harvey, V. L., Greer, K. R., Zhang, S.-R., Coster, A. J. (2020). Longitudinally dependent low-latitude ionospheric disturbances linked to the Antarctic sudden stratospheric warming of September 2019. *Journal of Geophysical Research: Space Physics*, *125*, e2020JA028199. https://doi.org/10.1029/2020JA028199

Received 4 MAY 2020
Accepted 26 JUN 2020
Accepted article online 15 JUL 2020

Abstract The strongest Southern Hemisphere minor sudden stratospheric warming (SSW) in the last 40 years occurred in September 2019 and resulted in unprecedented weakening of the stratospheric polar vortex. Ionospheric total electron content (TEC) observations are used to provide an overview of statistically significant anomalies in the low-latitude ionosphere during this event. Quasi-semidiurnal perturbations of TEC are observed in response to the SSW, similar to those seen during Northern Hemisphere SSWs. Analysis indicates the existence of quasi-periodic oscillations in TEC in the crests of the equatorial ionization anomaly, with strong 5- to 6-day and 2- to 3-day periodicities. Ionospheric anomalies from the combined effects of multiple mechanisms exceed a factor of 2, comparable to the strongest anomalies associated with Northern Hemisphere SSWs. These results also indicate a remarkable longitudinal variation in the character and magnitude of variations that could be related to a modulation of the non-migrating diurnal tide.

Plain Language Summary Sudden stratospheric warming, a large-scale meteorological disturbance, has been associated with profound anomalies in the Earth atmosphere, from troposphere all the way to the upper thermosphere and ionosphere. During the last decade, numerous studies showed that Arctic sudden stratospheric warmings cause especially large anomalies in the low-latitude ionosphere. However, it was not clear if similar ionospheric anomalies can be produced by Antarctic sudden stratospheric warming, mostly because Antarctic sudden stratospheric warmings are pretty rare. In this study, we provide an overview of ionospheric anomalies in total electron content observed in September 2019, when very strong sudden stratospheric warming developed over Antarctica. We conclude that Antarctic events produce even more dynamical changes in the ionosphere than Arctic events. We report for the first time large differences in the observed features at locations that are separated by only 30° in longitude. Our results indicate that stratospheric weather can strongly influence the state of the ionosphere not only during December–February period (winter in the Northern Hemisphere), but also during September (equinox conditions).

1. Introduction

A sudden stratospheric warming (SSW) event (Scherhag, 1952) is a large-scale disruption of the stratospheric polar vortex with concomitant warming at the pole and a weakening of the polar night jet stream (Butler et al., 2015). In recent years, SSWs have been linked to large variability throughout the ocean-atmosphere-ionosphere system (e.g., Pedatella et al., 2018). Since the late 2000s, observations have shown a large variety of ionospheric disturbances that have been associated with Arctic SSWs (see reviews by Chau et al., 2012; Goncharenko et al., 2021). Briefly, the most notable changes occur in the low-latitude ionosphere and include disturbances on three distinct temporal scales. The shorter temporal scale is associated with modification of tidal forcing during SSW and most frequently expressed as quasi-semidiurnal disturbances in, for example, vertical drift, electron density, and the equatorial electrojet (Chau et al., 2009; Fejer et al., 2010; Goncharenko, Chau, et al., 2010; Pedatella & Forbes, 2010; Yamazaki, 2013) that persist for multiple days or even weeks. The second temporal scale is associated with ionospheric oscillations with planetary wave time scales and observed as 2-, 5- to 6-, or 10- to 16-day quasi-periodic variations in peak electron density, peak height of the *F* region, and locations of the equatorial ionization anomaly (EIA) (Mo et al., 2014; Patra et al., 2014). The third temporal scale can last for 10–20 days or longer and is expressed as decreases in zonal and diurnal mean electron density and mean ionospheric peak height (Pancheva & Mukhtarov, 2011),

Journal of Geophysical Research: Space Physics 10.1029/2020JA028199

decrease in thermospheric density (Liu et al., 2011; Yamazaki et al., 2015), and decrease in thermospheric O/N_2 ratio (Oberheide et al., 2020). These observational studies have stimulated considerable advances in understanding the physical mechanisms that link the state of the stratosphere to low-latitude ionospheric variability. Three generally accepted mechanisms include (1) changes in the migrating and non-migrating solar and lunar tides (Forbes & Zhang, 2012; Jin et al., 2012; Liu et al., 2010; Pedatella & Forbes, 2010), (2) increases in stratospheric tropical ozone during SSWs that lead to an enhancement in the migrating tide (Goncharenko et al., 2012; Limpasuvan et al., 2016; Siddiqui et al., 2019), and (3) reductions in the thermospheric O/N_2 ratio due to tidal dissipation (Oberheide et al., 2020; Yamazaki & Richmond, 2013). Superposition of these and other mechanisms that are still yet to be discovered creates highly variable conditions in the quiet-time ionosphere-thermosphere system that can be observed in multiple upper atmospheric parameters. This topic is the subject of active research that will undoubtedly bring new insights as more observational and modeling results are obtained.

Due to larger planetary waves (PWs) in the Northern Hemisphere (NH) winter as compared to the Southern Hemisphere (SH) winter, Arctic SSWs (e.g., Charlton & Polvani, 2007) are far more common than their Antarctic counterparts (Kruger et al., 2005). An outstanding question is whether Antarctic SSWs can produce similar disturbances in the ionosphere-thermosphere system as Arctic SSWs. The main reason for this gap in understanding is that Antarctic SSWs occur much less frequently, with only one major SSW recorded in September 2002 and only several minor SSWs in the satellite era. Olson et al. (2013) examined equatorial ionospheric electric fields and currents during the 2002 event and reported enhanced quasi 2-day oscillations and multiday perturbations consistent with lunar tide. Mo and Zhang (2020) examined observations in the Asian sector and found quasi 10-day oscillations in total electron content (TEC) and location of crests of the EIA. However, both studies noted that enhanced geomagnetic activity during that period complicated interpretation of observations.

A renewed opportunity to investigate how the ionosphere and thermosphere reacts to Antarctic SSWs has emerged with the strong minor SSW that occurred over Antarctica in September 2019 (Lim et al., 2020). Yamazaki et al. (2020) examined middle atmospheric observations using Aura Microwave Limb Sounder satellite data alongside the ionospheric equatorial electrojet and the topside electron density from the Swarm satellite constellation and reported strong quasi 6-day variations in all parameters during this SSW. Specifically, these variations reached 20–40% for the topside electron density and 5–10% for the topside TEC and were observed simultaneously with 6-day wave activity in the lower thermosphere.

The main objective of this study is to examine ionospheric TEC and attribute anomalies in ionospheric TEC patterns to the Antarctic SSW. We note that analysis of TEC can uncover significantly different patterns of anomalies as compared to Yamazaki et al. (2020), as it examines all local times, in contrast to limited local time coverage available for Swarm data. However, as the ionospheric response to SSW varies with altitude, some patterns observed at fixed altitudes, like in Swarm (or other satellite) data, could be hard to detect in height-integrated TEC observations. This study reports SSW-induced TEC anomalies and their variation as a function of latitude, longitude, and local time, thus presenting different characteristics of ionospheric changes related to the Antarctic SSW of September 2019.

2. Results and Discussion

2.1. The 2019 Antarctic Minor SSW and Mesospheric Cooling

Figure 1 presents an overview of the meteorological conditions in the stratosphere and mesosphere from 15 August to 1 October 2019. The top panel shows an altitude time slice of zonal mean temperature at 80°S. The minor SSW is characterized here by the descent of the stratopause from 55 km in late August to 40 km in mid-September. As expected, there is simultaneous cooling in the polar mesosphere. The mesospheric response is most apparent in mid-September, at the same time the zonal winds are weakest (middle panel, red line). Indeed, to the extent that the speed of the stratospheric polar night jet can be used as a proxy for the strength of the polar vortex, the observed vortex weakening in the second week of September is unprecedented in the 40-year data record. During this time, the jet encircling the Antarctic vortex is even weaker than during the notorious vortex split year of 2002 (middle panel, blue line). The strong minor SSW and weak polar vortex in the Antarctic in 2019 are driven by large amplitude PWs, as evidenced in the bottom panel of Figure 1. These PW amplitudes maximize near the stratopause in early September but remain

Journal of Geophysical Research: Space Physics 10.1029/2020JA028199

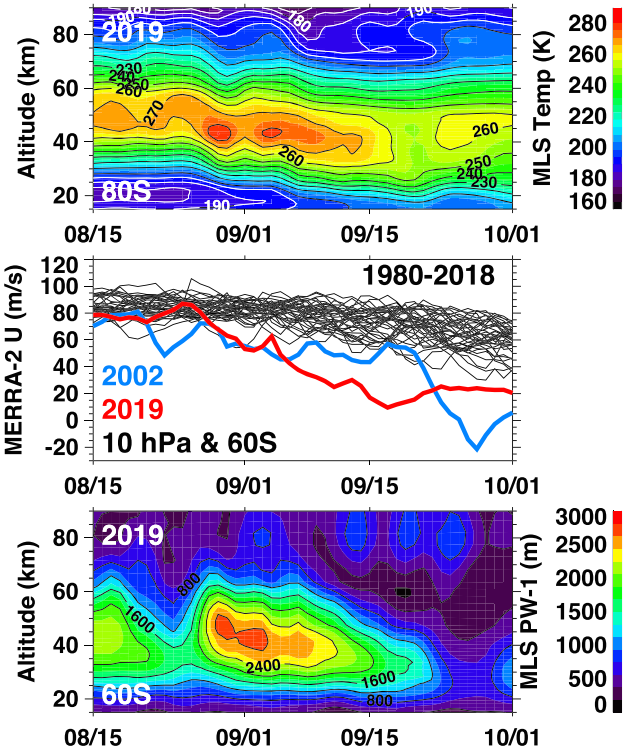

Figure 1. Time series from 15 August to 1 October of (top) zonal mean MLS temperatures at 80°S during 2019 as a function of altitude, (middle) MERRA-2 zonal mean zonal wind at 60°S and 10 hPa for 1980–2018 (black lines) highlighting 2002 (blue) and 2019 (red), and (bottom) MLS planetary wave 1 amplitude at 60°S during 2019 as a function of altitude.

large in the stratosphere through mid-September. Presented middle atmosphere dynamics is fully consistent with variations described by Lim et al. (2020) and Yamazaki et al. (2020). Of particular relevance to this work is the PW response in the mesosphere between 70 and 90 km in mid-September. Given the timing of the SSW and mesospheric cooling, and the concomitant PW activity in the stratosphere and mesosphere, we expect to see largest effects in the thermosphere and ionosphere in mid-September.

The 2019 SH SSW occurred during a period of very low solar activity; the F10.7 index varied from 67–70 SFU (1 SFU = 10^{-22} W/m^2/Hz) for most of September. Likewise, this time was also quiet geomagnetically, with an Ap index that ranged from 3 to 10 units. We note that one brief enhancement in the Kp index (on 16 September, Kp = 4 at 3–6 UT) does not influence our results. Overall, low and stable levels of solar and geomagnetic activity make it easier to unambiguously identify ionospheric anomalies related to SSW. In the subsequent analysis, we focus on the mid-September period.

2.2. Ionospheric Observations

We use TEC data provided by the Madrigal database and processed by Massachusetts Institute of Technology (MIT) Haystack Observatory as described by Rideout and Coster (2006) and Vierinen et al. (2016). These data have 1° × 1° latitude and longitude resolution and 5-min temporal resolution for locations that are covered by ground-based Global Navigation Satellite System (GNSS) receivers, resulting in data gaps over the oceans and areas without GNSS receivers. MIT Haystack Observatory currently processes data from more than 6,000 GNSS receivers. GLObal NAvigation Satellite System (GLONASS, operated by Russia) data were added recently to the processing, resulting in the ~30% improvement in the data density. For this study, we have analyzed 3 months of data from 1 August 2019 to 1 November 2019. Inspection of the TEC data for this time period shows high data quality, with a median error of a single data point equal to 0.92 TECu (1 TECu = 10^{16} electrons m^{-2}), and 99th percentile in error equal to 1.36 TECu. The error in TEC data exceeded 3 TECu in 0.01% of original data, and these data were excluded from the subsequent analysis.

To isolate effects of the September 2019 SSW, we first characterize the typical "dynamically quiet" ionospheric state for September under solar minimum conditions within three broad geographic areas: American sector (125°W to 25°W), African sector (20°W to 70°E), and Asian sector (110°E to 160°E). For each longitudinal sector, we have calculated median values of TEC and different percentiles for the following conditions: low solar activity (F10.7 daily index is 70 ± 5 SFU; 81-day average F10.7 index is 70 ± 5 SFU), low geomagnetic activity (daily Ap index < 15 for the current day and previous 24 h), average or below average stratospheric PW activity at 10 hPa and 60°S, and centered on 15 September with a ±15-day window. Average level of stratospheric PW activity was calculated from 40+ years of MERRA data. The Madrigal database contains 79 days that satisfy the aforementioned conditions, with data collected in 2008, 2009, and 2018. The TEC observations for the selected 79 days were then binned in 30-min intervals, resulting in several hundred data points per each 1° longitude × 1° latitude bin in areas with good data coverage. Areas with more limited data coverage (like over Africa) have more data from year 2018 in comparison with 2008 and 2009. Median TEC values determined from these bins were then used in this study as a baseline that describes the "dynamically quiet" ionosphere in each geographic sector with high resolution in latitude and longitude. We have included in the calculation of medians only areas that had more than 50 points in each 1° × 1° × 30-min bin, indicating that medians were calculated based on observations from at least 8 to 9 different days. As an example, the top two panels of Figure 2 show median TEC in the American sector at 17 UT (Figure 2a) and at 21 UT (Figure 2b). In addition, different percentile estimates obtained from these

Journal of Geophysical Research: Space Physics 10.1029/2020JA028199

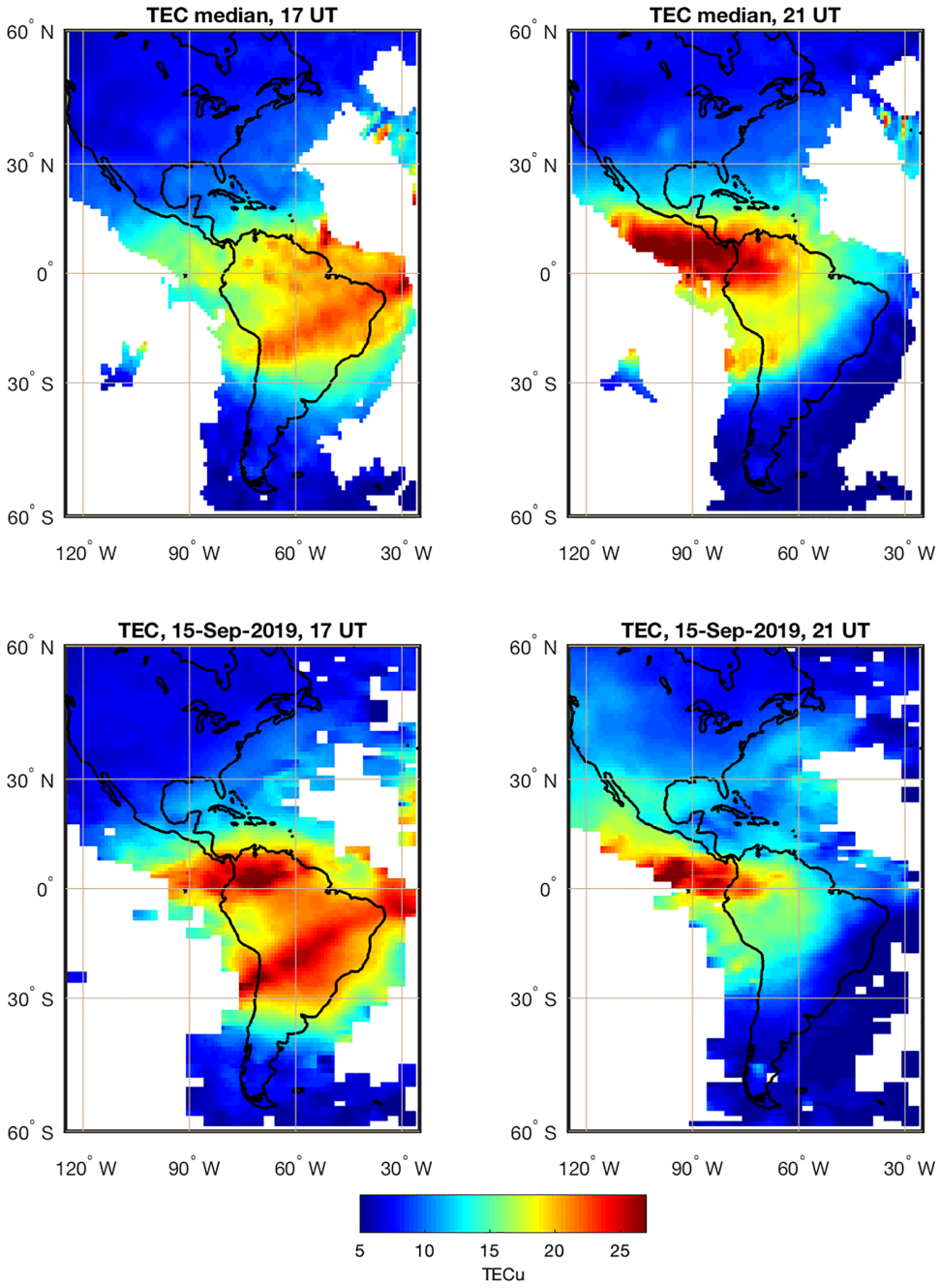

Figure 2. Maps of TEC over the American sector for low solar, geomagnetic, and stratospheric PW activity levels (top) and for 15 September 2019 (bottom). Left panels show TEC at 17 UT (noon in LT at 75°W), and right panels show TEC at 21 UT (afternoon sector at 75°W). Enhancement of TEC in the noontime sector on 15 September 2019 is followed by a strong depletion several hours later. This behavior is similar to TEC variations observed during Arctic SSW events and is driven by strong enhancements in tidal amplitudes during SSW.

79 days of data (e.g., difference between 10th and 90th percentiles or 25th and 75th percentiles) enabled quantitative description of typical ionospheric variability during dynamically quiet conditions.

Figure 2 compares the median, for example, "dynamically quiet state" TEC in the American sector around noontime (Figure 2a, 17 UT) and afternoon (Figure 2b, 21 UT), with observations during Antarctic SSW on 15 September 2019 during the same time, 17 UT (Figure 2c) and 21 UT (Figure 2d). Large increases in TEC

Journal of Geophysical Research: Space Physics 10.1029/2020JA028199

are observed at 17 UT during the SSW, with enhancements in both crests of the EIA, while the opposite behavior is observed several hours later, at 21 UT, with suppression of both crests of EIA. Similar quasi-semidiurnal deviations in TEC in the low-latitude ionosphere in the American sector have been previously reported to occur during Arctic SSW events (Goncharenko, Chau, et al., 2010, see their Figure 1). The mechanism driving this quasi-semidiurnal ionospheric variability is amplification of tidal amplitudes in the lower thermosphere (Jin et al., 2012; Liu et al., 2010; Pedatella et al., 2014). Anomalous tides modulate electric fields through the *E* region dynamo process and modify *F* region vertical drifts and, subsequently, *F* region electron densities. Although the roles of different mechanisms and different tides are a matter of active research (see reviews by Chau et al., 2012; Goncharenko et al., 2021), similar quasi-semidiurnal behavior was observed in multiple ionospheric and thermospheric parameters and during multiple Arctic SSW events, both major and minor. We thus conclude that a minor Antarctic SSW of September 2019 causes quasi-semidiurnal perturbations in the low-latitude ionosphere in a manner similar to Arctic SSW events.

The ionospheric response to the Antarctic SSW is both hemispheric in scale and regional in strength of specific features; in other words, qualitatively similar large-scale low-latitude ionospheric anomalies are observed in different geographic sectors, but the strength of these anomalies is different. Figure 3 illustrates this point and presents TEC anomalies observed on 15 September 2019 and calculated as a difference between observations and median values and expressed as percent change from median. Around noontime, positive TEC anomalies are seen over the American, African, and Asian sectors, albeit with varying strengths. In the American sector, noontime positive TEC anomalies are seen over a broad latitude band extending from 40°S to 40°N, including the EIA trough. The largest anomalies are observed in the areas several degrees poleward of the EIA crests, reaching ~40–60% poleward of the northern crest of EIA and ~60–80% poleward of the southern crest of EIA. Positive noontime anomalies are larger in the African sector where they reach 100%, while negative anomalies formed within ~20° latitude of the EIA trough. In contrast, in the Asian sector, positive TEC anomalies are rather weak and do not exceed 20–30%. To summarize the ionospheric anomalies over the globe, the afternoon and nighttime anomalies are more consistent between different geographic sectors and show predominant suppression of TEC which is stronger in the African and Asian sectors. These negative anomalies could result from a superposition of several mechanisms: a negative phase of a quasi-semidiurnal perturbation, general decrease of a thermospheric O/N_2 ratio related to the dissipation of enhanced tides (Oberheide et al., 2020; Yamazaki & Richmond, 2013), and perturbations in upper thermospheric winds that could contribute to the nighttime anomalies (Goncharenko et al., 2018; Pedatella & Maute, 2015). The positive TEC anomalies observed in the afternoon directly north of 20°N in the American sector (red area in the left side of the middle panel in Figure 3) do not exhibit a semidiurnal pattern. We hypothesize that they are produced by a different mechanism than the low-latitude anomalies and thus will be explored in a separate study.

One of the important distinctive features of this minor SSW is the fact that ionospheric anomalies are highly dynamic, with their phenomenology strongly varying from 1 day to another. This contrasts with typical TEC anomalies during Arctic major and minor SSW events where similar quasi-semidiurnal (Fagundes et al., 2015; Goncharenko, Coster, et al., 2010; Paes et al., 2014) or negative disturbances (Vieira et al., 2017) last for multiple days. For example, by 19 September, the American sector shows a negative TEC anomaly in the noontime sector, the African sector still shows a positive anomaly albeit with a reduced magnitude, but the Asian sector shows the strongest positive anomaly that exceeds 100% (Figure 4, compare to Figure 3).

Figure 5 further illustrates this behavior and depicts TEC variations for several selected days (14, 15, 17, and 19 September) in the northern crests of the EIA (Figures 5a and 5b) and in the southern crests of the EIA (Figures 5c and 5d) for geographic longitudes 75°W (left panels, Figures 5a and 5c) and 45°W (right panels, Figures 5b and 5d). The quasi-semidiurnal feature that was illustrated in Figure 2 is shown with blue and red lines in Figures 5a and 5c for 75°W, indicating TEC increase in the morning to early afternoon sector (prior to 19 UT) and TEC suppression in the late afternoon (after 19 UT). However, this quasi-semidiurnal departure from median values is short lived and present for only 2 days, 14 and 15 September. In the northern crest of EIA at 75°W (Figure 5a), on 16–18 September, it is replaced by a general increase in TEC for all daytime hours that at times exceeds the 90th percentile, and by 19 September, the dominant feature is the suppression of TEC below the 25th percentile for all daytime hours. Increase in TEC for all daytime hours followed by a decrease in TEC for all daytime hours 3 days later is likely a manifestation of ionospheric oscillation with ~6-day period. PWs, in particular quasi 6-day waves, affect TEC during all daytime hours (Qin

Journal of Geophysical Research: Space Physics 10.1029/2020JA028199

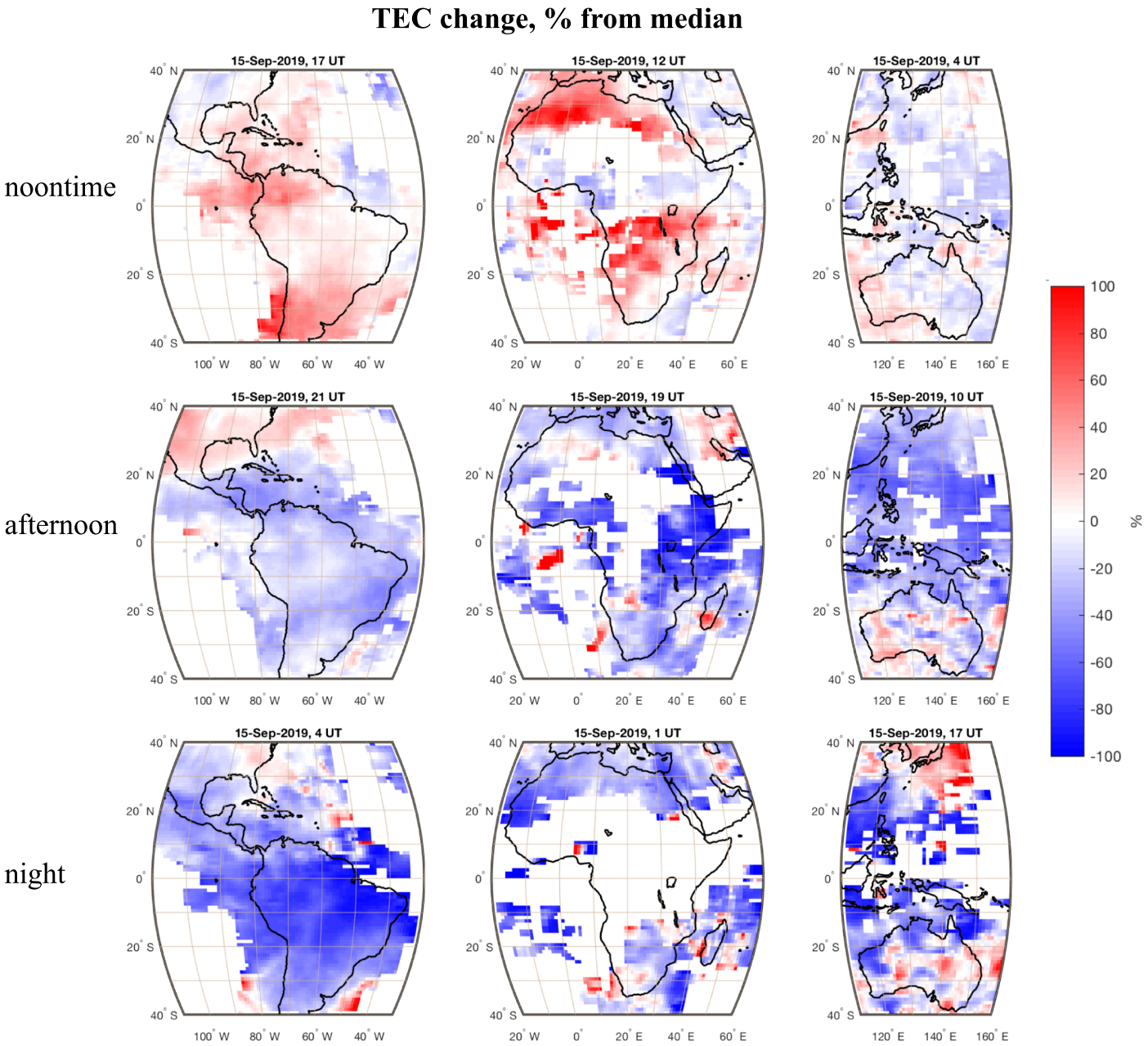

Figure 3. Change in TEC during Antarctic SSW on 15 September 2019 in different geographic regions and different local time sectors. Change is expressed as percentage from median values. Positive daytime anomalies are strongest in the African sector, but weak in the Asian sector. Negative anomalies in the afternoon and nighttime are more uniform for different geographic regions.

et al., 2019; Yamazaki et al., 2018), although this effect depends on solar local time and largest PW modulations of the ionosphere are observed in the afternoon hours (Gu et al., 2018; Liu et al., 2012). Thus, in the northern crest of EIA at 75°W, the low-latitude ionosphere exhibits signs of superposition of tidal effects and ~5- to 6-day PW effects that were discussed by Yamazaki et al. (2020). A plausible cause for the lack of persistence in quasi-semidiurnal anomalies during September 2019 SSW is the co-occurrence of a very strong quasi 6-day wave. We will discuss manifestations of 5- to 6-day wave and other PWs in a later portion of this study.

Figure 5 demonstrates another important aspect of ionospheric anomalies observed in September 2019: their phenomenology is different for geographic locations separated by as little as 30° in longitude. Figures 5b (for

Journal of Geophysical Research: Space Physics 10.1029/2020JA028199

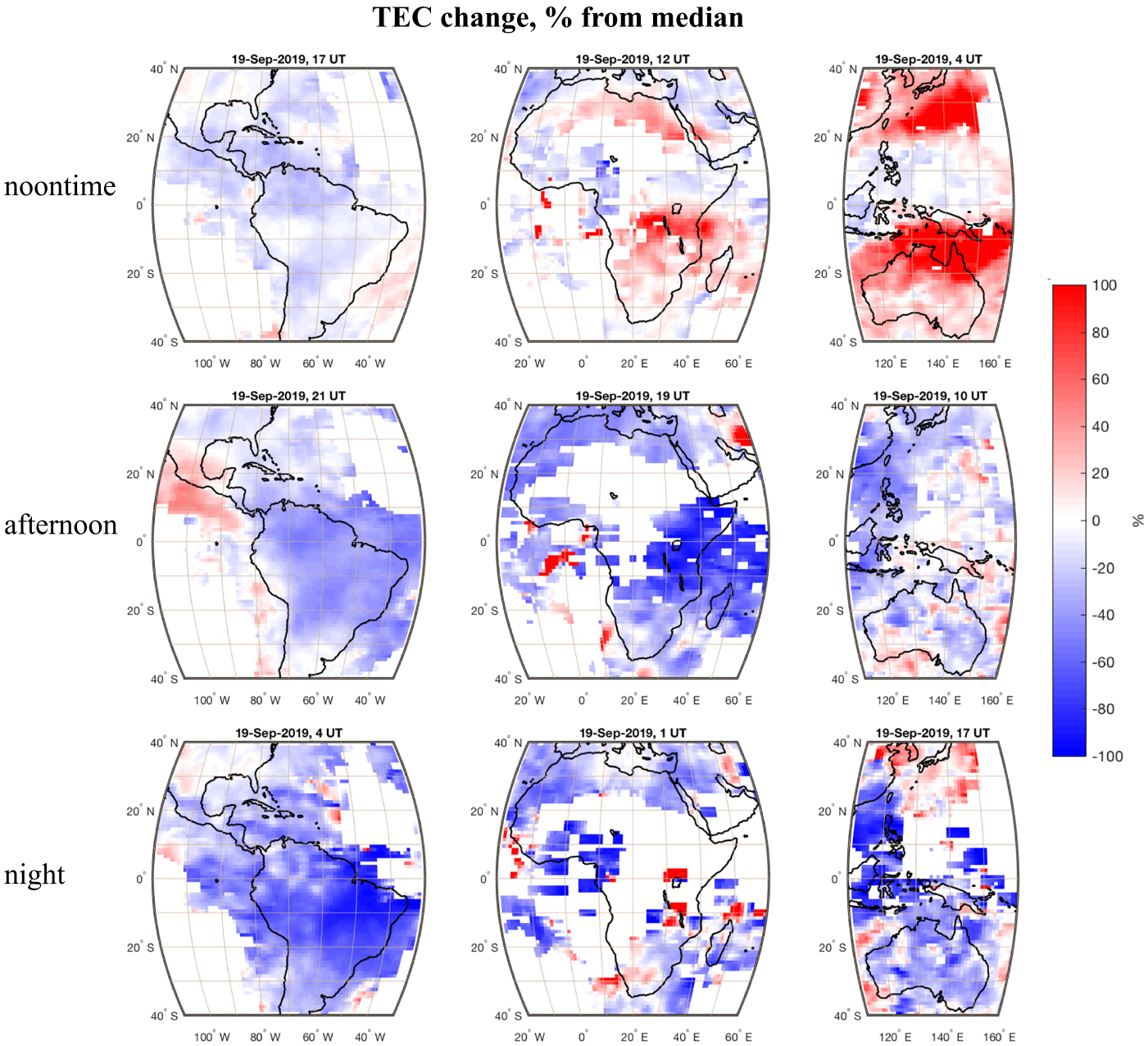

Figure 4. Same as Figure 3, but for 19 September 2019. Note large differences from 15 September 2019 at noontime.

the northern crest of EIA) and 5d (for the southern crest of EIA) show that at 45°W, TEC anomalies are much weaker than at 75°W in both absolute and relative magnitudes, with the exception of a large increase in the southern crest of the EIA on 17 September. The quasi-semidiurnal disturbance evident at 75°W is not present at 45°W, and the dominant variation is the TEC suppression, which is largest in the afternoon and nighttime hours. This contrasts with results obtained during several Arctic SSW, where TEC anomalies in the Brazilian sector (45°W) were found to be very similar to anomalies in the Peruvian sector (75°W) (Fagundes et al., 2015; Paes et al., 2014) and semidiurnal behavior was preserved for multiple days. For Arctic SSWs, EIA suppression in the Brazilian sector in the afternoon hours was stronger than intensification in the morning, in contrast to behavior in the Peruvian sector (Paes et al., 2014). However, Vieira et al. (2017) found that during a minor Arctic SSW of 2012, the dominating

Journal of Geophysical Research: Space Physics 10.1029/2020JA028199

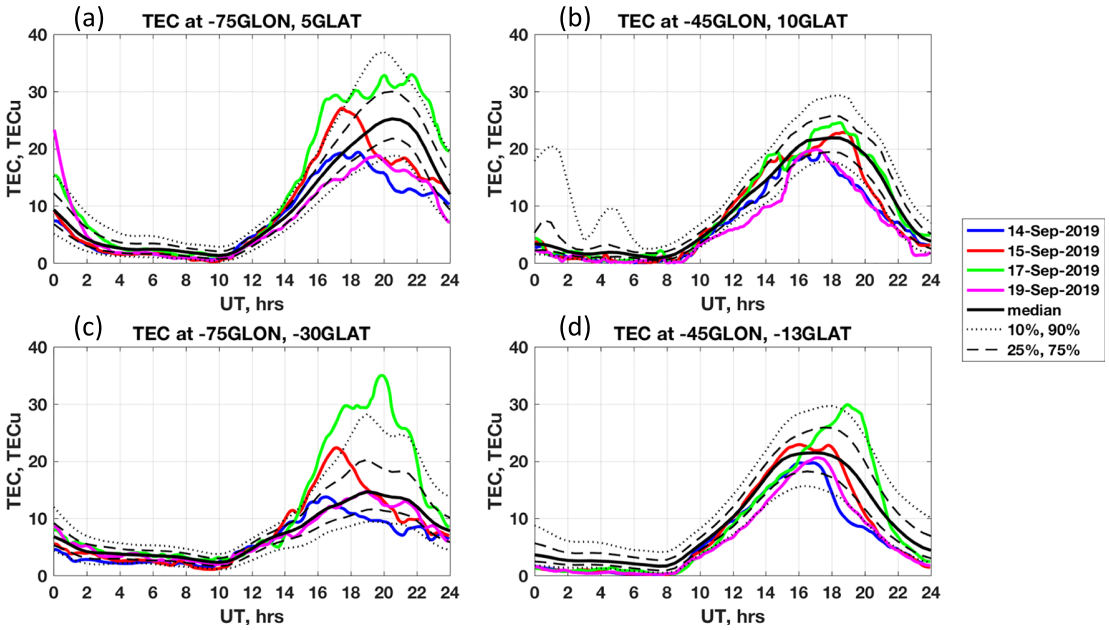

Figure 5. TEC variations on 14, 15, 17, and 19 September 2019 in the American sector at different longitudes, 75°W (left side) and 45°W (right side). Panels (a) and (b) show variations in the northern crest of EIA and panels (c) and (d) in the southern crest of EIA. Locations of EIA crests are given in geographic coordinates (GLON, GLAT).

ionospheric response is suppression of TEC during daytime hours, and this depletion is stronger in the eastern Brazilian sector than in the western sector. Different responses to different Arctic SSW events are likely related to different mechanisms dominating ionospheric changes, quasi-semidiurnal variation due to the amplification of semidiurnal tide in Paes et al.'s (2014) and Fagundes et al.'s (2015) studies or prolonged decrease in TEC due to the dissipation of amplified tides in Vieira et al.'s (2017) study. Although some differences between the Peruvian sector (75°W) and Brazilian sector (45°W) are expected due to the difference in the offset between the magnetic and geographic latitudes, Arctic SSW produces qualitatively similar ionospheric disturbances in these geographic areas. However, in the case of Antarctic SSW of September 2019, observed differences between these sectors are larger. This result indicates that Antarctic SSWs can produce larger dynamic variability in the ionosphere than Arctic SSWs.

Figure 6 further illustrates striking longitudinal differences in ionospheric disturbances during Antarctic SSW of September 2019. It depicts TEC variations in the northern crests of EIA in the African sector at 0°E and 30°E (Figures 6a and 6b) and in the Asian sector at 115°E and 145°E. We have analyzed observations only in the northern crests of EIA due to the lack of data in the southern crests of EIA in these sectors. The most dramatic differences between close longitudes are observed in the African sector (Figures 6a and 6b). The median TEC and quiet dynamic state variability (TEC variation between 10th and 90th percentiles) are significantly higher at 0°E than at 30°E. During the Antarctic SSW of September 2019, observations reveal increase in TEC above 75th and 90th percentiles or suppression below 25th and 10th percentiles at both longitudes in the African sector. However, the magnitude of these disturbances is higher at 0°E than at 30°E in both absolute TEC units and relative TEC units, as percentage change compared to the median value. Similar longitudinal differences are observed in the Asian sector, as illustrated by Figures 6c (115°E) and 6d (145°E): longitude with higher median TEC, such as 115°E, has higher quiet dynamic variability and higher disturbances during SSW of September 2019 in comparison with longitude with lower median TEC, such as 145°E. All four locations of EIA crests depicted in Figure 6 show a mixture of tidal effects and daily mean TEC suppression during SSW, but these effects are stronger at longitudes with higher median TEC.

Longitudinal variations in ionospheric parameters are expected to arise for several different reasons. One set of reasons is related to purely geometric effects arising from the longitudinal differences between the geomagnetic and geographic equator and variations in the magnetic declination as a function of longitude

Journal of Geophysical Research: Space Physics 10.1029/2020JA028199

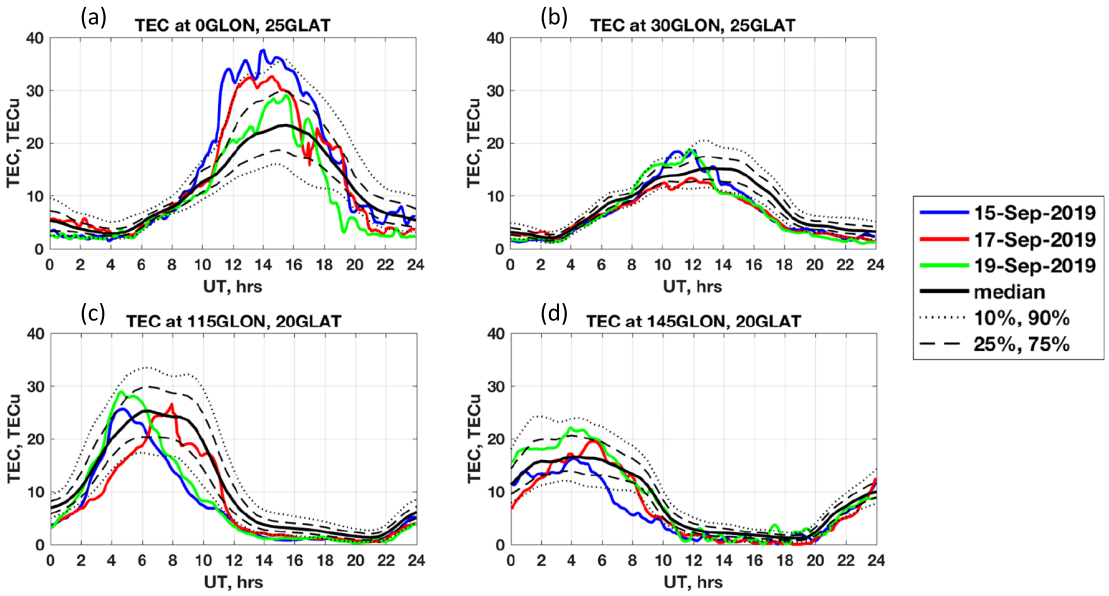

Figure 6. Variations in TEC during Antarctic SSW in the northern crests of EIA over African sector, panels (a) and (b), and Asian sector, panels (c) and (d).

(e.g., England, 2012, and references therein). The longitudinal variation in the difference between the geographic and geomagnetic equator leads to the longitudinal variation in the distance between the region with largest photoionization near the subsolar point of minimum solar zenith angle and the region of EIA trough as the plasma source of EIA. This reason could contribute to the observed longitudinal differences in TEC in the American sector (Figure 5 in this study), but could not be responsible for the observed differences in the African and Asian sectors (Figure 6 in this study). The longitudinal variation in the magnetic declination changes the angle between the neutral winds and geomagnetic field and, consequently, transport of ionospheric plasma. Effects of varying declination angle for locations separated by 30° in longitude are expected to be strongest in the low-latitude American sector, but weaker (though potentially non-negligible) in the African and Asian sectors. Thus, geometric effects related to the offset between geographic and geomagnetic equator and declination angle variations could not be a leading cause of the observed longitudinal TEC variations in the African and Asian sectors.

Previous studies concluded that non-migrating tides, in particular non-migrating diurnal eastward-propagating with zonal wavenumber-3 (DE3) tide can be a major driver of longitudinal variation in low-latitude ionospheric electron density. This longitudinal variation is expressed as a strong wavenumber-4 signature in a fixed local time frame and is reported in various ionospheric parameters, including equatorial electrojet (England et al., 2006), E × Bdrifts (Kil et al., 2007; Ren et al., 2009), and electron density (Lin et al., 2007; Scherliess et al., 2008). Amplitudes of DE3 tide reach their seasonal peaks in September in the lower thermosphere (Akmaev et al., 2008) and throughout the thermosphere (Oberheide et al., 2009). Consequently, the wavenumber-4 signature is expected to be strong in the low-latitude ionosphere in September 2019. Longitudes of higher and lower TEC reported in this study are consistent with longitudinal variations in ionospheric parameters related to DE3 tide (England et al., 2006; Kil et al., 2008; Scherliess et al., 2008). TEC observations presented in Figures 5 and 6 strongly suggest that observed longitudinal variations are related to the DE3 tide and not only for "dynamically quiet state," but also for the SSW conditions. Moreover, we suggest that Antarctic SSW of September 2019 led to the strong amplification of DE3 tide and, subsequently, to large longitudinal variation in ionospheric perturbations caused by SSW. Previous numerical simulations suggested that modification of semidiurnal non-migrating tides could contribute to ionospheric changes during Arctic SSWs (Fuller-Rowell et al., 2010; McDonald et al., 2015; Pedatella & Forbes, 2010). McDonald et al. (2018) suggested that interference of non-migrating diurnal tides can be a major contributor to TEC enhancements during Arctic SSW, even without enhanced amplitudes. To the best of our knowledge, our study presents first observational evidence of ionospheric changes that could

Journal of Geophysical Research: Space Physics 10.1029/2020JA028199

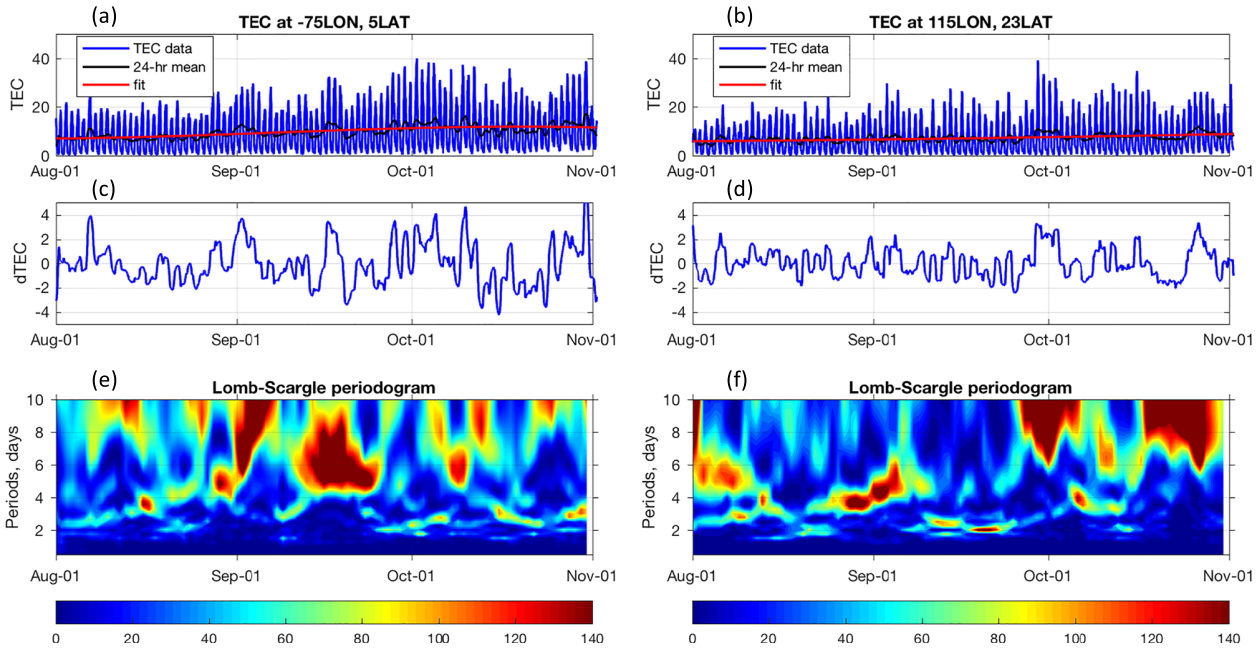

Figure 7. TEC variations in the northern crest of EIA in the American sector (left side,75°W, 5°N) and in the Asian sector (115°E, 23°N). Top panels (a, b) show TEC variations from 1 August to 1 November 2019 (blue line), 24-h running mean of this TEC (black line), and polynomial fit to 24-h mean (red line). The middle panels (c, d) show residual TEC. The bottom panels (e, f) show power spectra of residual TEC.

be related to the amplification of DE3 tide during Antarctic SSW. Additional observational and numerical studies are needed to test our suggestion about SSW modification of DE3 tide.

Our analysis also suggests that large longitudinal variation in ionospheric effects during Antarctic SSW of September 2019 is also manifested in different PW effects. Figure 7 compares these effects in the northern crest of EIA at 15° magnetic latitude in the American sector at 75°W, 5°N (Figure 7a) and Asian sector at 115°E, 23°N (Figure 7b). Top panels show diurnal variation in TEC at these locations from 1 August to 1 November 2019 (blue line) binned in 30-min intervals. To focus on multiday oscillations, we obtained a running 24-h mean of TEC (black line) and a seasonal variation of this 24-h mean from a polynomial fit (red line). The middle panels in Figure 7 present a difference between a running 24-h mean TEC and a seasonal variation. To extract temporal evolution in significant periodicities, we applied Lomb-Scargle analysis to 10-day segments of differential TEC, starting on 1 August 2019 and advancing 24 h at each step until 1 November 2019. As we preserved 30-min resolution from the initial data, our results are significant at 95% significance level for spectral power exceeding 9.1 units. The bottom panels of Figure 7 show periodograms produced by this procedure. In the American sector at 75°W, the most striking feature is a large amplification in the TEC oscillations with a 5- to 8-day period in the middle of September that coincides with decrease in stratospheric winds during Antarctic SSW. This 5- to 8-day wave corresponds to large TEC variations presented earlier in Figure 5a. It is also fully consistent with amplification in 5- to 6-day wave reported by Yamazaki et al. (2020) in Swarm daytime data. However, TEC observations at 115°E reveal a different behavior: oscillations with 5- to 6-day period during SSW in mid-September are weaker than during non-SSW periods. Instead, this longitude reveals an amplification with 2- to 3-day periods. PWs are not expected to propagate to ionospheric altitudes directly, but can impact the upper atmosphere indirectly, through modulation of tides extending into upper thermosphere (Liu, 2016; Liu et al., 2012; Oberheide et al., 2009), through modulation of equatorial vertical plasma drifts modified by tides propagating to the lower thermosphere (Liu & Richmond, 2013), through changes in thermospheric composition related to tidal dissipation (Yamazaki & Richmond, 2013; Yue & Wang, 2014), or through modulation of gravity waves (Liu, 2016). Our observations of large longitudinal differences in PW oscillations in TEC suggest that longitudes with higher median TEC and higher "quiet dynamic state" variability are also more influenced by upward-propagating

Journal of Geophysical Research: Space Physics 10.1029/2020JA028199

stratospheric PWs, presumably through modulation of non-migrating tides or gravity waves. We will further explore this suggestion in a more extended follow-up study.

3. Conclusions

The rare Antarctic SSW of September 2019 has provided a unique opportunity to examine whether stratospheric weather over Antarctica can produce ionospheric disturbances. Although the SSW of September 2019 is considered a minor event according to the standard World Meteorological Organization (WMO) definition, it was associated with several record-breaking changes in the SH stratosphere. We have examined TEC perturbations in the low-latitude ionosphere and have concluded the following.

1. Comparison of ionospheric TEC in mid-September of 2019 with "dynamically quiet" mean behavior reveals prominent quasi-semidiurnal variations that are similar to variations associated with Arctic SSW. However, the semidiurnal behavior does not persist for an extended period of time and strongly varies with longitude, indicating that the ionosphere is likely more dynamically disturbed during this Antarctic SSW than during a typical Arctic SSW.
2. We identify both positive and negative ionospheric disturbances that exceed 90th percentile (or decrease below 10th percentile) of TEC values for "dynamically quiet" September equinox and low solar flux conditions. In terms of absolute changes, TEC increased or decreased by up to a factor of 2 and more.
3. The observed TEC disturbances are consistent with several mechanisms previously identified for Arctic SSW events: perturbation of semidiurnal tides, enhanced disturbances with PW periods, in particular the 5- to 6-day wave and the 2-day wave, and decrease in daily mean TEC that could result from reduction in thermospheric O/N_2 density ratio. The study also suggests new aspects that connect the stratospheric weather to the state of the ionosphere.
4. We demonstrate a strong longitudinal variation in the observed TEC disturbances, when qualitatively different behavior can be observed at locations separated by as little as 30° in longitude.
5. Stronger TEC disturbances are observed at longitudes that correspond to higher electron density in response to variations in non-migrating diurnal eastward-propagating (DE3) tide. We suggest that amplification of DE3 tide during SSW plays a major role in the observed ionospheric behavior.
6. Our results indicate that stratospheric weather can strongly influence the state of the ionosphere not only during December–February period (winter in the NH), but also during September (equinox conditions).

Data Availability Statement

All of the data used in this paper are publicly available. GPS TEC data products and access through the Madrigal distributed data system are provided to the community (http://www.openmadrigal.org) by the Massachusetts Institute of Technology (MIT) under support from U.S. National Science Foundation grant AGS-1762141. Data for TEC processing are provided from the following organizations: UNAVCO, Scripps Orbit and Permanent Array Center, Institut Geographique National, France, International GNSS Service, The Crustal Dynamics Data Information System (CDDIS), National Geodetic Survey, Instituto Brasileiro de Geografia e Estatística, RAMSAC CORS of Instituto Geográfico Nacional de la República Argentina, Arecibo Observatory, Low-Latitude Ionospheric Sensor Network (LISN), Topcon Positioning Systems, Inc., Canadian High Arctic Ionospheric Network, Centro di Ricerche Sismologiche, Système d'Observation du Niveau des Eaux Littorales (SONEL), RENAG: REseau NAtional GPS permanent, GeoNet—the official source of geological hazard information for New Zealand, GNSS Reference Networks, Finnish Meteorological Institute, and SWEPOS—Sweden.

MLS v4.2 data are available from the NASA Goddard Space Flight Center for Earth Sciences Data and Information Services Center (DISC) at https://mls.jpl.nasa.gov/data/. MERRA-2 data are available at MDISC, managed by the NASA Goddard Earth Sciences (GES) DISC at https://gmao.gsfc.nasa.gov/reanalysis/.

Acknowledgments

L. P. G., V. L. H., and K. R. G. acknowledge support from NASA Grant 80NSSC19K0262. L. P. G., S. R. Z., and A. J. C. were also supported by ONR Grant N00014-17-1-2186. V. L. H. also acknowledges support by NASA Grants NNX17AB80G and 80NSSC18K1046.

References

Akmaev, R. A., Fuller-Rowell, T. J., Wu, F., Forbes, J. M., Zhang, X., Anghel, A. F., et al. (2008). Tidal variability in the lower thermosphere: Comparison of Whole Atmosphere Model (WAM) simulations with observations from TIMED. *Geophysical Research Letters*, *35*, L03810. https://doi.org/10.1029/2007GL032584

Butler, A., Seidel, D., Hardiman, S., Butchart, N., Birner, T., & Match, A. (2015). Defining sudden stratospheric warmings. *Bulletin of the American Meteorological Society*, *96*(11), 1913–1928. https://doi.org/10.1175/BAMS-D-13-00173.1

Charlton, A. J., & Polvani, L. M. (2007). A new look at stratospheric sudden warmings. Part I: Climatology and modeling benchmarks. *Journal of Climate*, *20*(3), 449–469. https://doi.org/10.1175/JCLI3996.1

Chau, J. L., Fejer, B. G., & Goncharenko, L. P. (2009). Quiet variability of equatorial ExB drifts during a sudden stratospheric warming event. *Geophysical Research Letters*, *36*, L05101. https://doi.org/10.1029/2008GL036785

Chau, J. L., Goncharenko, L. P., Fejer, B. G., & Liu, H.-L. (2012). Equatorial and low latitude ionospheric effects during sudden stratospheric warming events. *Space Science Reviews*, *168*(1-4), 385–417. https://doi.org/10.1007/s11214-011-9797-5

England, S. L. (2012). A review of the effects of non-migrating atmospheric tides on the Earth's low-latitude ionosphere. *Space Science Reviews*, *168*(1–4), 211–236. https://doi.org/10.1007/s11214-011-9842-4

England, S. L., Maus, S., Immel, T. J., & Mende, S. B. (2006). Longitudinal variation of the *E*-region electric fields caused by atmospheric tides. *Geophysical Research Letters*, *33*, L21105. https://doi.org/10.1029/2006GL027465

Fagundes, P. R., Goncharenko, L. P., de Abreu, A. J., Venkatesh, K., Pezzopane, M., de Jesus, R., et al. (2015). Ionospheric response to the 2009 sudden stratospheric warming over the equatorial, low, and middle latitudes in the South American sector. *Journal of Geophysical Research: Space Physics*, *120*, 7889–7902. https://doi.org/10.1002/2014JA020649

Fejer, B. G., Olson, M. E., Chau, J. L., Stolle, C., Lühr, H., Goncharenko, L. P., et al. (2010). Lunar-dependent equatorial ionospheric electrodynamic effects during sudden stratospheric warmings. *Journal of Geophysical Research*, *115*, A00G03. https://doi.org/10.1029/2010JA015273

Forbes, J. M., & Zhang, X. (2012). Lunar tide amplification during the January 2009 stratosphere warming event: Observations and theory. *Journal of Geophysical Research: Space Physics*, *117*, A12312. https://doi.org/10.1029/2012JA017963

Fuller-Rowell, T., Wu, F., Akmaev, R., Fang, T.-W., & Araujo-Pradere, E. (2010). A whole atmosphere model simulation of the impact of a sudden stratospheric warming on thermosphere dynamics and electrodynamics. *Journal of Geophysical Research*, *115*, A00G08. https://doi.org/10.1029/2010JA015524

Goncharenko, L., Harvey, V., Liu, H., & Pedatella, N. (2021). Sudden stratospheric warming impacts on the ionosphere-thermosphere system—A review of recent progress. In C. Huang & G. Lu (Eds.), *Space physics and aeronomy: Advances in ionospheric research: Current understanding and challenges* (Vol. 3). Hoboken, NJ: Wiley.

Goncharenko, L. P., Chau, J. L., Liu, H.-L., & Coster, A. J. (2010). Unexpected connections between the stratosphere and ionosphere. *Geophysical Research Letters*, *37*, L10101. https://doi.org/10.1029/2010GL043125

Goncharenko, L. P., Coster, A. J., Chau, J. L., & Valladares, C. E. (2010). Impact of sudden stratospheric warmings on equatorial ionization anomaly. *Journal of Geophysical Research*, *115*, A00G07. https://doi.org/10.1029/2010JA015400

Goncharenko, L. P., Coster, A. J., Plumb, R. A., & Domeisen, D. I. V. (2012). The potential role of stratospheric ozone in the stratosphere-ionosphere coupling during stratospheric warmings. *Geophysical Research Letters*, *39*, L08101. https://doi.org/10.1029/2012GL051261

Goncharenko, L. P., Coster, A. J., Zhang, S.-R., Erickson, P. J., Benkevitch, L., Aponte, N., et al. (2018). Deep Ionospheric Hole Created by Sudden Stratospheric Warming in the Nighttime Ionosphere. *Journal of Geophysical Research: Space Physics*, *123*, 7621–7633. https://doi.org/10.1029/2018JA025541

Gu, S.-Y., Ruan, H., Yang, C.-Y., Gan, Q., Dou, X., & Wang, N. (2018). The morphology of the 6-day wave in both the neutral atmosphere and *F* region ionosphere under solar minimum conditions. *Journal of Geophysical Research: Space Physics*, *123*, 4232–4240. https://doi.org/10.1029/2018JA025302

Jin, H., Miyoshi, Y., Pancheva, D., Mukhtarov, P., Fujiwara, H., & Shinagawa, H. (2012). Response of migrating tides to the stratospheric sudden warming in 2009 and their effects on the ionosphere studied by a whole atmosphere-ionosphere model GAIA with COSMIC and TIMED/SABER observations. *Journal of Geophysical Research*, *117*, A10323. https://doi.org/10.1029/2012JA017650

Kil, H., Oh, S. J., Kelley, M. C., Paxton, L. J., England, S. L., Talaat, E., et al. (2007). Longitudinal structure of the vertical E × B drift and ion density seen from ROCSAT-1. *Geophysical Research Letters*, *34*, L14110. https://doi.org/10.1029/2007GL030018

Kil, H., Talaat, E. R., Oh, S. J., Paxton, L. J., England, S. L., & Su, S. Y. (2008). Wave structures of the plasma density and vertical E × B drift in low-latitude *F* region. *Journal of Geophysical Research*, *113*, A09312. https://doi.org/10.1029/2008JA013106

Kruger, K., Naujokat, B., & Labitzke, K. (2005). The unusual midwinter warming in the Southern Hemisphere stratosphere 2002: A comparison to Northern Hemisphere phenomena. *Journal of Atmospheric Science*, *62*(3), 603–613. https://doi.org/10.1175/JAS-3316.1

Lim, E. P., Hendon, H. H., Butler, A. H., Garreaud, R. D., Polichtchouk, I., Shepherd, T. G., et al. (2020). The 2019 Antarctic sudden stratospheric warming. *SPARC Newsletter 54* (p. 10).

Limpasuvan, V., Orsolini, Y. J., Chandran, A., Garcia, R. R., & Smith, A. K. (2016). On the composite response of the MLT to major sudden stratospheric warming events with elevated stratopause. *Journal of Geophysical Research: Atmospheres*, *121*(9), 4518–4537. https://doi.org/10.1002/2015JD024401

Lin, C. H., Hsiao, C. C., Liu, J. Y., & Liu, C. H. (2007). Longitudinal structure of the equatorial ionosphere: Time evolution of the four-peaked EIA structure. *Journal of Geophysical Research*, *112*, A12305. https://doi.org/10.1029/2007JA012455

Liu, G. P., England, S. L., Immel, T. J., Kumar, K. K., Ramkumar, G., & Goncharenko, L. P. (2012). Signatures of the 3-day wave in the low-latitude and midlatitude ionosphere during the January 2010 URSI World Day campaign. *Journal of Geophysical Research*, *117*, A06305. https://doi.org/10.1029/2012JA017588

Liu, H., Yamamoto, M., Tulasi Ram, S., Tsugawa, T., Otsuka, Y., Stolle, C., et al. (2011). Equatorial electrodynamics and neutral background in the Asian sector during the 2009 stratospheric sudden warming. *Journal of Geophysical Research*, *116*, A08308. https://doi.org/10.1029/2011JA016607

Liu, H.-L. (2016). Variability and predictability of the space environment as related to lower atmosphere forcing. *Space Weather*, *14*, 634–658. https://doi.org/10.1002/2016SW001450

Liu, H. -L., & Richmond, A. D. (2013). Attribution of ionospheric vertical plasma drift perturbations to large-scale waves and the dependence on solar activity. *Journal of Geophysical Research: Space Physics*, *118*, 2452–2465. https://doi.org/10.1002/jgra.50265

Liu, H.-L., Wang, W., Richmond, A. D., & Roble, R. G. (2010). Ionospheric variability due to planetary waves and tides for solar minimum conditions. *Journal of Geophysical Research*, *115*, A00G01. https://doi.org/10.1029/2009JA015188

McDonald, S. E., Sassi, F., & Mannucci, A. J. (2015). SAMI3/SD-WACCM-X simulations of ionospheric variability during northern winter 2009. *Space Weather*, *13*, 568–584. https://doi.org/10.1002/2015SW001223

McDonald, S. E., Sassi, F., Tate, J., McCormack, J., Kuhl, D. D., Drob, D. P., et al. (2018). Impact of non-migrating tides on the low latitude ionosphere during a sudden stratospheric warming event in January 2010. *Journal of Atmospheric and Solar-Terrestrial Physics*, *171*, 188–200. https://doi.org/10.1016/j.jastp.2017.09.012

Journal of Geophysical Research: Space Physics 10.1029/2020JA028199

Mo, X., & Zhang, D. (2020). Quasi-10 d wave modulation of an equatorial ionization anomaly during the Southern Hemisphere stratospheric warming of 2002. *Annales Geophysicae*, *38*(1), 9–16.

Mo, X. H., Zhang, D. H., Goncharenko, L. P., Hao, Y. Q., & Xiao, Z. (2014). Quasi-16-day periodic meridional movement of the equatorial ionization anomaly. *Annales Geophysicae*, *32*, 121–131. https://doi.org/10.5194/angeo-32-121-2014

Oberheide, J., Forbes, J. M., Häusler, K., Wu, Q., & Bruinsma, S. L. (2009). Tropospheric tides from 80 to 400 km: propagation, interannual variability, and solar cycle effects. *Journal of Geophysical Research*, *114*, D00I05. https://doi.org/10.1029/2009JD012388

Oberheide, J., Pedatella, N. M., Gan, Q., Kumari, K., Burns, A. G., & Eastes, R. (2020). Thermospheric composition O/N_2 response to an altered meridional mean circulation during sudden stratospheric warmings observed by GOLD. *Geophysical Research Letters*, *47*, e2019GL086313. https://doi.org/10.1029/2019GL086313

Olson, M. E., Fejer, B. G., Stolle, C., Lühr, H., & Chau, J. L. (2013). Equatorial ionospheric electrodynamic perturbations during Southern Hemisphere stratospheric warming events. *Journal of Geophysical Research: Space Physics*, *118*, 1190–1195. https://doi.org/10.1002/jgra.50142

Paes, R. R., Batista, I. S., Candido, C. M. N., Jonah, O. F., & Santos, P. C. P. (2014). Equatorial ionization anomaly variability over the Brazilian region during boreal sudden stratospheric warming events. *Journal of Geophysical Research: Space Physics*, *119*, 7649–7664. https://doi.org/10.1002/2014JA019968

Pancheva, D., & Mukhtarov, P. (2011). Stratospheric warmings: The atmosphere-ionosphere coupling paradigm. *Journal of Atmospheric and Solar-Terrestrial Physics*, *73*, 1697–1702. https://doi.org/10.1016/j.jastp.2011.03.006

Patra, A. K., Pavan Chaitanya, P., Sripathi, S., & Alex, S. (2014). Ionospheric variability over Indian low latitude linked with the 2009 sudden stratospheric warming. *Journal of Geophysical Research: Space Physics*, *119*, 4044–4061. https://doi.org/10.1002/2014JA019847

Pedatella, N. M., Chau, J. L., Schmidt, H., Goncharenko, L. P., Stolle, C., Hocke, K., et al. (2018). How sudden stratospheric warming affects the whole atmosphere. *Eos*, *99*. https://doi.org/10.1029/2018EO092441

Pedatella, N. M., & Forbes, J. M. (2010). Evidence for stratosphere sudden warming-ionosphere coupling due to vertically propagating tides. *Geophysical Research Letters*, *37*, L11104. https://doi.org/10.1029/2010GL043560

Pedatella, N. M., Fuller-Rowell, T., Wang, H., Jin, H., Miyoshi, Y., Fujiwara, H., et al. (2014). The neutral dynamics during the 2009 sudden stratosphere warming simulated by different whole atmosphere models. *Journal of Geophysical Research: Space Physics*, *119*, 1306–1324. https://doi.org/10.1002/2013JA019421

Pedatella, N. M., & Maute, A. (2015). Impact of the semidiurnal lunar tide on the midlatitude thermospheric wind and ionosphere during sudden stratosphere warmings. *Journal of Geophysical Research: Space Physics*, *120*, 10,740–10,753. https://doi.org/10.1002/2015JA021986

Qin, Y., Gu, S.-Y., Dou, X., Gong, Y., Chen, G., Zhang, S., & Wu, Q. (2019). Climatology of the quasi-6-day wave in the mesopause region and its modulations on total electron content during 2003–2017. *Journal of Geophysical Research: Space Physics*, *124*, 573–583. https://doi.org/10.1029/2018JA025981

Ren, Z., Wan, W., Liu, L., & Xiong, J. (2009). Intra-annual variation of wave number 4 structure of vertical E × B driftin the equatorial ionosphere seen from ROCSAT-1. *Journal of Geophysical Research*, *114*, A05308. https://doi.org/10.1029/2009JA014060

Rideout, W., & Coster, A. (2006). Automated GPS processing for global total electron content data. *GPS Solutions*, *10*(3), 219–228. https://doi.org/10.1007/s10291-006-0029-5

Scherhag, R. (1952). Die explosionsartigen Stratosphärenerwärmungen des Spätwinter 1951/1952 (The explosive warmings in the stratosphere of the late winter 1951/1952). *Berichte des Deutschen Wetterdienstes in der US-Zone*, *38*, 51–63.

Scherliess, L., Thompson, D. C., & Schunk, R. W. (2008). Longitudinal variability of low-latitude total electron content: Tidal influences. *Journal of Geophysical Research*, *113*, A01311. https://doi.org/10.1029/2007JA012480

Siddiqui, T. A., Maute, A., & Pedatella, N. M. (2019). On the importance of interactive ozone chemistry in earth-system models for studying mesophere-lower thermosphere tidal changes during sudden stratospheric warmings. *Journal of Geophysical Research: Space Physics*, *124*, 10,690–10,707. https://doi.org/10.1029/2019JA027193

Vieira, F., Fagundes, P. R., Venkatesh, K., Goncharenko, L. P., & Pillat, V. G. (2017). Total electron content disturbances during minor sudden stratospheric warming, over the Brazilian region: A case study during January 2012. *Journal of Geophysical Research: Space Physics*, *122*, 2119–2135. https://doi.org/10.1002/2016JA023650

Vierinen, J., Coster, A. J., Rideout, W. C., Erickson, P. J., & Norberg, J. (2016). Statistical framework for estimating GNSS bias. *Atmospheric Measurement Techniques*, *9*(3), 1303–1312. https://doi.org/10.5194/amt-9-1303-2016

Yamazaki, Y. (2013). Large lunar tidal effects in the equatorial electrojet during northern winter and its relation to stratospheric sudden warming events. *Journal of Geophysical Research: Space Physics*, *118*, 7268–7271. https://doi.org/10.1002/2013JA019215

Yamazaki, Y., Kosch, M. J., & Emmert, J. T. (2015). Evidence for stratospheric sudden warming effects on the upper thermosphere derived from satellite orbital decay data during 1967–2013. *Geophysical Research Letters*, *42*, 6180–6188. https://doi.org/10.1002/2015GL065395

Yamazaki, Y., Matthias, V., Miyoshi, Y., Stolle, C., Siddiqui, T., Kervalishvili, G., et al. (2020). September 2019 Antarctic sudden stratospheric warming: Quasi-6-day wave burst and ionospheric effects. *Geophysical Research Letters*, *47*, e2019GL086577. https://doi.org/10.1029/2019GL086577

Yamazaki, Y., & Richmond, A. D. (2013). A theory of ionospheric response to upward-propagating tides: Electrodynamic effects and tidal mixing effects. *Journal of Geophysical Research: Space Physics*, *118*, 5891–5905. https://doi.org/10.1002/jgra.50487

Yamazaki, Y., Stolle, C., Matzka, J., & Alken, P. (2018). Quasi-6-day wave modulation of the equatorial electrojet. *Journal of Geophysical Research: Space Physics*, *123*, 4094–4109. https://doi.org/10.1029/2018JA025365

Yue, J., & Wang, W. (2014). Changes of thermospheric composition and ionospheric density caused by quasi 2 day wave dissipation. *Journal of Geophysical Research: Space Physics*, *119*, 2069–2078. https://doi.org/10.1002/2013JA019725

Appendix B

Goncharenko et al. (2021a)

Goncharenko, L. P., Harvey, V. L., Greer, K. R., Zhang, S.-R., Coster, A. J., Paxton, L. J. (2021). Impact of September 2019 Antarctic Sudden Stratospheric Warming on Mid-Latitude Ionosphere and Thermosphere over North America and Europe. Geophysical Research Letters, 48, e2021GL094517. https://doi.org/10.1029/2021GL094517

AGU ADVANCING EARTH AND SPACE SCIENCE

Geophysical Research Letters

RESEARCH LETTER
10.1029/2021GL094517

Key Points:

- Large regional ionospheric anomalies at northern hemisphere middle latitudes are linked to the 2019 Antarctic sudden stratospheric warming
- The ionospheric response has a quasi-semidiurnal behavior and is most likely driven by more than one mechanism
- We emphasize the potential role of thermospheric zonal wind and magnetic declination in the formation of these disturbances

Correspondence to:
L. P. Goncharenko,
lpg@mit.edu

Citation:
Goncharenko, L. P., Harvey, V. L., Greer, K. R., Zhang, S.-R., Coster, A. J., & Paxton, L. J. (2021). Impact of September 2019 Antarctic sudden stratospheric warming on mid-latitude ionosphere and thermosphere over North America and Europe. *Geophysical Research Letters*, *48*, e2021GL094517. https://doi.org/10.1029/2021GL094517

Received 24 MAY 2021
Accepted 12 JUL 2021

Impact of September 2019 Antarctic Sudden Stratospheric Warming on Mid-Latitude Ionosphere and Thermosphere Over North America and Europe

Larisa P. Goncharenko[1], V. Lynn Harvey[2], Katelynn R. Greer[2], Shun-Rong Zhang[1], Anthea J. Coster[1], and Larry J. Paxton[3]

[1]Massachusetts Institute of Technology, Haystack Observatory, Westford, MA, USA, [2]University of Colorado, Laboratory for Atmospheric and Space Physics, Boulder, CO, USA, [3]Applied Physics Laboratory, John Hopkins University, Laurel, MD, USA

Abstract Limited observational evidence indicates that ionospheric changes caused by Arctic sudden stratospheric warmings (SSWs) occur at middle latitudes in the Southern Hemisphere. However, it is not known if a similar interhemispheric linkage is produced by Antarctic SSWs. Here we examine thermospheric and ionospheric anomalies observed in September 2019 at middle latitudes in the Northern Hemisphere. We report persistent (at least 30 days) and strong (up to 80%–100%) positive anomalies in the daytime total electron content (TEC) and increases in the thermospheric O/N_2 ratio in the western region of North America. However, central and eastern regions of North America experience moderate suppression of TEC reaching 20%–40% of the baseline. Different positive and negative anomalies are observed over the European sector. We hypothesize that regional differences in the TEC response could be related to modulation of thermospheric winds during SSWs, changes in thermospheric composition, and differences in declination angle.

Plain Language Summary Sudden stratospheric warmings (SSWs) are large-scale meteorological disturbances that have been associated with profound anomalies in the Earth atmosphere, from troposphere all the way to the upper thermosphere and ionosphere. During the last decade, numerous studies shown that Arctic SSWs cause large anomalies in the low-latitude ionosphere, and few studies pointed out especially large disturbances at middle latitudes in the southern hemisphere ionosphere. However, it is not known if similar mid-latitude ionospheric anomalies on the other side of the globe are produced by Antarctic SSWs, mostly because Antarctic SSWs occur less often than Arctic ones. In this study we analyze ionospheric and thermospheric observations in September 2019, when a very strong SSW developed over Antarctica. We found both positive and negative disturbances in the thermospheric O/N_2 ratio and total electron content over North America and over Europe. Surprisingly, these disturbances are limited to narrow (20–40°) longitude ranges, differ between North America and Europe, and persist for a long time. We discuss the reasons why these anomalies occur only at specific longitudes and suggest that differences in magnetic declination angle play an important role as they affect how SSW-modified thermospheric wind influences ionospheric electron density.

1. Introduction

Significant progress in understanding mechanisms connecting the lower and upper atmosphere was achieved within the last decade by focusing on the analysis of sudden stratospheric warming events (SSWs). SSWs are large-scale phenomena characterized by rapid temperature increases in the winter high-latitude stratosphere, disruptions to the polar vortex, and decelerations or reversals of the stratospheric zonal winds. A review by Baldwin et al. (2021) summarizes the current state of knowledge about the mechanisms driving SSWs. Dramatic anomalies associated with SSWs are not limited to the stratosphere and have large impacts from the ocean to the ionosphere (see Pedatella et al., 2018 and references therein). Downward propagation of stratospheric disturbances affects tropospheric weather and leads to anomalous cold air outbreaks over Europe, Asia, and the eastern U.S. (Kolstad et al., 2010; King et al., 2019; Lehtonen & Karpechko, 2016). Dramatic changes are observed in the thermosphere and ionosphere where plasma temperatures can drop by ~100–150K (L. Goncharenko & Zhang, 2008; Conde & Nicolls, 2010) and plasma density varies by up to

Geophysical Research Letters 10.1029/2021GL094517

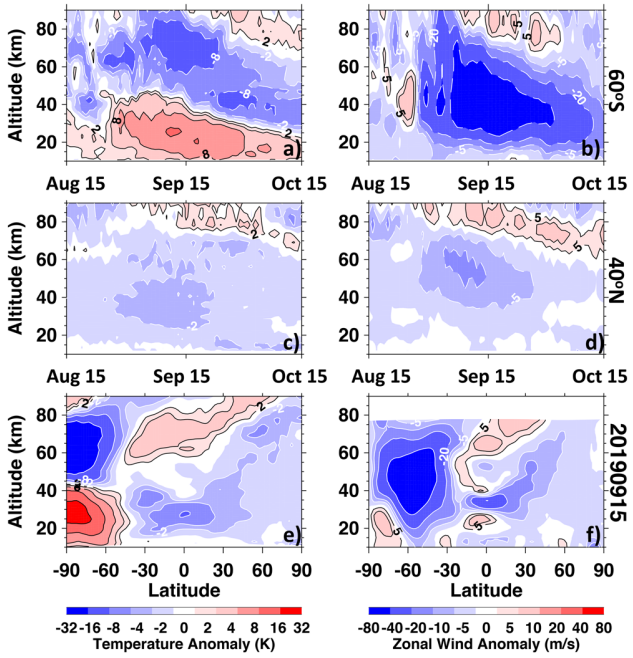

Figure 1. Altitude-time sections of temperature and zonal wind anomalies in the middle atmosphere during the September 2019 Antarctic sudden stratospheric warmings event. Anomalies are computed by subtracting the 2004–2020 (except 2019) average from each day in 2019. (a) Temperature anomaly at 60°S. (b) Zonal mean zonal wind anomaly at 60°S. (c) Temperature anomaly at 40°N. (d) Zonal mean wind anomaly at 40°N. (e) Latitude-height section of the temperature anomaly on September 15, 2019. (f) Latitude-height section of the zonal wind anomaly on September 15, 2019. Panels (a)–(e) use Aura MLS data, panel (f) is based on MERRA2 data. Note the nonlinear color bar levels for both temperature and zonal wind anomalies.

a factor of 2 (Chau et al., 2010; L. P. Goncharenko et al., 2010; L. Goncharenko et al., 2013). Ionospheric and thermospheric anomalies related to SSWs are discussed in reviews by Chau et al. (2012) and L. Goncharenko et al. (2021).

One of the surprising features of ionospheric disturbances during Arctic SSWs is that the largest variations are seen not at the high or middle latitudes of the Northern Hemisphere (NH), but at low latitudes and middle latitudes of the Southern Hemisphere (SH). Low-latitude variations have a semi-diurnal character and reach their peaks near the crests of Equatorial Ionization Anomaly (EIA), located within 10–20° latitude of the magnetic equator. Both observational and modeling studies suggest that tropical variations are produced mainly through the vertical transport of plasma by enhanced electric field due to amplification of the E-region dynamo mechanism (Fang et al., 2012; Pedatella & Liu, 2013). Ionospheric variations at the SH middle latitudes are much less understood. Fagundes et al. (2015) reported increases in total electron content (TEC) by almost a factor of 2 at a mid-latitude location (Rio Grande: 53.8°S, 67.8°W), during the 2009 SSW. L. P. Goncharenko et al. (2018) saw similarly large increases in the daytime peak electron density N_mF2 in Port Stanley (51.6°S, 57.9°W) ionosonde data during the 2013 SSW event. Analysis of TEC data along the 75°W longitude for the same event shows that nighttime decreases in TEC are largest near 40°S, and much weaker in the NH middle latitudes (L. P. Goncharenko et al., 2018). Pedatella and Maute (2015) noted larger ionospheric variations during two Arctic SSW events in the SH mid-latitudes using both observations and simulations. They suggested that the mechanism responsible for these mid-latitude disturbances is a modulation of thermospheric wind by an amplified semidiurnal lunar tide (Forbes & Zhang, 2012). However, simulations by Limpasuvan et al. (2016) indicated stronger amplification of semidiurnal tides in NH. This conclusion implies a stronger ionospheric response to Arctic SSWs in the NH, which contrasts with observational results discussed above.

SSW-induced ionospheric anomalies in the middle latitudes of the opposite hemisphere and the mechanisms responsible for such anomalies are not fully understood. One of the reasons for this is the scarcity of observational data at SH middle latitudes. A record strong Antarctic SSW that occurred in September 2019 (Lim et al., 2020; Shen et al., 2020) enables addressing the question of inter-hemispheric coupling during SSWs with unprecedented detail, as NH middle latitudes have exceptional coverage due to the dense networks of GNSS receivers. Studies of this SSW event demonstrate a record strong quasi 6-days wave (Q6DW) in the mesosphere-lower thermosphere (MLT) region and low-latitude ionosphere (Yamazaki et al., 2020), multiple dynamo processes driving the Q6DW in the ionosphere (Lin et al., 2020), propagation of the Q6DW to 25–30°N in the Asian sector and a strong longitudinal variation in the ionospheric Q6DW at low latitudes (L. P. Goncharenko et al., 2020; Gu et al., 2021; Yamazaki et al., 2020). Other features include a Q10DW in the NH MLT (He et al., 2020), a Q2DW in TEC in the Asian sector at low latitudes, and quasi-semidiurnal disturbances in TEC at low latitudes (L. P. Goncharenko et al., 2020). Here we utilize a variety of observational data to demonstrate that this Antarctic SSW produced anomalies in the middle-latitude thermosphere and ionosphere in the NH and to suggest mechanisms responsible for these anomalies.

2. Results and Discussion

2.1. Stratospheric and Mesospheric Anomalies

Figure 1 illustrates spatio-temporal variations in anomalies from the stratosphere to the MLT during the September 2019 SSW. These anomalies follow a well-known "quad pattern", when polar SH stratospheric warming and mesospheric cooling are accompanied by tropical stratospheric cooling and mesospheric

Geophysical Research Letters 10.1029/2021GL094517

warming (Limpasuvan et al., 2016; Randel, 1993). This quad pattern is associated with anomalous stratospheric and mesospheric circulation cells that result in adiabatic warming in the polar stratosphere and adiabatic cooling in the tropical stratosphere (and vice versa in the mesosphere). Figures 1a and 1b show the development of temperature and zonal wind anomalies, respectively, at 60°S. Positive stratospheric temperature anomalies at 60°S (values exceeding 8K, Figure 1a) persisted from late August to early October and peaked on 13 September. Mesospheric cooling between 60 and 80 km also reached its peak in mid-September. Negative zonal wind anomalies at 60°S (values less than −20 m/s, Figure 1b) which are physically consistent with the temperature anomalies, persist from late August through mid-October, and peak in mid-September. Figures 1c and 1d demonstrate that long-lasting middle atmospheric anomalies, while significantly weaker, are also observed at 40°N. Figure 1c shows SSW-induced stratospheric cooling of 2–3 K at 40°N in mid-September. Likewise, Figure 1d shows negative zonal wind anomalies in September, with values less than −5 m/s (a strengthening of the summer easterly jet) from 40–60 km. We note that the negative zonal wind anomaly reaches 9 m/s at 40°N and 50 km and represents a significant departure from the average background wind of −12 m/s (not shown here). The negative temperature (Figure 1c) and zonal wind (Figure 1d) anomalies are accompanied by positive anomalies near 80 km, as expected (e.g., Goldberg et al., 2004; Gumbel & Karlsson, 2011). Figure 1e further illustrates the global nature of the SSW-induced temperature anomalies on September 15, 2019. In the extreme case of the September 2019 SSW, tropical temperature anomalies extend to the NH mid-latitudes. Zonal wind anomalies (Figure 1f) also extend to middle and high latitudes of the NH, albeit they are weaker than in the SH. Pedatella and Liu (2013) showed that changes in the zonal mean middle atmospheric winds and temperatures are the primary drivers of the enhancement in the semidiurnal solar and lunar tides during SSWs, thus we can expect that during this Antarctic SSW event, semidiurnal tidal amplitudes are enhanced from SH high latitudes to NH mid-latitudes.

2.2. Ionospheric Anomalies

For the purposes of this study, we used the CEDAR Madrigal TEC database and "quiet dynamic state" baseline (L. Goncharenko, 2021), as it provides a quantitative description of typical variability. The TEC data we used has a 1 × 1 degree resolution in latitude and longitude and 5 min resolution in time, and provides excellent coverage over continental U.S. and Europe (Vierinen et al., 2016). To clearly identify effects of the SSW and separate them from ionospheric variations due to changes in solar cycle, season, and geomagnetic activity, we tested two approaches for the description of background conditions. In the first approach, we followed the methodology originally described in L. P. Goncharenko et al. (2020) to develop the "quiet dynamic state" baseline for September low solar activity conditions (L. Goncharenko, 2021). We have also tested an alternative approach through the use of the empirical North America TEC model (Chen et al., 2015). We have concluded that these two approaches are consistent within 1.2–2.0 TECu average error estimates. Results of this study therefore do not depend on the selected method to describe background conditions.

This study focuses on anomalies over North America and Europe, where TEC data quality is highest. We hypothesize that the striking regional anomaly over the western U.S. is caused by an abatement or even reversal of the thermospheric zonal wind modified by the SSW, as zonal winds strongly influence ionospheric electron density in areas with larger magnetic declination angles (S.-R. Zhang et al., 2011; 2012). Figure 2 illustrates the spatial development of ionospheric anomalies at NH middle latitudes. Figures 2a and 2b show TEC anomalies over North America on September 15, 2019 during morning (14 UT) and afternoon (22 UT) hours, respectively. Anomalies are expressed as a percentage change relative to the quiet time baseline. In the morning sector (Figure 2a), the prevailing change is a decrease of TEC by 20%–40%, with largest decreases over southern California (110–125°W, 30–50°N). In the afternoon sector (22UT, Figure 2b), the most striking feature is an increase up to 80%–100% in TEC observed at the same location. This positive daytime anomaly reaches its maximum at 40°N and is separated from low-latitude anomalies observed near the crests of the EIA (L. P. Goncharenko et al., 2020). The central and eastern regions of North America experience only minor TEC variations, within the expected daily variability. The inlets on the right side of Figure 2 show declination angles (in degrees) over specific regions. The TEC variations observed over the western U.S. where declination angle exceeds 10° could be generated by an enhanced semidiurnal tide in the zonal wind, with more eastward wind in the morning (providing downward plasma motion and faster recombination) and more westward wind in the afternoon (providing upward plasma motion and slower

Geophysical Research Letters 10.1029/2021GL094517

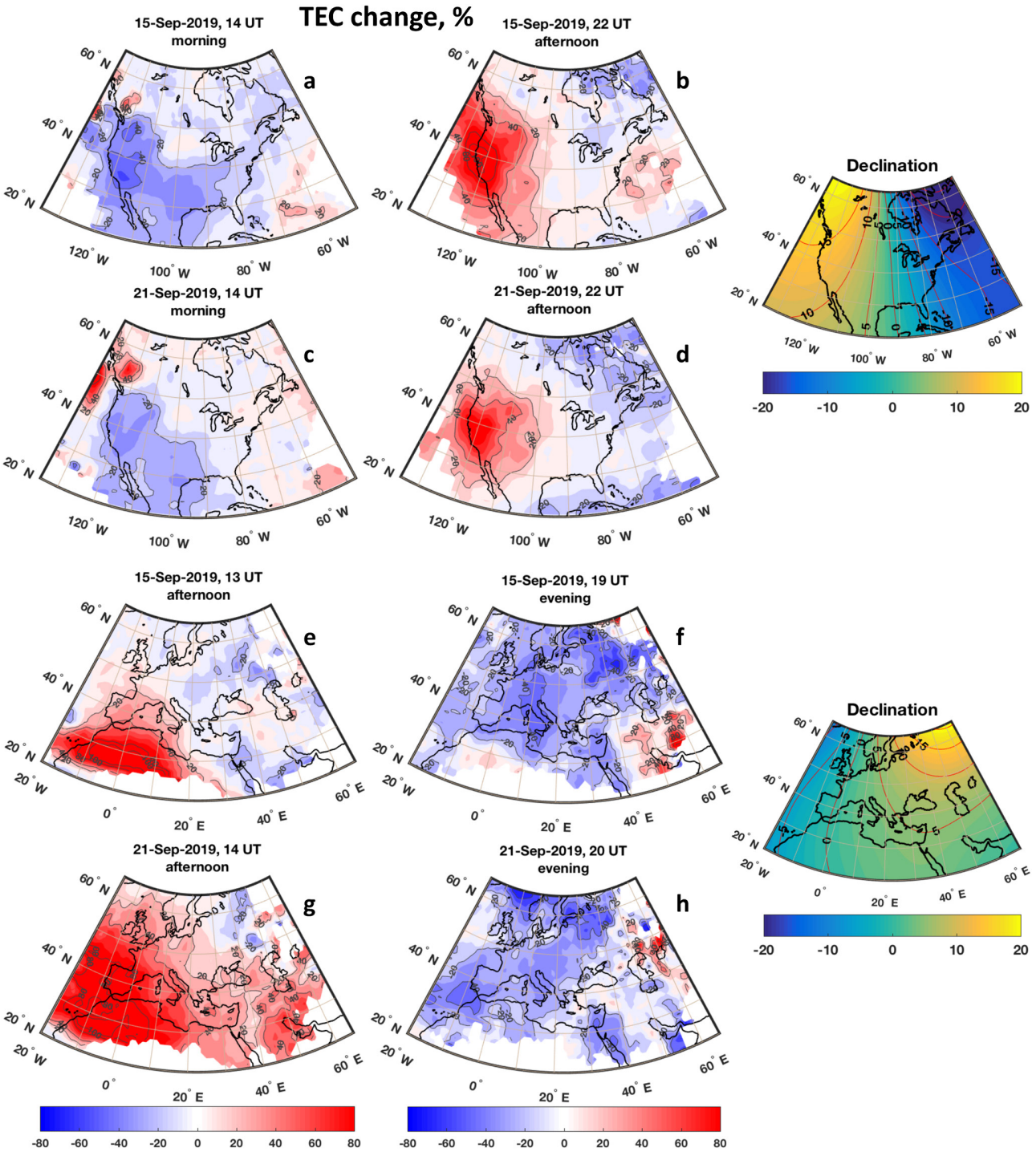

Figure 2. Ionospheric anomalies observed in September 2019. (a) and (b) Anomalies on September 15, 2019 over North America in the morning sector (14 UT) and afternoon sector (22 UT). (c) and (d) Same as (a)–(b), but for September 21, 2019. (e) and (f) Anomalies over North Africa and Europe on September 15, 2019 around noontime (13 UT) and in the evening (19 UT). (g) and (h) Same as (e)–(f), but for September 21, 2019. Inlets on the right side show variations in the magnetic declination angle over given regions.

Geophysical Research Letters 10.1029/2021GL094517

recombination). The observed quasi-semidiurnal variation in TEC is strongest in mid-September, but is sustained for an extended period of time, as shown in Figures 2c and 2d for September 21, 2019.

The nature of TEC anomalies over Europe is very different, as illustrated in Figures 2e and 2f for September 15, 2019. Large positive anomalies, 100%–120% from the baseline, are seen in the early afternoon (13 UT) in a narrow longitudinal region (20°W–20°E) at 25–30°N, that is, near the northern crest of the EIA. Positive anomalies subside to 10%–20% poleward of 40°N. The magnetic equator is located at ∼10°N at these longitudes and ionospheric disturbances at the EIA crests are strongly linked to perturbations in vertical drifts and electric fields through the E-region dynamo (Liu 2016). The positive disturbances over northwest Africa and western Europe are likely driven by perturbations in the electric field. The negative 20%–40% disturbances over Europe, which are observed several hours later at 19UT (Figure 2f), are not connected to the EIA and are seen over a broader range of latitudes, indicating contributions from mechanisms other than the electric field. Although TEC anomalies over Europe also exhibit quasi-semidiurnal variations, similar to the quasi-semidiurnal anomalies over North America, the local times of positive and negative variations are different, indicating contributions from different mechanisms.

As geomagnetic activity often increases during equinox (Lyatsky et al., 2001; Russell & McPherron, 1973), our observations of ionospheric anomalies related to this Antarctic SSW illustrate the need to include lower atmospheric forcing in ionosphere-thermosphere studies to avoid misinterpretation of drivers and mechanisms, as suggested by Hagan et al. (2015) and Pedatella (2016). The largest positive TEC anomalies over Europe are seen on September 21, 2019 (Figure 2g), reaching higher latitudes and spanning a wider range of longitudes than on September 15. Negative TEC anomalies observed several hours later remained at the 20%–40% level (Figure 2h). As the SSW of September 2019 is associated with a record strong quasi-6-days wave in the middle atmosphere and low-latitude ionosphere (L. P. Goncharenko et al., 2020; Gu et al., 2021; Lin et al., 2020; Miyoshi & Yamazaki, 2020; Yamazaki et al., 2020), the timing of the peak TEC anomalies on September 15, 2019 and September 21, 2019 indicates that they are linked to quasi-6-days oscillations that peak near the crests of EIA. Spectral analysis of TEC (not shown here) confirms the presence of oscillations with periods of 4–8 days in the extended latitudinal span in the European sector The regional nature of these disturbances could be related to secondary waves generated by the non-linear interaction between the quasi-6 days wave and the migrating semidiurnal tide (Miyoshi & Yamazaki, 2020). We note that both days, September 15 and 21, 2019 (as well as preceding days) were geomagnetically very quiet, with Kp = 1–3 and Kp = 1–2+. The magnitude of the TEC disturbances observed at middle latitudes during this SSW event is comparable to positive and negative effects (Buonsanto, 1999; Prolss, 1995) of geomagnetic storms.

The differences in the baseline TEC behavior between the western and eastern U.S. are particularly large in our solar minimum condition case, and are likely to be enhanced by longitudinal differences in thermospheric zonal winds (K. Zhang et al., 2018). Strong daytime eastward winds seen by K. Zhang et al. (2018) at longitudes with positive magnetic declination (90–150°W) work to decrease electron density by moving ionospheric plasma to lower altitudes with higher recombination rates. Weakening or a reversal in this eastward zonal wind direction increases electron density and leads to higher TEC values. Observations of larger daytime TEC increases and larger nighttime decreases over the western U.S. in comparison with the eastern U.S. seen in Figures 2a–2d, 3a and 3b suggest that changes in the zonal wind during SSWs lead to the observed TEC behavior. As our ability to properly interpret TEC observations is hindered by the lack of observations of thermospheric winds, this hypothesis needs to be tested with model simulations and additional case studies. Figure 3 compares the baseline (median) with TEC observations during September 14–16, 2019 over North America (left panels, Figures 3a and 3b) and during September 20–22, 2019 over Europe (right panels, Figures 3c and 3d). Dramatic daytime (∼18–24 UT) increases in TEC in the western part of the U.S. (Figure 3a) exceed the 90th percentile of typical variability. TEC suppression is observed from nighttime to morning hours (∼3–15 UT), with negative anomalies often below tenth percentile. Maximum negative and positive variations occur several hours apart and exhibit a semidiurnal pattern. Similar disturbances are seen between 125 and 90°W (not shown), albeit with reduced strength. The TEC variations over the central and eastern U.S. have the same general character but smaller magnitudes and are mostly within expected quiet-time variability.

Over the eastern U.S. (75°W, Figure 3b), the dominant signature is TEC suppression which is observed at most times of the day. We note large differences in the baseline TEC behavior (solid black line) between the

Geophysical Research Letters 10.1029/2021GL094517

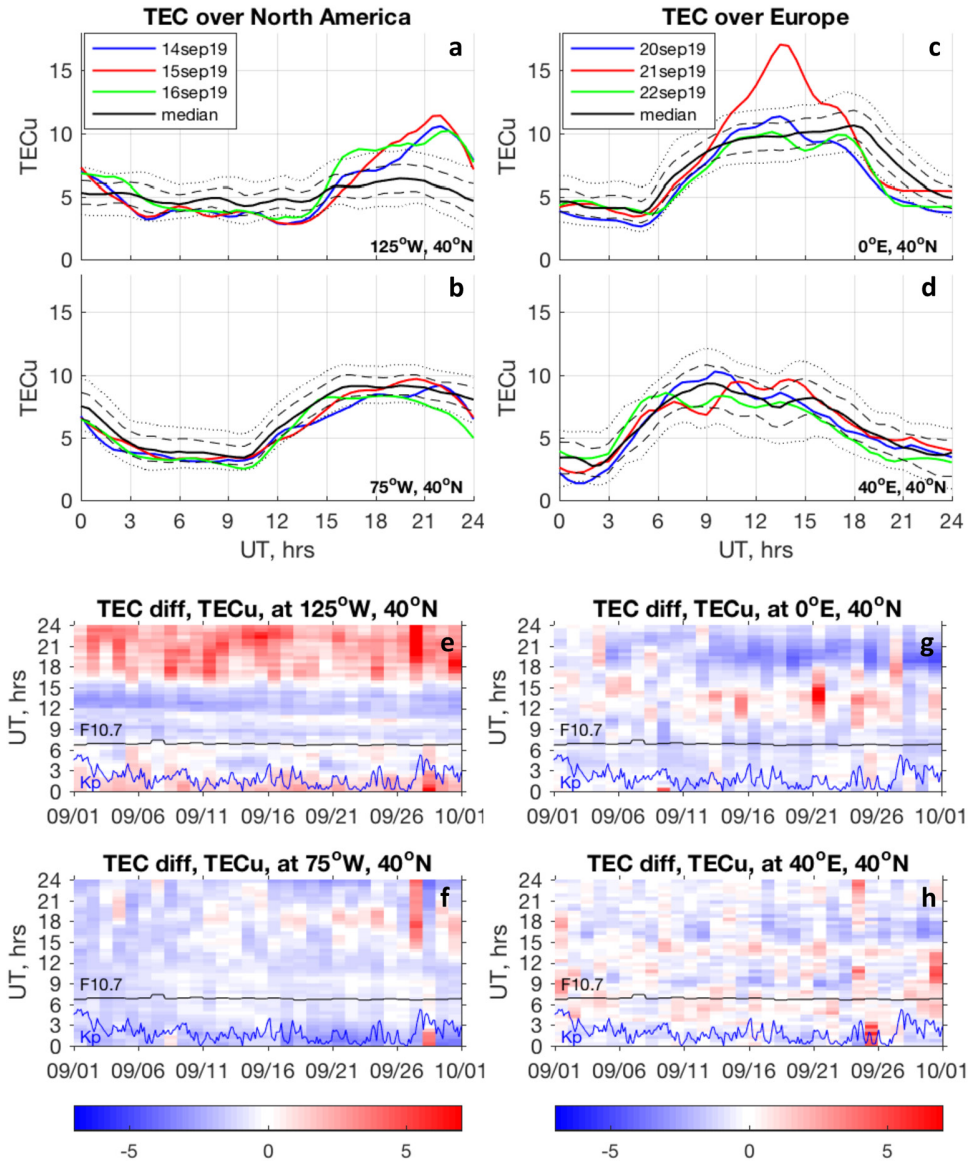

Figure 3. (Top part) TEC variations at 40°N at different longitudes in comparison with baseline. Panels (a–b) show variations over North America on September 14-16, 2019. Panels (c–d) show variations over Europe on September 20–22, 2019. Thin dash lines show 25th and 75th percentiles and dotted lines show 10th and 90th percentiles to illustrate the level of typical quiet-time variability. (Bottom part) Evolution of TEC anomalies in absolute units (TECu) in September 2019 at selected mid-latitude locations over North America (panels e–f) and Europe (panels g–h). Variations in F10.7 index (divided by 10, black line) and Kp index (blue line) provide context for the TEC anomalies.

western U.S. (125°W, Figure 3a) and the eastern U.S. (75°W, Figure 3b): daytime TEC is much larger over the eastern U.S. than over the western U.S., while nighttime TEC is higher over the western U.S. In other words, the ratio of the diurnal TEC maximum to the diurnal TEC minimum is larger over the eastern U.S. than over the western U.S. Such longitudinal differences in the baseline are produced by combined effects of thermospheric zonal winds and magnetic declination (S.-R. Zhang et al., 2011, 2012) and are at least partially responsible for the regional nature of the observed TEC anomalies.

The TEC variations over Europe are illustrated in Figures 3c and 3d (right panels) for September 20–22, 2019, around the time of the largest disturbances shown in Figure 2g. A sharp daytime peak on September 21 to highly anomalous TEC values (30% higher than the 90th percentile) was accompanied by a strong

Geophysical Research Letters 10.1029/2021GL094517

decrease in the afternoon. Surrounding days experienced only minor daytime increases, within typical quiet time variations, and TEC suppression that dominated at most times of the day. Similar to observations over North America, significant positive TEC variations are seen only in a narrow longitudinal band; this signature subsides toward the east (at 20°E), and no obvious disturbances are seen at 40°E (Figure 3d) or 60°E (not shown).

The long-lasting changes in TEC over the western U.S. and Europe are consistent with long-lasting anomalies in the middle atmosphere shown in Figure 1 and imply that prolonged anomalies in the stratospheric wind system are imprinted on the thermosphere-ionosphere system for an extended period of time. To illustrate the duration of the ionospheric anomalies, the bottom portion of Figure 3 presents the evolution of TEC anomalies over North America (panels 3e–3f) and over Europe (panels 3g–3h) for the entire month of September 2019 at the same locations as shown in the top portion of Figure 3. The most striking feature is that in the western U.S. (125°W, Figure 3e), positive TEC anomalies are observed for the entire month of September during the daytime (~16–3 UT) while negative anomalies are observed at nighttime (~6–15 UT). This behavior is seen only in a narrow longitude band (100–130°W) and subsides to the east of 100°W (not shown). Minimal TEC anomalies are seen over the central U.S. (90°W, not shown). The eastern U.S. (75°W, panel 3f) experiences moderate suppression of TEC for most local times (except minor increases during daytime, ~17–19 UT). The TEC suppression becomes stronger, has a more pronounced quasi-semidiurnal behavior, and extends for most of September over central Europe (0–20°E, Figure 3g), but subsides by 40°E (Figure 3h).

2.3. Thermospheric Anomalies

Numerous simulations have demonstrated that dissipation of upward propagating tides can affect vertical transport of atomic oxygen in the lower thermosphere that results in a reduction of thermospheric O/N_2 ratio and, in turn, can contribute to a depletion in ionospheric electron density or TEC (Jones, Forbes & Hagan, 2014; Jones, Forbes, Hagan & Maute, 2014; Pedatella et al., 2016; Yamazaki & Richmond, 2013). Similarly, reduction in O/N_2 ratio and electron density is also expected due to the dissipation of gravity waves (Jones et al., 2020) and planetary waves (Yue & Wang, 2014). We use observations of column O/N_2 ratio ($\Sigma O\ /\ N_2$) by the Global Ultraviolet Imager (GUVI) onboard the Thermosphere, Ionosphere, Mesosphere Energetics, and Dynamics (TIMED) satellite (Meier, 2021; Paxton et al., 2017, 2021; Strickland et al., 1995; Y. Zhang & Paxton, 2021) to examine whether anomalous $\Sigma O\ /\ N_2$ variations can be attributed to the SSW of September 2019. Background thermospheric $\Sigma O\ /\ N_2$ is calculated as a median value of all observations collected from 2008 to 2018, 2020 for low solar flux conditions (F10.7 < 80), low geomagnetic activity (Ap for the current day and previous day < 13), and centered on September 15 ± 10 days. Figure 4 compares background $\Sigma O\ /\ N_2$ (black) to $\Sigma O\ /\ N_2$ observations on September 15, 2019 (red) as a function of latitude as sampled along different orbits. The main difference between the background and SSW conditions seen at all longitude sectors is a ~5%–15% depletion in $\Sigma O\ /\ N_2$ at low latitudes, ~20°S to 20°N. This depletion is consistent with a 5%–10% $\Sigma O\ /\ N_2$ decrease in Global-scale Observations of the Limb and Disk data reported by Oberheide et al. (2020) during the Arctic SSW in January 2019. It is also consistent with numerical simulations cited above, and is likely to be produced by the changes in the residual mean circulation related to the dissipation of SSW-amplified tides and waves. This decrease in the low-latitude $\Sigma O\ /\ N_2$ observation could contribute to a pronounced depletion of low-latitude TEC (L. P. Goncharenko et al., 2020), as changes in $\Sigma O\ /\ N_2$ are well correlated with changes in TEC (Tsugawa et al., 2007; Y. Zhang & Paxton, 2021; Zhao et al., 2007). However, at middle latitudes (30–50°S and 30–50°N) the $\Sigma O\ /\ N_2$ change is more complex and depends on longitude. A decrease in $\Sigma O\ /\ N_2$ seen at middle latitudes over Europe (Figures 4a and 4b) and the central and eastern U.S. (Figures 4c and 4d) likely contributes to TEC depletions that dominate ionospheric responses at these locations (Figures 3b, 3c, 3d, 3f, 3g, and 3h). However, the $\Sigma O\ /\ N_2$ anomaly becomes positive at middle latitudes over the western U.S. (Figures 4e and 4f), where an increase in the daytime TEC is observed (Figures 2b, 3a and 3e), and thus can contribute to the formation of positive ionospheric changes over this region.

Geophysical Research Letters 10.1029/2021GL094517

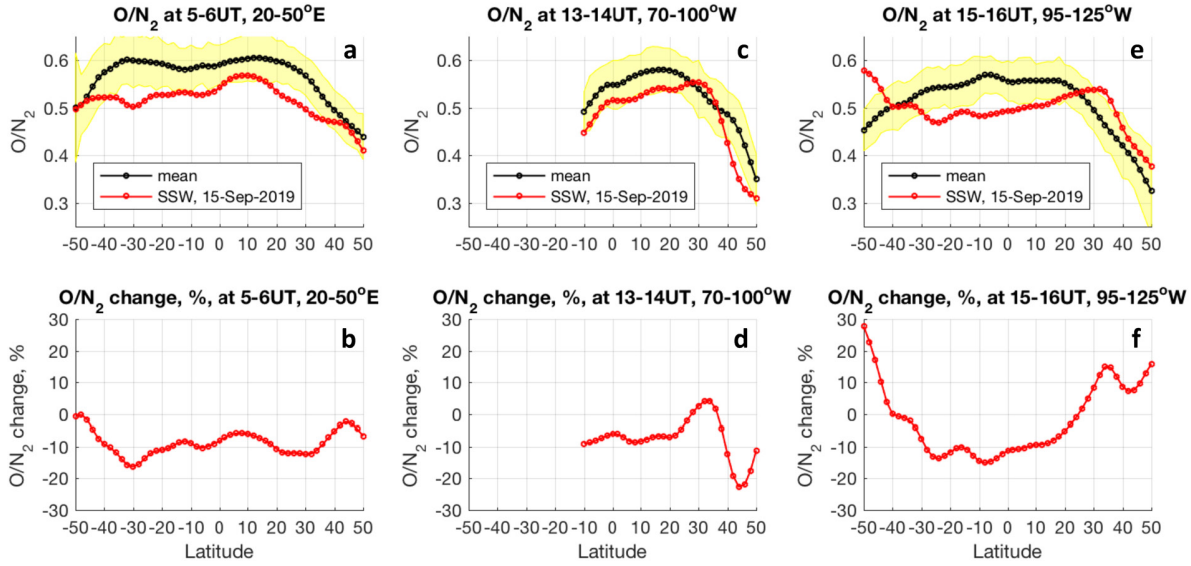

Figure 4. Evolution of thermospheric O/N2 at different longitudes. Top panels (a, c, e) compare O/N_2 variations on September 15, 2019 (red) with background O/N_2 behavior (black). Yellow shade indicates 1σ variation. Bottom panels (b, d, f) show differences in O/N_2 between the background and the SSW day.

3. Conclusions

Ionospheric observations in September 2019 provide evidence of large (50%–100%) regional anomalies at middle latitudes of the northern hemisphere linked to the Antarctic sudden stratospheric warming. We expect that changes in thermospheric zonal wind play a major role in the formation of ionospheric anomalies, especially over western North America. The ionospheric response has a quasi-semidiurnal behavior and is most likely driven by more than one mechanism, including variations in $\Sigma O / N_2$ induced by dissipation of waves (tides, gravity waves, planetary waves), variations in plasma drift due to the E-region dynamo mechanism, and variations in thermospheric wind. This study emphasizes the potential role of thermospheric zonal wind and magnetic declination in the formation of regional ionospheric disturbances at middle latitudes, in addition to the role of secondary waves generated through the interaction of quasi-6-days waves and tides previously discussed in the literature. The strongest responses are limited to narrow longitudinal areas with widths of 20–40°, while other longitudes experience similar types of perturbations but with magnitudes within typical day-to-day variability. Positive and negative anomalies over the western U.S. (100–130°W) persist for the entire month of September. Over Europe (20°W to 20°E) the dominating response is long-lasting TEC suppression superimposed on a quasi-6-days variation. Both positive and negative changes are observed in the thermospheric $\left(\Sigma O / N_2\right)$ ratio and can contribute to regional increases and suppressions of TEC.

The paper's additional key finding is that we cannot understand the variability and response of the thermosphere and ionosphere without understanding the episodic forcing from below and the extent of the persistent response of the system. Further, our ability to interpret ionospheric observations is limited by the uncertainty about the behavior of underlying thermospheric parameters, in particular the altitude profiles of winds, composition, and neutral density. The progress in understanding physical mechanisms responsible for the observed ionospheric behavior is hindered by the lack of thermospheric observations with appropriate spatio-temporal resolution.

Data Availability Statement

The TEC data used as “quiet dynamic state” baseline in this study is available at Zenodo via http://doi.org/10.5281/zenodo.5083832. MLS v4.2 data are available from the NASA Goddard Space Flight Center for Earth Sciences Data and Information Services Center (DISC) at https://mls.jpl.nasa.gov/data/. MERRA-2

data are available at https://gmao.gsfc.nasa.gov/reanalysis/. TIMED GUVI O/N2 data are available at http://guvitimed.jhuapl.edu/data_products.

Acknowledgments
Larisa P. Goncharenko, V. Lynn Harvey, and Katelynn R. Greer acknowledge support from NASA Grant 80NSSC19K0262. GNSS TEC data are provided at http://cedar.openmadrigal.org/ by MIT under support from NSF grant AGS-1952737. Larisa P. Goncharenko, Anthea J. Coster, and Shun-Rong Zhang also acknowledge support from ONR grant N00014-17-1-2186; Shun-Rong Zhang acknowledges MURI grant FA9559-16-1-0364.

References

Baldwin, M. P., Ayarzagüena, B., Birner, T., Butchart, N., Butler, A. H., Charlton-Perez, A. J., et al. (2021). Sudden stratospheric warmings. *Reviews of Geophysics*, *59*(1), e2020RG000708. https://doi.org/10.1029/2020rg000708

Buonsanto, M. (1999). Ionospheric storms—A review. *Space Science Reviews*, *88*(3–4), 563–601. https://doi.org/10.1023/A:1005107532631

Chau, J. L., Aponte, N. A., Cabassa, E., Sulzer, M. P., Goncharenko, L. P., & Gonzalez, S. A. (2010). Quiet time ionospheric variability over Arecibo during sudden stratospheric warming events. *Journal of Geophysical Research*, *115*, A00G06. https://doi.org/10.1029/2010JA015378

Chau, J. L., Goncharenko, L. P., Fejer, B. G., & Liu, H.-L. (2012). Equatorial and Low Latitude Ionospheric Effects During Sudden Stratospheric Warming Events. *Space Science Reviews*, *168*, 385–417. https://doi.org/10.1007/s11214-011-9797-5

Chen, Z., Zhang, S.-R., Coster, A. J., & Fang, G. (2015). EOF analysis and modeling of GPS TEC climatology over North America. *Journal of Geophysical Research: Space Physics*, *120*, 3118–3129. https://doi.org/10.1002/2014JA020837

Conde, M. G., & Nicolls, M. J. (2010). Thermospheric temperatures above Poker Flat, Alaska, during the stratospheric warming event of January and February 2009. *Journal of Geophysical Research*, *115*, D00N05. https://doi.org/10.1029/2010JD014280

Fagundes, P. R., Goncharenko, L. P., de Abreu, A. J., Venkatesh, K., Pezzopane, M., de Jesus, R., et al. (2015). Ionospheric response to the 2009 sudden stratospheric warming over the equatorial, low- and mid-latitudes in the South American sector. *Journal of Geophysical Research: Space Physics*, *120*, 7889–7902. https://doi.org/10.1002/2014JA020649

Fang, T.-W., Fuller-Rowell, T., Akmaev, R., Wu, F., Wang, H., & Anderson, D. (2012). Longitudinal variation of ionospheric vertical drifts during the 2009 sudden stratospheric warming. *Journal of Geophysical Research*, *117*, A03324. https://doi.org/10.1029/2011JA017348

Forbes, J. M., & Zhang, X. (2012). Lunar tide amplification during the January 2009 stratosphere warming event: Observations and theory. *Journal of Geophysical Research*, *117*, A12312. https://doi.org/10.1029/2012JA017963

Goldberg, R. A., Fritts, D. C., Williams, B. P., Lübken, F. J., Rapp, M., Singer, W., et al. (2004). The MaCWAVE/MIDAS rocket and ground-based measurements of polar summer dynamics: Overview and mean state structure. *Geophysical Research Letters*, *31*(24), L24S02. https://doi.org/10.1029/2004gl019411

Goncharenko, L. (2021). TEC over continental US and Europe for the fall equinox and low solar flux conditions [Data set]. Zenodo. https://doi.org/10.5281/zenodo.5083832

Goncharenko, L., Chau, J. L., Condor, P., Coster, A., & Benkevitch, L. (2013). Ionospheric effects of sudden stratospheric warming during moderate-to-high solar activity: Case study of January 2013. *Geophysical Research Letters*, *40*, 4982–4986. https://doi.org/10.1002/grl.50980

Goncharenko, L., Harvey, V. L., Liu, H., & Pedatella, N. (2021). Sudden stratospheric warming impacts on the ionosphere-thermosphere system—A review of recent progress. In C. Huang, & G. Lu (Eds.), *Space physics and aeronomy: Advances in ionospheric research: Current understanding and challenges* (Vol. 3). Wiley.

Goncharenko, L., & Zhang, S. (2008). Ionospheric signatures of sudden stratospheric warming: Ion temperature at middle latitude. *Geophysical Research Letters*, *35*, L21103. https://doi.org/10.1029/2008GL035684

Goncharenko, L. P., Coster, A. J., Chau, J. L., & Valladares, C. E. (2010). Impact of sudden stratospheric warmings on equatorial ionization anomaly. *Journal of Geophysical Research*, *115*, A00G07. https://doi.org/10.1029/2010JA015400

Goncharenko, L. P., Coster, A. J., Zhang, S.-R., Erickson, P. J., Benkevitch, L., Aponte, N., et al. (2018). Deep ionospheric hole created by sudden stratospheric warming in the nighttime ionosphere. *Journal of Geophysical Research: Space Physics*, *123*, 7621–7633. https://doi.org/10.1029/2018JA025541

Goncharenko, L. P., Harvey, V. L., Greer, K. R., Zhang, S.-R., & Coster, A. J. (2020). Longitudinally dependent low-latitude ionospheric disturbances linked to the Antarctic sudden stratospheric warming of September 2019. *Journal of Geophysical Research: Space Physics*, *125*, e2020JA028199. https://doi.org/10.1029/2020JA028199

Gu, S.-Y., Teng, C.-K., Li, N., Jia, M., Li, G., Xie, H., et al. (2021). Multivariate analysis on the ionospheric responses to planetary waves during the 2019 Antarctic SSW event. *Journal of Geophysical Research: Space Physics*, *126*, e2020JA028588. https://doi.org/10.1029/2020ja028588

Gumbel, J., & Karlsson, B. (2011). Intra- and inter-hemispheric coupling effects on the polar summer mesosphere. *Geophysical Research Letters*, *38*, L14804. https://doi.org/10.1029/2011GL047968

Hagan, M. E., Häusler, K., Lu, G., Forbes, J. M., & Zhang, X. (2015). Upper thermospheric responses to forcing from above and below during 1-10 April 2010: Results from an ensemble of numerical simulations. *Journal of Geophysical Research: Space Physics*, *120*, 3160–3174. https://doi.org/10.1002/2014JA020706

He, M., Chau, J. L., Forbes, J. M., Thorsen, D., Li, G., Siddiqui, T. A., et al. (2020). Quasi-10-day wave and semidiurnal tide nonlinear interactions during the Southern Hemispheric SSW 2019 observed in the Northern Hemispheric Mesosphere. *Geophysical Research Letters*, *47*(23), e2020GL091453. https://doi.org/10.1029/2020gl091453

Jones, M., Jr., Forbes, J. M., & Hagan, M. E. (2014). Tidal-induced net transport effects on the oxygen distribution in the thermosphere. *Geophysical Research Letters*, *41*, 5272–5279. https://doi.org/10.1002/2014GL060698

Jones, M., Jr., Forbes, J. M., Hagan, M. E., & Maute, A. (2014). Impacts of vertically propagating tides on the mean state of the ionosphere-thermosphere system. *Journal of Geophysical Research: Space Physics*, *119*, 2197–2213. https://doi.org/10.1002/2013JA019744

Jones, M., Jr., Siskind, D. E., Drob, D. P., McCormack, J. P., Emmert, J. T., Dhadly, M. S., et al. (2020). Coupling from the middle atmosphere to the exobase: Dynamical disturbance effects on light chemical species. *Journal of Geophysical Research: Space Physics*, *125*, e2020JA028331. https://doi.org/10.1029/2020JA028331

King, A. D., Butler, A. H., Jucker, M., Earl, N. O., & Rudeva, I. (2019). Observed relationships between sudden stratospheric warmings and European climate extremes. *Journal of Geophysical Research: Atmospheres*, *124*, 13943–13961. https://doi.org/10.1029/2019JD030480

Kolstad, E. W., Breiteig, T., & Scaife, A. A. (2010). The association between stratospheric weak polar vortex events and cold air outbreaks in the Northern Hemisphere. *Quarterly Journal of the Royal Meteorological Society*, *136*(649), 886–893. https://doi.org/10.1002/qj.620

Lehtonen, I., & Karpechko, A. Y. (2016). Observed and modeled tropospheric cold anomalies associated with sudden stratospheric warmings. *Journal of Geophysical Research: Atmospheres*, *121*, 1591–1610. https://doi.org/10.1002/2015JD023860

Lim, E. P., Hendon, H. H., Butler, A. H., Garreaud, R. D., Polichtchouk, I. Shepherd, T. G. et al. (2020). The 2019 Antarctic sudden stratospheric warming. *SPARC Newsletter*, 54, 10–13.

Limpasuvan, V., Orsolini, Y. J., Chandran, A., Garcia, R. R., & Smith, A. K. (2016). On the composite response of the MLT to major sudden stratospheric warming events with elevated stratopause. *Journal of Geophysical Research - D: Atmospheres*, *121*, 4518–4537. https://doi.org/10.1002/2015JD024401

Lin, J. T., Lin, C. H., Rajesh, P. K., Yue, J., Lin, C. Y., & Matsuo, T. (2020). Local-time and vertical characteristics of quasi-6-day oscillation in the ionosphere during the 2019 Antarctic sudden stratospheric warming. *Geophysical Research Letters*, *47*, e2020GL090345. https://doi.org/10.1029/2020GL090345

Liu, H.-L. (2016). Variability and predictability of the space environment as related to lower atmosphere forcing. *Space Weather*, *14*, 634–658. https://doi.org/10.1002/2016SW001450

Lyatsky, W., Newell, P. T., & Hamza, A. (2001). Solar illumination as cause of the equinoctial preference for geomagnetic activity. *Geophysical Research Letters*, *28*(12), 2353–2356. https://doi.org/10.1029/2000gl012803

Meier, R. R. (2021). The thermospheric column O/N_2 ratio. *Journal of Geophysical Research: Space Physics*, *126*, e2020JA029059. https://doi.org/10.1029/2020JA029059

Miyoshi, Y., & Yamazaki, Y. (2020). Excitation mechanism of ionospheric 6-day oscillation during the 2019 September sudden stratospheric warming event. *Journal of Geophysical Research: Space Physics*, *125*, e2020JA028283. https://doi.org/10.1029/2020JA028283

Oberheide, J., Pedatella, N. M., Gan, Q., Kumari, K., Burns, A. G., & Eastes, R. (2020). Thermospheric composition O/N_2 response to an altered meridional mean circulation during Sudden Stratospheric Warmings observed by GOLD. *Geophysical Research Letters*, *47*, e2019GL086313. https://doi.org/10.1029/2019GL086313

Paxton, L. J., Schaefer, R. K., Zhang, Y., & Kil, H. (2017). Far ultraviolet instrument technology. *Journal of Geophysical Research: Space Physics*, *122*(2), 2706–2733. https://doi.org/10.1002/2016ja023578

Paxton, L. J., Zhang, Y., Kil, H., & Schaefer, R. K. (2021). Exploring the upper atmosphere: Using optical remote sensing. *Upper Atmosphere Dynamics and Energetics*, 487–522. https://doi.org/10.1002/9781119815631.ch23

Pedatella, N. M. (2016). Impact of the lower atmosphere on the ionosphere response to a geo-magnetic superstorm. *Geophysical Research Letters*, *43*, 9383–9389. https://doi.org/10.1002/2016GL070592

Pedatella, N. M., Chau, J. L., Schmidt, H., Goncharenko, L. P., Stolle, C., Hocke, K., et al. (2018). How sudden stratospheric warming affects the whole atmosphere. *Eos*, *99*, Published on 20 March 2018. https://doi.org/10.1029/2018EO092441

Pedatella, N. M., & Liu, H. L. (2013). The influence of atmospheric tide and planetary wave variability during sudden stratosphere warmings on the low latitude ionosphere. *Journal of Geophysical Research: Space Physics*, *118*, 5333–5347. https://doi.org/10.1002/jgra.50492

Pedatella, N. M., & Maute, A. (2015). Impact of the semidiurnal lunar tide on the midlatitude thermospheric wind and ionosphere during sudden stratosphere warmings. *Journal of Geophysical Research*, *120*(10), 10740–10753. https://doi.org/10.1002/2015JA021986

Pedatella, N. M., Richmond, A. D., Maute, A., & Liu, H.-L. (2016). Impact of semidiurnal tidal variability during SSWs on the mean state of the ionosphere and thermosphere. *Journal of Geophysical Research: Space Physics*, *121*, 8077–8088. https://doi.org/10.1002/2016JA022910

Prolss, G. W. (1995). Ionospheric F region storms. In H. Volland (Ed.), *Handbook of atmospheric electrodynamics* (pp. 195–248). CRC Press.

Randel, W. J. (1993). Global variations of zonal mean zonal ozone during stratospheric warming events. *Journal of the Atmospheric Sciences*, *50*, 3308–3321. https://doi.org/10.1175/1520-0469(1993)050<3308:gvozmo>2.0.co;2

Russell, C. T., & McPherron, R. L. (1973). Semiannual variation of geomagnetic activity. *Journal of Geophysical Research*, *78*(1), 92–108. https://doi.org/10.1029/ja078i001p00092

Shen, X., Wang, L., & Osprey, S. (2020). The Southern Hemisphere sudden stratospheric warming of September 2019. *Science Bulletin*, *65*(21), 1800–1802. https://doi.org/10.1016/j.scib.2020.06.028

Strickland, D. J., Evans, J. S., & Paxton, L. J. (1995). Satellite remote sensing of thermospheric O/N_2 and solar EUV: 1. Theory. *Journal of Geophysical Research*, *100*(A7), 12217–12226. https://doi.org/10.1029/95JA00574

Tsugawa, T., Zhang, S. R., Coster, A. J., Otsuka, Y., Sato, J., Saito, A., et al. (2007). Summer-winter hemispheric asymmetry of the sudden increase in ionospheric total electron content and of the O/N2 ratio: Solar activity dependence. *Journal of Geophysical Research*, *112*(A8), A08301. https://doi.org/10.1029/2007ja012415

Vierinen, J., Coster, A. J., Rideout, W. C., Erickson, P. J., & Norberg, J. (2016). Statistical framework for estimating GNSS bias. *Atmospheric Measurement Techniques*, *9*(3), 1303–1312. https://doi.org/10.5194/amt-9-1303-2016

Yamazaki, Y., Matthias, V., Miyoshi, Y., Stolle, C., Siddiqui, T., Kervalishvili, G., et al. (2020). September 2019 Antarctic sudden stratospheric warming: Quasi-6-day wave burst and ionospheric effects. *Geophysical Research Letters*, *47*, e2019GL086577. https://doi.org/10.1029/2019GL086577

Yamazaki, Y., & Richmond, A. D. (2013). A theory of ionospheric response to upward-propagating tides: Electrodynamic effects and tidal mixing effects. *Journal of Geophysical Research: Space Physics*, *118*, 5891–5905. https://doi.org/10.1002/jgra.50487

Yue, J., & Wang, W. (2014). Changes of thermospheric composition and ionospheric density caused by quasi 2 day wave dissipation. *Journal of Geophysical Research: Space Physics*, *119*, 2069–2078. https://doi.org/10.1002/2013JA019725

Zhang, K., Wang, W., Wang, H., Dang, T., Liu, J., & Wu, Q. (2018). The longitudinal variations of upper thermospheric zonal winds observed by the CHAMP satellite at low and midlatitudes. *Journal of Geophysical Research: Space Physics*, *123*, 9652–9668. https://doi.org/10.1029/2018JA025463

Zhang, S.-R., Foster, J. C., Coster, A. J., & Erickson, P. J. (2011). East-west coast differences in total electron content over the continental U.S. *Geophysical Research Letters*, *38*, L19101. https://doi.org/10.1029/2011GL049116

Zhang, S.-R., Foster, J. C., Holt, J. M., Erickson, P. J., & Coster, A. J. (2012). Magnetic declination and zonal wind effects on longitudinal differences of ionospheric electron density at midlatitudes. *Journal of Geophysical Research*, *117*, A08329. https://doi.org/10.1029/2012JA017954

Zhang, Y., & Paxton, L. J. (2021). Storm-time neutral composition changes in the upper atmosphere. *Upper Atmosphere Dynamics and Energetics*, 115–133. https://doi.org/10.1002/9781119815631.ch7

Zhao, B., Wan, W., Liu, L., Mao, T., Ren, Z., Wang, M., & Christensen, A. B. (2007). Features of annual and semiannual variations derived from the global ionospheric maps of total electron content. *Annales Geophysicae*, *25*, 2513–2527. https://doi.org/10.5194/angeo-25-2513-2007

Appendix C

Goncharenko et al. (2022)

Goncharenko LP, Harvey VL, Randall CE, Coster AJ, Zhang S-R, Zalizovski A, Galkin I and Spraggs M (2022) Observations of Pole-to-Pole, Stratosphere-to-Ionosphere Connection. Front. Astron. Space Sci. 8:768629. doi: 10.3389/fspas.2021.768629

frontiers in Astronomy and Space Sciences

BRIEF RESEARCH REPORT
published: 19 January 2022
doi: 10.3389/fspas.2021.768629

Observations of Pole-to-Pole, Stratosphere-to-Ionosphere Connection

L. P. Goncharenko[1], V. L. Harvey[2,3], C. E. Randall[2,3], A. J. Coster[1], S.-R. Zhang[1], A. Zalizovski[3,4,5], I. Galkin[6] and M. Spraggs[7]*

[1]Massachusetts Institute of Technology, Haystack Observatory, Westford, MA, United States, [2]Laboratory for Atmospheric and Space Physics, University of Colorado, Boulder, CO, United States, [3]Atmospheric and Oceanic Sciences Department, University of Colorado, Boulder, CO, United States, [4]National Antarctic Scientific Center of Ukraine, Kharkiv, Ukraine, [5]Space Research Centre of Polish Academy of Sciences, Warsaw, Poland, [6]University of Massachusetts, Lowell, MA, United States, [7]Department of Atmospheric and Oceanic Sciences, University of Wisconsin-Madison, Madison, WI, United States

The behavior of the Earth's middle atmosphere and ionosphere is governed by multiple processes resulting not only from downward energy transfer from the Sun and magnetosphere but also upward energy transfer from terrestrial weather. Understanding the relative importance of mechanisms beyond solar and geomagnetic activity is essential for progress in multi-day predictions of the Earth's atmosphere-ionosphere system. The recent development of research infrastructure, particularly in Antarctica, allows the observation of new ionospheric features. Here we show for the first time that large disturbances observed in the Arctic winter polar stratosphere (20–50 km above ground and at 60–90°N) during a sudden stratospheric warming event are communicated across the globe and cause large disturbances in the summertime ionospheric plasma over Antarctica (60–90°S). Ionospheric anomalies reach ~100% of the background level and are observed for multiple days. We suggest several possible terrestrial mechanisms that could contribute to the formation of upper atmospheric and ionospheric anomalies in the southern hemisphere.

Keywords: sudden stratospheric warming, stratosphere, ionosphere, Antarctica, tides

OPEN ACCESS

Edited by:
Yoshizumi Miyoshi,
Nagoya University, Japan

Reviewed by:
Alexei V. Dmitriev,
Lomonosov Moscow State University, Russia
Nickolay Ivchenko,
Royal Institute of Technology, Sweden

****Correspondence:***
L. P. Goncharenko
lpg@mit.edu

Specialty section:
This article was submitted to Space Physics, a section of the journal Frontiers in Astronomy and Space Sciences

Received: *31 August 2021*
Accepted: *22 December 2021*
Published: *19 January 2022*

Citation:
Goncharenko LP, Harvey VL, Randall CE, Coster AJ, Zhang S-R, Zalizovski A, Galkin I and Spraggs M (2022) Observations of Pole-to-Pole, Stratosphere-to-Ionosphere Connection. Front. Astron. Space Sci. 8:768629. doi: 10.3389/fspas.2021.768629

INTRODUCTION

As the Earth's ionosphere—the charged portion of the atmosphere with maximum ionization at ~300 km—is created primarily by solar ionizing flux, conventional thinking implies that major variations in ionospheric electron density are related to solar and geomagnetic activity. While these factors are the primary drivers of ionospheric variability, many studies demonstrate significant variations in electron density due to the influences from the lower atmosphere through effects of gravity waves (Fritts and Lund, 2011, and references therein), tides (England, 2011, and references therein), and planetary waves (Pancheva and Mukhtarov, 2011). Terrestrial influences on ionospheric variability are often thought to be limited to a narrow geographic region or a short time frame. In the last decade it has become widely accepted that large (50–100% deviations from the background), persistent (>2 weeks) ionospheric variations are driven by middle atmosphere changes that are particularly enhanced during dramatic meteorological events called sudden stratospheric warmings (SSWs) (e.g., Goncharenko et al., 2010, 2021; Chau et al., 2012). SSWs cause large-scale

variations in temperature, wind, and ozone density in the Arctic wintertime stratosphere at high latitudes (60–90°N). SSW-induced variations extend both above and below the stratosphere, and across the equator to the tropics and summer polar mesosphere (e.g., Karlsson et al., 2007, 2009; Smith et al., 2020), and to the tropical ionosphere (e.g., Pedatella et al., 2018). However, known ionospheric disturbances associated with such changes are believed to be greatest at low latitudes (0–20°) and to fall off rapidly in the mid-latitudes (Pancheva and Mukhtarov, 2011), implying complex mechanisms of atmospheric connections in both the vertical and horizontal directions.

The Earth's ionosphere has been monitored for several decades, mostly by ionosondes due to their simplicity (Reinisch, 1986); however, such instruments allow studies of only local conditions. For the last 2 decades, large progress in understanding the spatial and temporal evolution of the ionosphere was achieved through observations of Total Electron Content (TEC) by ground-based Global Navigation Satellite System (GNSS) receivers. Although thousands of GNSS receivers are currently used in ionospheric research, data gaps over the oceans and hard-to-reach areas impact the utility of GNSS TEC data and hinder understanding of ionospheric behavior over those regions. Current knowledge of ionospheric physics is heavily influenced by observational data in the northern hemisphere, while the ionosphere above the sparsely instrumented southern hemisphere remains less understood. The last several years have seen an important development with the installation of new instrumentation in South America and Antarctica, enabling fundamentally new types of studies. This is the first work to leverage new instrumentation in South America and Antarctica to show that ionospheric variations at the summer high latitudes may be attributed to SSW. This study presents observations from independent techniques that show large-scale mesospheric and ionospheric variations in response to the Arctic SSW in January 2013. These variations occur not only at low latitudes, but at the middle latitudes and polar latitudes of the southern (opposite) hemisphere. The interhemispheric coupling mechanism (IHC, Becker et al., 2004) was invoked by de Wit et al. (2015) to explain variability at the summer polar mesopause during January 2013. Here we forge new territory by showing SSW-induced variability in the summer polar ionosphere.

DATA AND METHODS

This work requires the use of disparate data to study pole-to-pole teleconnections between the winter stratosphere and summer ionosphere during January 2013. We use temperature measurements from the Aura Microwave Limb Sounder (MLS) (Waters et al., 2006) to determine the response of the middle atmosphere to the SSW 2013 event. Temperature anomalies are computed by removing the 2004–2021 average from each day; however, this average does not include the day in question.

Polar mesospheric cloud (PMC) frequencies are derived from measurements made by the Cloud Imaging and Particle Size (CIPS) instrument (McClintock et al., 2009), which is a nadir-viewing panoramic imager that measures scattered radiation at 265 nm. CIPS was launched in 2007 aboard the Aeronomy of Ice in the Mesosphere (AIM) satellite (Russell et al., 2009), and is still operational. CIPS is a nadir-viewing panoramic imager that measures scattered radiation at 265 nm. It provides high resolution images of PMC albedo near the summer polar mesopause every day over the entire summer polar cap (Lumpe et al., 2013). This work uses the v5.20r05 level 3c data, which has a spatial resolution of 56 km^2.

To determine characteristics of ionospheric disturbances, we employ global TEC maps that utilize ground-based vertical TEC values (measured with TEC unit TECU; one TECU = 10^{16} e^-/m^2) from several thousand GNSS receivers. The resolution of this data is 1°longitude by 1°latitude every 5 min. This work uses 17 years of data from 2000–2016. On each day, all TEC data in the American sector (75°W ± 7.5°) is averaged in 1°latitude by 1-h local time bins. To separate effects of meteorological or other types of forcing from known effects of solar, geomagnetic activity, and seasonal variations, we use an empirical model of TEC based on the same 17 years of data. See Goncharenko et al. (2018) for details on model formulation and performance. We construct the TEC model for 75°W by fitting each latitude and local time bin with a formula that combines a dependence on the F10.7 solar flux proxy, a dependence on the Ap geomagnetic activity index and its history, a sinusoidal parameterization of seasonal variation, and a modulation of seasonal variations by solar activity. Fitting coefficients are obtained independently for every 1°latitude and 1-h local time bin, thus avoiding artificial features that can be introduced by fitting with 24-, 12-, and 8-h tides. Subtracting empirical model estimates from the observational data produces residuals that we interpret as having a meteorological origin. Note that inclusion of additional terms in the fit formula does not change the residuals significantly and does not change the results of this study. The TEC model was developed only for 75°W due to the relative data scarcity at other longitudes; however, this approach can be applied in the future to other locations as more data for a variety of conditions becomes available.

For comparison with TEC results, we have analyzed ionosonde data on maximum F-region density (*NmF2*) that is highly correlated with TEC. We used data from two instruments that are located in the American longitudinal sector, the Port Stanley (51.6°S, 57.9°W) digisonde and the Vernadsky (65.1°S, 64.2°W) ionosonde. The Port Stanley digisonde data was provided by the Lowell GIRO Data Center (http://spase.info/VWO/NumericalData/GIRO/CHARS.PT15M) which is discussed by Reinisch and Galkin (2011). The Vernadsky ionosonde data is provided by the National Antarctic Scientific Center of Ukraine, which has operated Vernadsky station since 1996. We use Port Stanley data collected in 1997–2015 and Vernadsky data collected in 2011–2013 to construct empirical models of *NmF2* in the same manner as described above for GNSS TEC.

RESULTS

In January 2013, a major Arctic SSW caused significant disturbances in Earth's middle atmosphere. **Figure 1A** (top

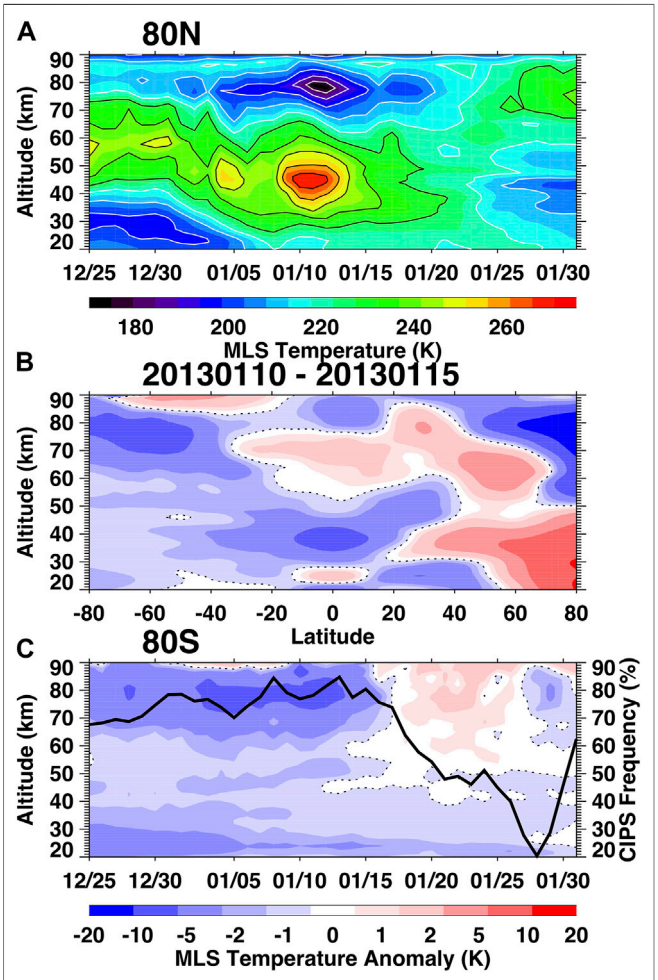

FIGURE 1 | (A) Altitude-time section of zonal mean MLS temperature averaged at 80°N from December 25, 2012 through January 31, 2013, **(B)** Latitude-altitude section of zonal mean temperature anomalies (deviations from the time mean) averaged from 10 to 15 January 2013, **(C)** Altitude-time section of temperature anomalies at 80° S from December 25, 2012 through January 31, 2013. The thick black line indicates daily CIPS PMC frequencies (number of pixels in which a PMC was detected relative to the total number of pixels, in %) at 80°S for clouds with albedos greater than 5×10^{-6} sr^{-1}, smoothed over 3 days.

panel) shows the temperature impacts, using MLS satellite observations. This major SSW was associated with the growth of planetary wave-2, which split the stratospheric polar vortex. As is typical for SSWs, the momentum deposited by the planetary wave breaking altered the mesospheric residual circulation, leading to anomalous descent and warming in the polar winter stratosphere and upwelling and cooling in the polar winter mesosphere, as indicated in **Figure 1A**. Stratospheric polar temperatures maximized on January 11th and mesospheric cooling peaked on January 12th.

The teleconnection pattern whereby planetary wave disturbances in the winter stratosphere lead to temperature variations at the summer mesopause is referred to as interhemispheric coupling (IHC) (e.g., Becker and Schmitz, 2003; Becker et al., 2004; Becker and Fritts, 2006; Karlsson et al., 2007; 2009). **Figure 1B** shows 5-days average temperature anomalies for 10–15 January, during the peak SSW and mesospheric cooling. The classic quadrupole pattern in temperature anomalies is in an agreement with de Wit et al. (2015) (**Figure 4**), who documented IHC coupling during the same SSW. This panel illustrates the low latitude and summer hemisphere extension of SSW-induced temperature perturbations. Several IHC mechanisms are described as follows. The cooling in the tropical stratosphere and warming in the tropical mesosphere causes meridional temperature gradients (and thus zonal winds) in the summer hemisphere to strengthen. The tropical warm anomaly in the mesosphere (red area in **Figure 1B**) increases the summer hemisphere equator-to-pole temperature gradient, leading to a westerly shift in the zonal winds in the summer upper mesosphere. According to Körnich and Becker (2010), this causes a lowering of the zero wind line, and thus a lowering of the altitude at which gravity waves break. The resulting downward shift in the ascending branch of the residual circulation then leads to warming near the summer polar mesopause. Smith et al. (2020) found repeatable temperature correlations between the winter stratosphere and the summer mesopause that exhibited expected IHC latitude-altitude structures (Randel, 1993) in 195 simulated years in the Whole Atmosphere Community Climate Model; however, they could not confirm that gravity wave filtering was the primary coupling mechanism in the model. Rather, they concluded that IHC in the model is due to a compensating circulation that arises to restore balance to the zonal mean atmosphere. Further, France et al. (2018) and Lieberman et al. (2021) showed that warming at the summer mesopause can arise due to inertial instability-triggered growth of the quasi-2-days wave. Thus, while IHC is both observed and simulated, the mechanisms responsible for the coupling remain elusive.

Figure 1C shows the time evolution of temperature anomalies in the stratosphere and mesosphere of the summer hemisphere. Prior to the SSW, the summer mesosphere was significantly colder than average, as evidenced by the persistent negative anomalies above ~60 km over the southern polar cap in late December and early January. However, within days of the SSW, the negative temperature anomalies decreased in magnitude and then turned positive. This is due to warming in the polar summer mesosphere; this warming is consistent with a sharp decrease in PMC frequencies (given by the thick black line). The changes in Antarctic summer mesopause temperatures and PMC frequencies are consistent with robust IHC processes.

To understand ionospheric behavior during this period, we focus on GNSS TEC in the American longitudinal sector, where evolution of TEC with latitude can be investigated in detail due to the dense network of GNSS receivers. Large, long-lasting ionospheric disturbances in response to this SSW event were reported in earlier studies at low latitudes and peaked in mid-January (Goncharenko et al., 2013; Jonah et al., 2014). **Figure 2A** shows the latitudinal variation in the TEC anomaly at 75°W on January 16, 2013, a geomagnetically quiet day (Ap = 5) during moderate solar activity (F10.7 = 137). The TEC anomaly is calculated as a difference between TEC observations and expected TEC behavior, which is provided by the empirical

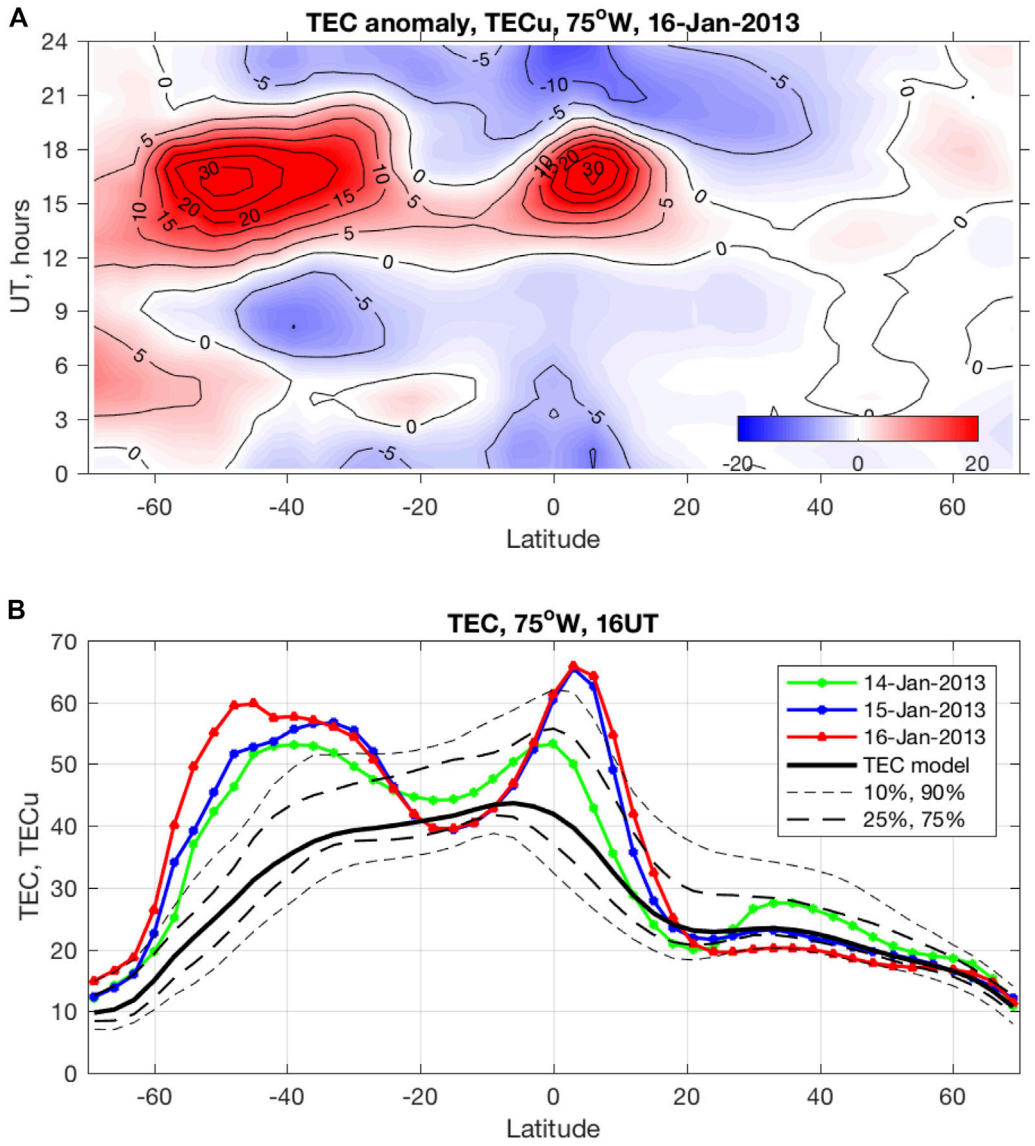

FIGURE 2 | (A) Anomaly in the total electron content at 75°W on Jan 16, 2013 extends from equatorial to high latitudes of the southern hemisphere. **(B)** TEC variation with latitude for 75°W and 16 UT (11 AM Local Time). Shown are TEC values observed on January 14–16, 2013 (green, blue, red) compared with TEC values expected for this season and solar activity as predicted by the empirical model (black). Thick dash lines show 25th and 75th percentiles of all available data, thin dash lines show 10th and 90th percentiles. Percentiles were calculated using TEC observations with close solar flux conditions (127 < F10.7 < 136) and from mid-December to mid-February.

TEC model described in *Data and Methods* and in Goncharenko et al. (2018). The anomaly in TEC (**Figure 2A**) includes a large increase in the northern crest of the Equatorial Ionization Anomaly (EIA, 0–15°N) in the morning-noon sector (12–18 UT) and a decrease in the afternoon and evening sectors (21–3 UT), as was reported for multiple SSW events in numerous studies (see reviews Chau et al., 2012; Goncharenko et al., 2021).

Observations in January 2013 show that an even larger morning-noon TEC anomaly develops in the southern hemisphere, centered at 40–60°S and extending to high latitudes, as seen in **Figure 2A**. **Figure 2B** shows the latitudinal variation in TEC at 16 UT (11:00 AM local time) for three consecutive geomagnetically quiet days, 14–16 January 2013; similar TEC variations are observed over the 10-days period. Continuous extension of TEC anomalies up to a factor of two from the expected value is observed from ~20°S all the way to the high latitudes in the southern hemisphere. Recent modeling studies are coming to a consensus that amplification in solar and lunar semidiurnal tides during SSWs is the most likely physical mechanism driving variations in the electric field and plasma velocity at the magnetic equator and, consequently, in plasma density in the EIA region (Fang et al., 2012; Jin et al., 2012; Pedatella and Liu, 2013; Wang et al., 2014). Solar semidiurnal

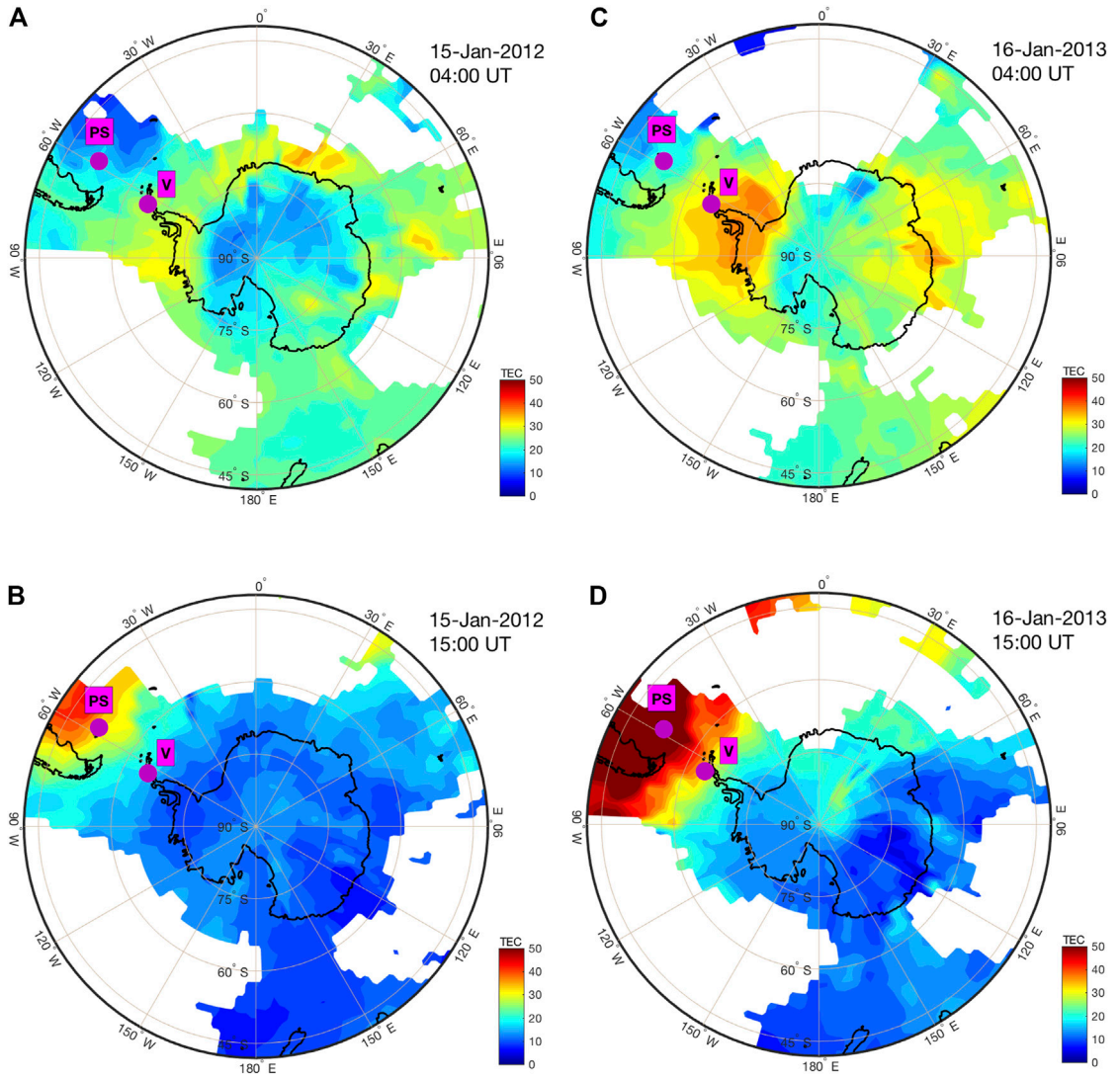

FIGURE 3 | Southern hemisphere polar maps showing TEC behavior during undisturbed Arctic conditions in January 2012 (left side, **A, B**) and during an SSW in January 2013 (right side, **C, D**). Top panels show snapshots at 4:00 UT and demonstrate increases in TEC over the entire Antarctic continent, with particularly large enhancement around the Antarctic Peninsula (30–120°W). Bottom panels (snapshots at 15:00 UT) demonstrate a strong increase in TEC from ~60°E to 120°W, with largest increases in the American longitudinal sector. Magenta dots indicate the locations of the Port Stanley and Vernadsky ionosondes stations.

migrating tides (SW2) experience stronger amplifications in the mid-latitude southern hemisphere than in the northern hemisphere (Liu et al., 2010). Upward propagation of these tides can modulate the thermospheric wind system and directly influence the ionosphere, particularly at middle latitudes. Pedatella and Maute (2015) also suggest that semidiurnal lunar tides amplified during SSWs propagate all the way to the upper thermosphere, leading to the quasi-semidiurnal variation of the F-region peak height and, consequently, electron density. As lunar tides were strongly amplified during the 2013 SSW (Zhang and Forbes, 2014), our observations of increased TEC at southern hemisphere mid-latitudes support both solar and lunar semidiurnal tide mechanisms.

In addition to the morning-noon enhancement, nighttime (3-8 UT) electron density is also enhanced at latitudes higher than ~45°S (**Figure 2A**); for example, the ionospheric Weddell Sea Anomaly, a phenomenon when the nighttime electron density exceeds the daytime electron density (Penndorf, 1965; He et al., 2009), is modified during both nighttime and daytime hours, as seen in **Figure 2A** at 60–70°S. We note that **Figure 2** extends only to 70°S, as empirical TEC model did not include higher latitudes due to the data scarcity. **Figure 3** further illustrates extension of the observed ionospheric anomalies to the high latitudes in the southern hemisphere, up to the South Pole. Polar maps compare TEC distributions on January 15, 2012, an undisturbed Arctic winter day the previous year (panels (3A) and (3B), to January 16, 2013, a SSW day (panels 3C and 3D). The control day of January

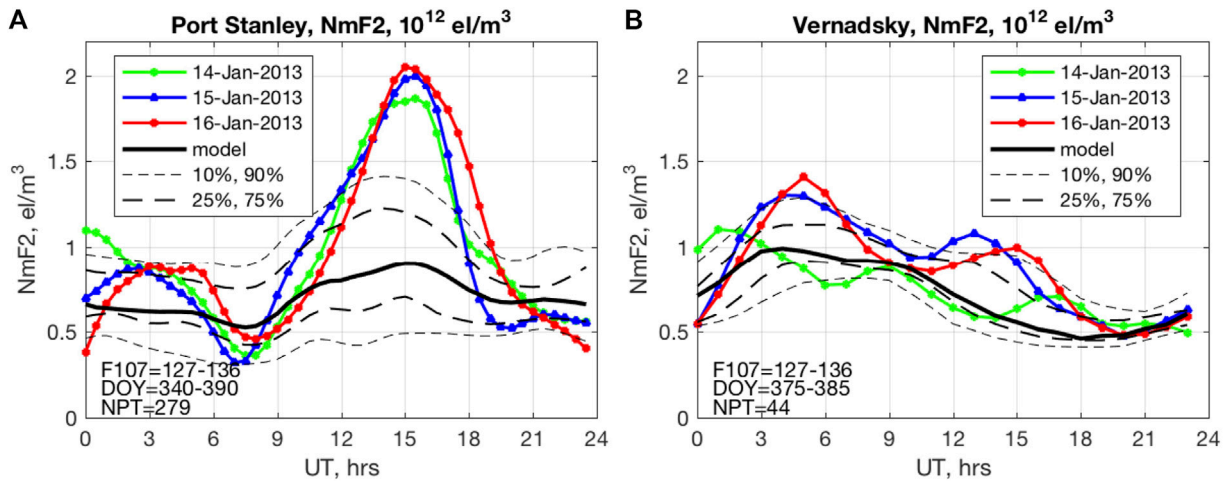

FIGURE 4 | Variations in the peak electron density *NmF2* as measured by ionosondes at Port Stanley **(A)** and Vernadsky **(B)**. Highly anomalous increases in *NmF2* are observed at both locations during the SSW, as illustrated with data from January 14–16, 2013.

15, 2012 was chosen to minimize differences due to seasonal change, solar flux, and geomagnetic activity (F10.7 = 133, Ap = 4 on Jan 15, 2012; F10.7 = 137, Ap = 5 on Jan 16, 2013). The TEC increase on January 16, 2013 (SSW day) at 4 UT is observed over the entire Antarctic continent, as seen in **Figure 3C**. The largest enhancements are over the Antarctic Peninsula and the Weddell Sea in the western hemisphere and near the Antarctic coast and 90°E. At 15 UT (**Figure 3D**), increases in TEC over the Antarctic Peninsula and the Weddell Sea are clearly an extension of the TEC change that peaked in the middle latitudes of the southern hemisphere, as shown in **Figures 2A,B**. Ionospheric disturbances similar to those presented in **Figures 3C,D** were observed for several days and maximized on January 14–16, 2013, simultaneously with disturbances at lower latitudes seen in **Figure 2**.

Independent confirmation of the impact of an Arctic SSW on the ionosphere over the middle and high latitudes of southern hemisphere is further obtained using a different observational technique, namely ionosondes. **Figure 4** shows diurnal variations in the peak electron density *NmF2* at mid- and high-latitude stations: Port Stanley (51.6°S, 57.9°W) and Vernadsky (65.1°S, 64.2°W), respectively. Typical diurnal variations of *NmF2* (black lines) at these locations are very different. Daytime *NmF2* (at ~12–18 UT) over Port Stanley (**Figure 4A**) exceeds nighttime *NmF2* (at ~1-6 UT) by ~50–60%, as expected in the mid-latitude summer hemisphere, consistent with effects of maximum photo-ionization rates at noon due to the smallest solar zenith angle and indicating that solar photoionization is the dominant mechanism responsible for *NmF2* behavior. In contrast to middle latitude, at high latitude over the Vernadsky location (**Figure 4B**) nighttime *NmF2* exceeds daytime *NmF2* by a factor of ~2, as expected for the area of the Weddell Sea Anomaly. This behavior in typical *NmF2* indicates significant contributions to *NmF2* from ionospheric dynamics, including thermospheric neutral wind and *E x B* drift, and from composition (Chen et al., 2011; Richards et al., 2017). During the SSW, similar ionospheric anomalies are observed at both locations: dramatic increases (up to a factor of 2) in *NmF2* during daytime hours (~12–18 UT), weaker increases at night (1-6 UT), and a slight decrease in the morning hours (6-9 UT). These anomalies are fully consistent with the GNSS TEC observations shown in **Figures 2**, **3**. The similarity of the diurnal behavior in ionospheric anomalies in the geographic mid- and high-latitude southern hemisphere suggest that they could be driven by the same mechanism, despite very different mechanisms being responsible for the typical/climatological ionospheric behavior in these regions. Seasonal variations in the meridional wind have long been considered an important driver of the Weddell Sea Anomaly (Jee et al., 2009). Thus, we suggest that SSW-associated semidiurnal variations in the upper thermospheric wind system is likely a leading mechanism responsible for large ionospheric disturbances in the high-latitude southern hemisphere during this SSW event.

DISCUSSION

Our observations demonstrate that during the 2013 Arctic SSW event, an extended region of atmospheric anomalies formed in the southern hemisphere. This region spans the mesosphere (60–90 km) to the ionosphere (~100–1,000 km) and from summer mid-latitudes to the South Pole, and persists for days. The formation of mesospheric and ionospheric anomalies in the mid- and high-latitude southern hemisphere during the northern hemisphere winter SSW presents a fascinating example of atmospheric coupling that is most likely driven by multiple mechanisms. Although we do not fully understand how the Arctic SSW leads to the ionospheric variability in the summer hemisphere, the following discussion presents some hypotheses about associated mechanisms. These hypotheses need to be tested with both additional observations and numerical simulations.

In the mesosphere, warming of the summer mesopause region in late January 2013 and associated decrease in the frequency of

PMCs has been attributed to IHC. The notion that large planetary wave activity and warming in the polar winter stratosphere is correlated with increasing temperatures at the polar summer mesopause is well accepted. However, as explained above, several mechanisms have been proposed to explain this global teleconnection. It is still unclear whether one or more of these mechanisms are at play in different situations. The weakened ascent near the summer mesopause due to IHC is also consistent with the SSW-induced weakening of the residual circulation in the lower thermosphere reported by Miyoshi et al. (2015).

In the ionosphere, the formation of anomalous features over the entire Antarctic continent likely results from thermospheric wind changes brought about by the SSW. At thermospheric altitudes, the wind changes could result from the superposition of migrating semidiurnal solar tides (SW2), non-migrating solar semidiurnal tides (SW1), and semidiurnal lunar tides (M1, M2). Enhancement of the SW2 tide during SSWs is a well-known phenomenon documented in both observations and simulations (Liu et al., 2010; Pedatella and Liu, 2013; Limpasuvan et al., 2016). The SW1 tide is generated through interaction of planetary wave 1 with solar semidiurnal migrating tide SW2. Simulations by Liu et al. (2010) indicate that amplitudes of the resulting SW1 tide in the meridional wind are larger in the mid-latitude southern hemisphere than in the northern hemisphere, and are particularly strongly enhanced in the high-latitude southern hemisphere. The SW1 tide remains strong even in the high-latitude upper thermosphere, making it potentially a key component for ionospheric variability above Antarctica. The semidiurnal lunar tide was particularly strongly amplified during the January 2013 SSW, as reported by Zhang and Forbes (2014). Liu et al. (2021) found that lunar tides in ionospheric TEC are not symmetric in latitude in several cases of analyzed SSW events, and signatures of lunar tides extend deep into middle latitudes of the southern hemisphere and weaken the Weddell Sea Anomaly. We thus can expect that amplification of any of the above-mentioned tides in association with SSWs can influence thermospheric winds at middle to high latitudes in the southern hemisphere. Superposition of these tidal components (SW2, SW1, M1, M2) of varying amplitudes and phases creates a complicated pattern of anomalies in the thermospheric wind and, consequently, in the ionosphere above Antarctica.

Additionally, Miyoshi et al. (2015) found that the effect of a winter SSW is to weaken the summer residual circulation between ~80 and ~400 km, including decreased descent in the summer polar lower thermosphere and weakened ascent above ~120 km. These thermospheric circulation changes are compounded with IHC effects to weaken ascent near the summer mesopause. In general, upwelling decreases the O/N_2 ratio and tends to decrease ionospheric electron density (e.g., Rishbeth, 1998). Weaker upwelling in the upper thermosphere at high latitudes of the southern hemisphere predicted by Miyoshi et al. (2015) would result in a higher thermospheric O/N_2 ratio and contribute to an overall increase in ionospheric electron density and TEC observed over Antarctica. Such an increase is seen in **Figure 2A** as a general enhancement in TEC at 60–70°S, which is observed in addition to the quasi-semidiurnal variation discussed above. An increase in TEC at even higher latitudes, including the overall increase in TEC above Antarctica seen in **Figure 3C**, might also be linked to SSW-induced variations in thermospheric composition. Pedatella et al. (2016) reveled a slight increase in O/N_2 at high latitudes of the southern hemisphere in TIE-GCM simulations and in COSMIC zonal mean peak electron density during the SSW of January 2009. Although their study was limited to lower latitudes than Antarctica, it is consistent with the general increase in TEC above Antarctica reported here. We note that SSW-induced changes in the thermospheric composition can vary strongly with latitude, as they are driven by variations in thermospheric circulation. Other simulations emphasized changes in thermospheric composition [such as (O), (O_2), (N_2), (H)] induced by the dissipation of amplified tides and generally predicted a decrease in the O/N_2 ratio at low and middle latitudes that would lead to a decrease in ionospheric electron density and TEC (Yamazaki and Richmond, 2013; Pedatella et al., 2016; Jones et al., 2020). The topic of changes in composition of different species has not been explored yet with sufficient detail and requires additional observational and modeling effort.

We cannot rule out the influence on ionospheric electron density that is produced by electric fields; these effects contribute significantly to the vertical plasma motion in the low-latitude ionosphere and are a well-known driver of the EIA (Anderson, 1981). Usually, effects of the electric field are not expected to contribute significantly to variations in electron density at middle and high latitudes, due to the high inclination angle of the Earth's magnetic field lines closer to its poles. However, the inclination angle at high latitudes in the southern hemisphere (58 at Vernadsky) is smaller than in the northern hemisphere (for American longitudes), and an electric field can produce non-negligible electron density variations. Numerical simulations demonstrate that significant perturbations in the mid-to-high latitude F-region vertical ion drift can be generated by inclusion of planetary waves at the model's lower boundary (Liu et al., 2010).

CONCLUSION

This study investigated the behavior of the mesosphere and ionosphere at geographic high latitudes of the southern hemisphere during and after the Arctic SSW of January 2013. We use a combination of stratospheric, mesospheric, and ionospheric ground-based and satellite data to demonstrate anomalous behavior in multiple parameters during a multi-day period in January 2013—neutral temperature, PMC frequency, TEC, and peak electron density. Our observations show that persistent mesospheric and ionospheric anomalies that are observed above Antarctica in January 2013 may be related to the SSW in the Arctic stratosphere. The results provide strong observational evidence that SSW events generate truly global disturbances that reach the high latitudes of the opposite hemisphere; thus, this study extends the concept of inter-hemispheric coupling to polar ionosphere. A variety of mechanisms is proposed to interpret the observed atmospheric and ionospheric variations at middle and high latitudes in the southern hemisphere, but their relative importance is not known yet. This paper aims to spark curiosity and encourage the

scientific community to quantify the contributions of the different mechanisms proposed here, and to suggest or consider other mechanisms responsible for the mesospheric and ionospheric variability seen in the observations. Continuous, high-quality observations of mesospheric, thermospheric and ionospheric parameters are critical for the robust identification of essential features. As the southern hemisphere remains poorly instrumented, detailed studies of this coupling remain a matter of future research.

DATA AVAILABILITY STATEMENT

Publicly available datasets were analyzed in this study. This data can be found here: MLS satellite data is available *via* http://mls.jpl.nasa.gov/. GNSS TEC data are publicly available through the CEDAR Madrigal database at http://cedar.openmadrigal.org. The Port Stanley digisonde data is available at http://giro.uml.edu/. Data obtained by Vernadsky ionosonde is available at http://geospace.com.ua/databrowser.

AUTHOR CONTRIBUTIONS

LPG: all aspects of paper; VLH and CER: analysis and interpretation of MLS and CIPS data; S-RZ: interpretation of ionospheric data; AJC: TEC data coordination and interpretation; AZ and IG: ionosonde data coordination and interpretation; MS: TEC data processing.

FUNDING

Research and operations at MIT Haystack Observatory are supported by the cooperative agreement AGS-1952737 between the US National Science Foundation and the Massachusetts Institute of Technology. LPG was also supported by the NASA grant 80NSSC19K0262 and NSF grant AGS-1132267. VLH was supported by the NASA grants 80NSSC18K1046 and 80NSSC20K0628. CER was supported by the NASA Small Explorer Program through contract # NAS5-03132. CER and VLH were also supported by the NASA grant 80NSSC20K0628. SZ was supported by the AFOSR FA9559-16-1-0364. AZ is partially supported through EOARD-STCU- IRA NASU Partner projects P667 and P735. MS was supported by the Research Experience for Undergraduates grant for her internship at MIT Haystack Observatory.

ACKNOWLEDGMENTS

We thank the MLS science team for processing and freely distributing the satellite data *via* http://mls.jpl.nasa.gov/. GNSS TEC data are publicly available through the CEDAR Madrigal database at http://cedar.openmadrigal.org. We thank the operators of the digisonde at Port Stanley (United Kingdom) for sharing their data through http://giro.uml.edu/. Data obtained by Vernadsky ionosonde is available at http://geospace.com.ua/databrowser.

REFERENCES

Anderson, D. N. (1981). Modeling the Ambient, Low Latitude F-Region Ionosphere-A Review. *J. Atmos. Terrestrial Phys.* 43, 753–762. doi:10.1016/0021-9169(81)90051-9

Becker, E., and Fritts, D. C. (2006). Enhanced Gravity-Wave Activity and Interhemispheric Coupling during the MacWAVE/MIDAS Northern Summer Program 2002. *Ann. Geophys.* 24, 1175–1188. doi:10.5194/angeo-24-1175-2006

Becker, E., Müllemann, A., Lübken, F.-J., Körnich, H., Hoffmann, P., and Rapp, M. (2004). High Rossby-Wave Activity in Austral winter 2002: Modulation of the General Circulation of the MLT during the MaCWAVE/MIDAS Northern Summer Program. *Geophys. Res. Lett.* 31, L24S03. doi:10.1029/2004GL019615

Becker, E., and Schmitz, G. (2003). Climatological Effects of Orography and Land-Sea Heating Contrasts on the Gravity Wave-Driven Circulation of the Mesosphere. *J. Atmos. Sci.* 60, 103–118. doi:10.1175/1520-0469(2003)060<0103:ceooal>2.0.co;2

Chau, J. L., Goncharenko, L. P., Fejer, B. G., and Liu, H.-L. (2012). Equatorial and Low Latitude Ionospheric Effects during Sudden Stratospheric Warming Events. *Space Sci. Rev.* 168, 385–417. doi:10.1007/s11214-011-9797-5

Chen, C. H., Huba, J. D., Saito, A., Lin, C. H., and Liu, J. Y. (2011). Theoretical Study of the Ionospheric Weddell Sea Anomaly Using Sami2. *J. Geophys. Res.* 116, a–n. doi:10.1029/2010JA015573

de Wit, R. J., Hibbins, R. E., Espy, P. J., and Hennum, E. A. (2015). Coupling in the Middle Atmosphere Related to the 2013 Major Sudden Stratospheric Warming. *Ann. Geophys.* 33, 309–319. doi:10.5194/angeo-33-309-2015

England, S. L. (2011). A Review of the Effects of Non-migrating Atmospheric Tides on the Earth's Low-Latitude Ionosphere. *Space Sci. Rev.* 168, 211–236. doi:10.1007/s11214-011-9842-4

Fang, T.-W., Fuller-Rowell, T., Akmaev, R., Wu, F., Wang, H., and Anderson, D. (2012). Longitudinal Variation of Ionospheric Vertical Drifts during the 2009 Sudden Stratospheric Warming. *J. Geophys. Res.* 117, A03324. doi:10.1029/2011JA017348

France, J. A., Randall, C. E., Lieberman, R. S., Harvey, V. L., Eckermann, S. D., Siskind, D. E., et al. (2018). Local and Remote Planetary Wave Effects on Polar Mesospheric Clouds in the Northern Hemisphere in 2014. *J. Geophys. Res. Atmos.* 123, 5149–5162. doi:10.1029/2017JD028224

Fritts, D. C., and Lund, T. S. (2011). "Gravity Wave Influences in the Thermosphere and Ionosphere: Observations and Recent Modeling," in *A. Bhattacharyya (Coed.), Aeronomy of the Earth's Atmosphere and Ionosphere, IAGA Special Sopron Book Series 2*. Editors M. A. Abdu and D. Pancheva (© Springer Science+Business Media B.V), 109–130. doi:10.1007/978-94-007-0326-1_8

Goncharenko, L., Chau, J. L., Condor, P., Coster, A., and Benkevitch, L. (2013). Ionospheric Effects of Sudden Stratospheric Warming during Moderate-To-High Solar Activity: Case Study of January 2013. *Geophys. Res. Lett.* 40, 4982–4986. doi:10.1002/grl.50980

Goncharenko, L., Harvey, V., Liu, H., and Pedatella, N. (2021). "Sudden Stratospheric Warming Impacts on the Ionosphere-thermosphere System—A Review of Recent Progress,". *Space Physics and Aeronomy: Advances in Ionospheric Research: Current Understanding and Challenges*. Editors C. Huang and G. Lu (Hoboken, NJ: Wiley), Vol. 3.

Goncharenko, L. P., Chau, J. L., Liu, H.-L., and Coster, A. J. (2010). Unexpected Connections between the Stratosphere and Ionosphere. *Geophys. Res. Lett.* 37. doi:10.1029/2010GL043125

Goncharenko, L. P., Coster, A. J., Zhang, S. R., Erickson, P. J., Benkevitch, L., Aponte, N., et al. (2018). Deep Ionospheric Hole Created by Sudden Stratospheric Warming in the Nighttime Ionosphere. *J. Geophys. Res. Space Phys.* 123, 7621–7633. doi:10.1029/2018JA025541

He, M., Liu, L., Wan, W., Ning, B., Zhao, B., Wen, J., et al. (2009). A Study of the Weddell Sea Anomaly Observed by FORMOSAT-3/COSMIC. *J. Geophys. Res.* 114 (A12). doi:10.1029/2009ja014175

Jee, G., Burns, A. G., Kim, Y.-H., and Wang, W. (2009). Seasonal and Solar Activity Variations of the Weddell Sea Anomaly Observed in the TOPEX Total Electron Content Measurements. *J. Geophys. Res.* 114. doi:10.1029/2008JA013801

Jin, H., Miyoshi, Y., Pancheva, D., Mukhtarov, P., Fujiwara, H., and Shinagawa, H. (2012). Response of Migrating Tides to the Stratospheric Sudden Warming in 2009 and Their Effects on the Ionosphere Studied by a Whole Atmosphere-Ionosphere Model GAIA with COSMIC and TIMED/SABER Observations. *J. Geophys. Res.* 117, 463. doi:10.1029/2012JA017650

Jonah, O. F., de Paula, E. R., Kherani, E. A., Dutra, S. L. G., and Paes, R. R. (2014). Atmospheric and Ionospheric Response to Sudden Stratospheric Warming of January 2013. *J. Geophys. Res. Space Phys.* 119, 4973–4980. doi:10.1002/2013JA019491

Jones, M., Jr., Siskind, D. E., Drob, D. P., McCormack, J. P., Emmert, J. T., Dhadly, M. S., et al. (2020). Coupling from the Middle Atmosphere to the Exobase: Dynamical Disturbance Effects on Light Chemical Species. *J. Geophys. Res. Space Phys.* 125, e2020JA028331. doi:10.1029/2020JA028331

Karlsson, B., Körnich, H., and Gumbel, J. (2007). Evidence for Interhemispheric Stratosphere-Mesosphere Coupling Derived from Noctilucent Cloud Properties. *Geophys. Res. Lett.* 34, L16806. doi:10.1029/2007GL030282

Karlsson, B., Randall, C. E., Benze, S., Mills, M., Harvey, V. L., Bailey, S. M., et al. (2009). Intra-seasonal Variability of Polar Mesospheric Clouds Due to Inter-hemispheric Coupling. *Geophys. Res. Lett.* 36, L20802. doi:10.1029/2009GL040348

Körnich, H., and Becker, E. (2010). A Simple Model for the Interhemispheric Coupling of the Middle Atmosphere Circulation. *Adv. Space Res.* 45 (5), 661–668. doi:10.1016/j.asr.2009.11.001

Lieberman, R. S., France, J., Ortland, D. A., and Eckermann, S. D. (2021). The Role of Inertial Instability in Cross-Hemispheric Coupling. *J. Atmos. Sci.* 78, 1113–1127. doi:10.1175/JAS-D-20-0119.1

Limpasuvan, V., Orsolini, Y. J., Chandran, A., Garcia, R. R., and Smith, A. K. (2016). On the Composite Response of the MLT to Major Sudden Stratospheric Warming Events with Elevated Stratopause. *J. Geophys. Res. Atmos.* 121, 4518–4537. doi:10.1002/2015JD024401

Liu, H.-L., Wang, W., Richmond, A. D., and Roble, R. G. (2010). Ionospheric Variability Due to Planetary Waves and Tides for Solar Minimum Conditions. *J. Geophys. Res.* 115. doi:10.1029/2009JA015188

Liu, J., Zhang, D., Goncharenko, L. P., Zhang, S. R., He, M., Hao, Y., et al. (2021). The Latitudinal Variation and Hemispheric Asymmetry of the Ionospheric Lunitidal Signatures in the American Sector during Major Sudden Stratospheric Warming Events. *J. Geophys. Res. Space Phys.* 126 (5), e2020JA028859. doi:10.1029/2020JA028859

Lumpe, J. D., Bailey, S. M., Carstens, J. N., Randall, C. E., Rusch, D. W., Thomas, G. E., et al. (2013). Retrieval of Polar Mesospheric Cloud Properties from CIPS: Algorithm Description, Error Analysis and Cloud Detection Sensitivity. *J. Atmos. Solar-Terrestrial Phys.* 104, 167–196. doi:10.1016/j.jastp.2013.06.007

McClintock, W. E., Rusch, D. W., Thomas, G. E., Merkel, A. W., Lankton, M. R., Drake, V. A., et al. (2009). The Cloud Imaging and Particle Size experiment on the Aeronomy of Ice in the Mesosphere mission: Instrument Concept, Design, Calibration, and On-Orbit Performance. *J. Atmos. Solar-Terrestrial Phys.* 71, 340–355. doi:10.1016/j.jastp.2008.10.011

Miyoshi, Y., Fujiwara, H., Jin, H., and Shinagawa, H. (2015). Impacts of Sudden Stratospheric Warming on General Circulation of the Thermosphere. *J. Geophys. Res. Space Phys.* 120, 10,897–10,910. doi:10.1002/2015JA021894

Pancheva, D., and Mukhtarov, P. (2011). Stratospheric Warmings: the Atmosphere- Ionosphere Coupling Paradigm. *J. Atmos. Sol. Terr. Phys.* 73, 1697–1702. doi:10.1016/j.jastp.2011.03.006

Pedatella, N. M., Chau, J. L., Schmidt, H., Goncharenko, L. P., Stolle, C., Hocke, K., et al. (2018). *How Sudden Stratospheric Warming Impacts on the Whole Atmosphere*. Eos, 99. doi:10.1029/2018EO092441

Pedatella, N. M., and Liu, H.-L. (2013). The Influence of Atmospheric Tide and Planetary Wave Variability during Sudden Stratosphere Warmings on the Low Latitude Ionosphere. *J. Geophys. Res. Space Phys.* 118, 5333–5347. doi:10.1002/jgra.50492

Pedatella, N. M., and Maute, A. (2015). Impact of the Semidiurnal Lunar Tide on the Midlatitude Thermospheric Wind and Ionosphere during Sudden Stratosphere Warmings. *J. Geophys. Res. Space Phys.* 120, 10740–10753. doi:10.1002/2015JA021986

Pedatella, N. M., Richmond, A. D., Maute, A., and Liu, H. L. (2016). Impact of Semidiurnal Tidal Variability during SSWs on the Mean State of the Ionosphere and Thermosphere. *J. Geophys. Res. Space Phys.* 121, 8077–8088. doi:10.1002/2016JA022910

Penndorf, R. (1965). The Average Ionospheric Conditions over the Antarctic. *Geomagnetism Aeronomy: Stud. Ionosphere, Geomagnetism Atmos. Radio Noise* 4, 1–45. doi:10.1029/ar004p0001

Randel, W. J. (1993). Global Variations of Zonal Mean Ozone during Stratospheric Warming Events. *J. Atmos. Sci.* 50, 3308–3321. doi:10.1175/1520-0469(1993)050<3308:gvozmo>2.0.co;2

Reinisch, B. W., and Galkin, I. A. (2011). Global Ionospheric Radio Observatory (GIRO). *Earth Planet. Sp* 63, 377–381. doi:10.5047/eps.2011.03.001

Reinisch, B. W. (1986). New Techniques in Ground-Based Ionospheric Sounding and Studies. *Radio Sci.* 21 (3), 331–341. doi:10.1029/rs021i003p00331

Richards, P. G., Meier, R. R., Chen, S. P., Drob, D. P., and Dandenault, P. (2017). Investigation of the Causes of the Longitudinal Variation of the Electron Density in the Weddell Sea Anomaly. *J. Geophys. Res. Space Phys.* 122, 6562–6583. doi:10.1002/2016JA023565

Rishbeth, H. (1998). How the Thermospheric Circulation Affects the Ionospheric F2-Layer. *J. Atmos. Solar-Terrestrial Phys.* 60 (14), 1385–1402. doi:10.1016/s1364-6826(98)00062-5

Russell, J. M., III, Bailey, S. M., Gordley, L. L., Rusch, D. W., Horányi, M., Hervig, M. E., et al. (2009). The Aeronomy of Ice in the Mesosphere (AIM) mission: Overview and Early Science Results. *J. Atmos. Solar-Terrestrial Phys.* 71, 289–299. doi:10.1016/j.jastp.2008.08.011

Smith, A. K., Pedatella, N. M., and Mullen, Z. K. (2020). Interhemispheric Coupling Mechanisms in the Middle Atmosphere of WACCM6. *J. Atmos. Sci.* 77, 1101–1118. doi:10.1175/JAS-D-19-0253.1

Wang, H., Akmaev, R. A., Fang, T.-W., Fuller-Rowell, T. J., Wu, F., Maruyama, N., et al. (2014). First Forecast of a Sudden Stratospheric Warming with a Coupled Whole-Atmosphere/ionosphere Model IDEA. *J. Geophys. Res. Space Phys.* 119, 2079–2089. doi:10.1002/2013JA019481

Waters, J. W., Froidevaux, L., Harwood, R. S., Jarnot, R. F., Pickett, H. M., Read, W. G., et al. (2006). The Earth Observing System Microwave Limb Sounder (EOS MLS) on the Aura Satellite. *IEEE Trans. Geosci. Remote Sens.* 44, 1075–1092. doi:10.1109/TGRS.2006.873771

Yamazaki, Y., and Richmond, A. D. (2013). A Theory of Ionospheric Response to Upward-Propagating Tides: Electrodynamic Effects and Tidal Mixing Effects. *J. Geophys. Res. Space Phys.* 118, 5891–5905. doi:10.1002/jgra.50487

Zhang, X., and Forbes, J. M. (2014). Lunar Tide in the Thermosphere and Weakening of the Northern Polar Vortex. *Geophys. Res. Lett.* 41, 8201–8207. doi:10.1002/2014GL062103

Conflict of Interest: The authors declare that the research was conducted in the absence of any commercial or financial relationships that could be construed as a potential conflict of interest.

Appendix D

Curriculum Vitæ

Larisa P. Goncharenko

Research Scientist

MIT Haystack Observatory, Westford, MA 01886, USA

617-715-5622 (office)

lpg@mit.edu

EDUCATION and PROFESSIONAL PREPARATION

MIT Haystack Observatory	Massachusetts, USA	Post-Doc	1996-1997
Kharkiv National Polytechnic University, School of Graduate Studies	Kharkiv, Ukraine	Radiophysics	1991-1996
Kharkiv National Polytechnic University	Kharkiv, Ukraine	Physics (Honors)	M.S. 1988

Note: Upon completing my graduate courses in 1995, it was not possible to pursue defense of my Ph.D. thesis. Shortly after Ukraine became an independent country, it did not have administrative and academic structures for considering Ph.D. candidates and awarding respective degrees in my field of research. In 1994, I was invited to the U.S. to work at the MIT Haystack Observatory as visiting scientist, where based on my scientific achievements and skills I was hired as a postdoc in 1996.

WORK EXPERIENCE

11/1997 - present, MIT Haystack Observatory, Research Scientist. Over 25 years of work experience as a Research Scientist at the MIT Haystack Observatory. My responsibilities and effort have progressed from the execution of research projects under the supervision of a senior colleague to leading independent developments of new research topics and innovative interdisciplinary science. I am currently a Principal Investigator (PI) in charge of two NASA awards and one AFOSR award, and a Co-PI on five other projects for NASA, NSF, and ONR, including an NSF Facilities grant that supports operations of the Millstone Hill Geospace Facility.

My research activities focus on a comprehensive understanding of thermospheric and ionospheric variability recorded by ground-based and space-based observations, with an emphasis on variability generated by the lower atmosphere drivers. I conduct observational and modeling studies of various meteorological drivers affecting ionospheric and thermospheric dynamics - such as sudden stratospheric

warmings, meteorological disturbances, solar eclipses, planetary waves, tides, and gravity waves. I study traveling ionospheric disturbances and their physical sources in the context of orographic gravity waves, polar vortex dynamics, geomagnetic activity, and related interhemispheric coupling. My research interests also encompass long-term change and empirical modeling. My research activities include yearly organization of international multi-instrument observational Sudden Stratospheric Warming campaigns (2008-2024) and coordination of collaborative data analysis. I am actively involved in the international research effort and collaborate with numerous colleagues outside of USA.

My management and administration efforts include setting strategic research goals for the group, development and implementation of new lines of research, with several proposals submitted to different agencies on the yearly basis, tracking and managing budgets on existing grants, assisting younger group members in developing their research proposals, recruiting and hiring junior staff and post-docs, and mentoring undergraduate students and post-docs.

03/1996 – 10/1997, MIT Haystack Observatory, Post-Doc. I analyzed lower thermospheric winds calculated from the Millstone Hill incoherent scatter radar data and co-located Durham meteor radar. This data served as a core dataset to determine tidal patterns in the mesosphere and lower thermosphere at middle latitudes.

11/1994 – 01/1995, MIT Haystack Observatory, Visiting Scientist. My efforts included intercomparison of techniques and methods used at Kharkiv and Millstone Hill incoherent scatter radars (ISR), learning about Millstone Hill ISR data products and technical characteristics, and translating relevant documentation.

03/1988 – 02/1996: Institute of Ionosphere, Kharkiv Polytechnic Institute, Research Scientist My responsibilities included design and execution of experiments on perturbations in the ionosphere created by high-power high-frequency radio waves and diagnostics of ionospheric perturbations with the Kharkiv ISR and co-located ionosonde. I also taught undergraduate classes in the Department of Radiophysics and Radioelectronics at the Kharkiv Polytechnic Institute.

RECOGNITION AND AWARDS

- American Meteorological Society Outstanding Committee Service (2021)
- MIT Buonsanto Lecture Award (2018)
- CEDAR Prize Lecture Award (2012)
- NASA Group Achievement Award (2008)
- MIT Excellence Award (2003)
- Excellence in Reviewing Awards:
  - Journal of Atmospheric and Solar-Terrestrial Physics, 2013
  - Earth, Planets and Space Journal, 2015

PROFESSIONAL LEADERSHIP AND SERVICE ACTIVITIES

- Member of the USA National Academy of Science Committee on Solar and Space Physics (Mar 2023 - present)

- Chair of the USA National Science Foundation CEDAR (Coupling, Energetics, and Dynamics of Atmospheric Regions) Science Steering Committee (2020 - 2023)
- Member of the NASA Heliophysics Advisory Committee (2017 - 2022)
- Member of the Space Weather Committee of the American Meteorological Society (2015+)
- National Academy of Science - Space Weather Operations and Research Infrastructure Panel member (2022)
- NASA Heliophysics 2050 panel member (2021)
- Member of the NASA Science and Technology Definition Team for GDC (Geospace Dynamics Constellation), 2018-2019
- Secretary, American Geophysical Union, Space Physics and Aeronomy section (2008-2010 term, 2010-2012 term)

Appendix E

Selected Publications

I am an author or coauthor of ∼120 publications. Full list of publications can be found on Google Scholar profile. The following list contains several selected publications (in reverse chronological order) that are relevant to the topic of the thesis and were published within the last 5 years.

- Q Gan et al. (2023). "GOLD Synoptic Observations of Quasi-6-Day Wave Modulations of Post-Sunset Equatorial Ionization Anomaly During the September 2019 Antarctic Sudden Stratospheric Warming". In: *Geophysical Research Letters* 50.12, e2023GL103386
- Katelynn R Greer et al. (2023). "Polar vortex strength impacts on the longitudinal structure of thermospheric composition and ionospheric electron density". In: *Journal of Geophysical Research: Space Physics* 128.9, e2023JA031797
- VL Harvey et al. (2023). "CIPS observations of gravity wave activity at the edge of the polar vortices and coupling to the ionosphere". In: *Journal of Geophysical Research: Atmospheres* 128.12, e2023JD038827
- M Jones Jr et al. (2023). "Understanding Nighttime Ionospheric Depletions Associated With Sudden Stratospheric Warmings in the American Sector". In: *Journal of Geophysical Research: Space Physics* 128.6, e2022JA031236
- Erich Becker et al. (2022a). "Multi-step vertical coupling during the January 2017 sudden stratospheric warming". In: *Journal of Geophysical Research: Space Physics* 127.12, e2022JA030866
- Katrina Bossert et al. (2022). "Large-Scale Traveling Atmospheric and Ionospheric Disturbances Observed in GUVI With Multi-Instrument Validations". In: *Geophysical Research Letters* 49.16, e2022GL099901
- Larisa P Goncharenko et al. (2022). "Observations of pole-to-pole, stratosphere-to-ionosphere connection". In: *Frontiers in Astronomy and Space Sciences* 8, p. 768629
- V Lynn Harvey et al. (2022). "Improving ionospheric predictability requires accurate simulation of the mesospheric polar vortex". In: *Frontiers in astronomy and space sciences* 9, p. 1041426
- Larisa P Goncharenko et al. (2021a). "Impact of September 2019 Antarctic sudden stratospheric warming on mid-latitude ionosphere and thermosphere over North America and Europe". In: *Geophysical Research Letters* 48.15, e2021GL094517

- Larisa P Goncharenko et al. (2021b). "Sudden Stratospheric Warming Impacts on the Ionosphere–Thermosphere System: A Review of Recent Progress". In: *Ionosphere dynamics and applications*, pp. 369–400
- Larisa P Goncharenko et al. (2021c). "A new model for ionospheric total electron content: The impact of solar flux proxies and indices". In: *Journal of Geophysical Research: Space Physics* 126.2, e2020JA028466
- Jing Liu et al. (2021). "The latitudinal variation and hemispheric asymmetry of the ionospheric lunitidal signatures in the American sector during major Sudden Stratospheric Warming events". In: *Journal of Geophysical Research: Space Physics* 126.5, e2020JA028859
- Larisa P Goncharenko et al. (2020). "Longitudinally dependent low-latitude ionospheric disturbances linked to the Antarctic sudden stratospheric warming of September 2019". In: *Journal of Geophysical Research: Space Physics* 125.8, e2020JA028199
- Larisa P Goncharenko et al. (2018). "Deep ionospheric hole created by sudden stratospheric warming in the nighttime ionosphere". In: *Journal of Geophysical Research: Space Physics* 123.9, pp. 7621–7633
- NM Pedatella et al. (2018). "How Sudden stratospheric warmings affect the whole atmosphere". In: *EOS* 99

Declaration of Authorship

I, Larisa GONCHARENKO, herewith, declare the following:

- The opportunity for this PhD project was not communicated to me commercially. In particular, I have not engaged any organisation that, for money, seeks supervisors for the drawing up of dissertations or that performs entirely or partially on my behalf the duties incumbent upon me regarding the examinations.
- I hereby declare under oath that I have completed the work submitted here independently and have composed it without outside assistance. Furthermore, I have not used anything other than the resources and sources stated and where I have taken sections from these works in terms of content or text, I have identified this appropriately.

Signed:

Date: February 12, 2024